Functional Regeneration of Brachial Sensory Afferents to Targets in the Brainstem

A dissertation

submitted by

Laura Elisabeth Wong

In partial fulfillment of the requirements

for the degree of

Doctor of Philosophy

in

Neuroscience

TUFTS UNIVERSITY

Sackler School of Graduate Biomedical Sciences

Date

April 2014

Advisor

Eric Frank, Ph.D.

Abstract

Spinal cord injury leads to devastating paralysis and paresis, in large part because damaged axons in the central nervous system fail to regenerate. Recovery following a spinal cord injury will require axons to restore synaptic connectivity with denervated targets several centimeters from the site of injury. This will require therapeutic agents that promote regeneration across long distances. Here, we report that brief systemic artemin treatment promotes regeneration of sensory axons to the brainstem following brachial dorsal root crush in an adult rat. Axon regeneration to the brainstem takes more than three months, consistent with slow growth across the three to four centimeter distance to reach the brainstem. Artemin not only stimulates robust regeneration of large, myelinated sensory axons to the brainstem, but it also promotes functional reinnervation of the appropriate target region, the cuneate nucleus. Remarkably, axons regenerate appropriately in the dorsal columns and establish connections with the correct nucleus in the brainstem without the addition of exogenous guidance molecules.

Artemin signals primarily through the RET tyrosine kinase, an interaction that requires the non-signaling co-receptor GFRα3. Previous studies report limited GFRα3 expression on large sensory neurons, suggesting that artemin could not signal in these neurons. Our findings, however, demonstrate that artemin promotes robust regeneration of large, myelinated sensory afferents suggesting some manner by which artemin signals in these neurons. Using a cell sorting technique, we demonstrated that the expression of GFRα3 is similar in myelinated and unmyelinated adult sensory neurons.

This suggests that artemin likely induces long-distance regeneration by binding GFRα3 and RET.

Although artemin is delivered for just two-weeks, regeneration to the brainstem requires more than three months, suggesting that brief trophic support may initiate intrinsic growth programs that remain active until targets are reached. Artemin may therefore represent a promising therapy for targeted sensory axon regeneration and functional reinnervation after spinal cord injury. In addition, understanding the mechanism by which artemin promotes regeneration may provide important insights into the development of future therapeutics to promote recovery following spinal cord injury.

For Steven Robinow,

who taught me that there is no greater joy than

discovering something no one else has seen

by looking through a microscope

Acknowledgements

The work presented in this dissertation would not have been possible without the contributions of many individuals throughout my time as a graduate student. I am grateful for the mentorship and guidance of my mentor, Dr. Eric Frank, who generously shared his time and expertise. His enthusiasm for discovery, for the results, and for the scientific method was a constant source of motivation as we pursued the next result and the next experiment. Thanks also to Dr. Pamela Harvey and Dr. Zhi Wang, whose guidance during the start of the regeneration project was critical to its success. I am also grateful to the members of my committee, Dr. Kathleen Dunlap, Dr. Daniel Jay, and Dr. James Schwob, as well as to my outside examiner, Dr. Zhigang He, who skillfully guided my training, shared their expertise and gave much needed advice during the difficult portions of this project. A special thanks to Eric Frank, Roger Wu, Daniel Wong and Molly Gibson for critical review of portions of this manuscript.

I must thank Molly Gibson, my best friend, partner in crime, and the “Stim 2” to my “Stim 1” (paired pulses make the best nerdy Halloween costume), for her numerous contributions to this project. Molly was more than a technician in the lab; she made the many of the experiments possible by running the electrophysiology rig by my side, brainstorming, reading drafts of proposals, and listening to presentations until we both knew them by heart. Molly made coming to work everyday more enjoyable and going to conferences all the more fun. I am grateful for our friendship and all the days spent together with our thinking caps on, both the metaphorical and tinfoil ones.

It is impossible to adequately thank my parents, Tom and Karen Wong, who tirelessly supported me every step along this journey. They have listened to me during times of triumph and despair. My dad’s logical approach to solving every problem that

comes along, and the precision and skill with which my mom approaches every endeavor inspired me to pursue this path and gave me the courage to fearlessly chase every dream I had.

Along my journey, I have had the privilege of working with and learning from several remarkable people at Tufts. Stephen Kwok, Alenka Lovy and Hiroko Nagase taught me technical skills that were required to complete this project. Daniel Wong, Bina Julian, Stephen Schworer, Adam Skibinski and Vallent Lee have shared their knowledge, their challenges, and supported me, making Tufts a second home. I must also thank the programs and departments I have had the pleasure of being a part of. Members of the neuroscience and physiology departments have nurtured my curiosity, shared reagents and created memories that will never be forgotten. In addition, I am grateful for the MSTP program for the support and wisdom of the students and administration,

Lastly, to my partner Roger Wu, who has shared in my trials and tribulations: I thank you for supporting me every day for the last four years. I feel so lucky to have a loving, smart and wonderful partner with whom to share this triumph. You bring out the best parts of me, challenging me to see the good in everything. It has been a joy to share this experience with my partner and best friend and I look forward to the future adventures we will share.

Table of Contents

List of Tables

Chapter 3

List of Figures

Chapter 1

Chapter 2

List of Abbreviations

Akt	Serine/threonine specific protein kinase
ARTN	Artemin
cAMP	Cyclic adenosine monophosphate
CGRP	Calcitonin gene related peptide
CNS	Central nervous system
CREB	cAMP response element binding protein
CSF	Cerebrospinal fluid
cSp5	Caudal spinal trigeminal tract
CSPG	Chondroitin sulfate proteoglycan
CST	Corticospinal tract
DR	Dorsal root
DREZ	Dorsal root entry zone
DRG	Dorsal root ganglion
ECM	Extracellular matrix
ELISA	Enzyme linked immunosorbent assay
ERK	Extracellular signal related kinase
FACS	Fluorescence activated cell sorting
GAG	Glycosaminoglycan
GDNF	Glial-Derived Neurotrophic Factor
GFL	GDNF-family ligand
GFRα	GDNF receptor family
GPI	Glycosylphosphatidylinositol
HAM	Human amniotic membrane
HSPG	Heparin sulfate proteoglycan

IB4	Isolectin B4
Ig	Immunoglobulin
JAK	Janus kinase
JNK	Jun N-terminal kinase
KIRA	Kinase receptor activation
KLF	Kruppel-like factor
MAG	Myelin-associated glycoprotein
MAPK	Mitogen-activated protein kinase
mTOR	Mammalian target of rapamycin
MVA	Motor vehicle accident
NCAM	Neural cell adhesion molecule
NF200	Neurofilament heavy chain
NGF	Nerve growth factor
NgR	Nogo receptor
NT-3	Neurotrophin-3
NRTN	Neurturin
OMgp	Oligodendrocyte myelin glycoprotein
PI3K	Phospho inositide 3 kinase
PKA	Protein kinase A
PLCγ	Phospholipase C-γ
PNS	Peripheral nervous system
PSPN	Persephin
PTEN	Phosphatase and tensin homolog
QPCR	Quantitative polymerase chain reaction
RB	Rose Bengal
SCG	Superior cervical ganglion

SCI	Spinal cord injury
Sema3	Type 3 semaphorins
SFK	Src-family kinase
SOCS3	Suppressor of cytokine signaling 3
Sp5	Spinal trigeminal tract
STAT	Signal transducers and activators of transcription
TGF-β	Transforming growth factor β
Trp	Transient receptor potential

CHAPTER 1

Introduction

Spinal Cord Injury

Spinal Cord Injuries. Spinal cord injury (SCI) is devastating, frequently resulting in permanent loss of movement and sensation. Current estimates indicate that more than 250,000 Americans have some form of SCI, with nearly 12,000 new cases occurring each year (Silva et al. 2013).

Most central nervous system (CNS) axons do not regenerate, resulting in little functional improvement following SCI. While much of the disability caused by SCI is due to loss of axonal connectivity, patients often experience complications related to CNS dysfunction such as hyperreflexia, autonomic dysfunction and contracture, in addition to non-neurological complications including increased urinary tract infections, bowel problems, and cardiac and respiratory dysfunction (Dobkin and Havton 2004; Silva et al. 2013). Despite tremendous gains in the understanding of the molecular and cellular events caused by SCI, there has been little improvement in the prognosis for functional recovery. Current treatment options are limited to high-dose methylprednisone, surgical interventions to stabilize and decompress the spinal cord, and rehabilitation (Kwon et al. 2010; Silva et al. 2013). Ongoing research aims to “cure” SCI by restoring connectivity between ascending and descending pathways in the spinal cord.

The pathobiology of SCI is complex. Mechanical trauma to the spinal cord leads to direct neuronal death and axon damage. Trauma triggers a cascade of biological events in the hours and days that follow, leading to ionic imbalance, glutamate excitotoxicity, inflammation, and oxidative stress; this ultimately results in delayed neuronal death (Dobkin and Havton 2004; Kwon et al. 2010; Silva et al. 2013). The chronic phase of SCI, occurring days to years later, involves demyelination, the deposition of connective tissue and reactive gliosis, the end product of which is glial scar

formation. Recovery after SCI requires bridging the glial scar and promoting regeneration of injured axons, sprouting of uninjured axons, extension of axons within white matter tracts, and restoration of synaptic contact with correct target regions. Effective therapies will require stimulation of each of these processes.

Brachial plexus injuries. The brachial plexus is the network of nerves connecting the spinal cord to the shoulder, arm, and hand. Injuries to the brachial plexus interrupt the flow of information between the CNS and peripheral tissues, resulting in loss of movement and sensation in the limb ipsilateral to the injury. Injuries to the dorsal roots (DRs) result in degeneration of the axon distal to the injury. Recovery of function in these types of injury is notoriously poor because these axons must regenerate in the inhibitory environment of the CNS in order to restore synaptic connectivity. Axons damaged in the DR face the same barriers to regeneration as axons damaged in the spinal cord.

High velocity motor vehicle accidents (MVA), particular motorcycle accidents, are responsible for 50-80% of brachial plexus injuries in the adult population (Terzis and Kostopoulos 2007; Limthongthang et al. 2013). Penetrating trauma, gunshot wounds and violent falls are responsible for much of the remainder. Given that extreme sporting accidents and high speed MVA are responsible for many of these injuries, it is not surprising that young men between the ages of 15 to 25 are most affected by brachial plexus injuries (Midha 1997; Moran et al. 2005).

Brachial plexus injury is most commonly caused by traction, where the arm and shoulder are forced away from the head and neck (Moran et al. 2005; Mannan and Carlstedt 2006; Terzis and Kostopoulos 2007; Giuffre et al. 2010; Limthongthang et al. 2013). Injuries can vary in severity on a spectrum from localized myelin damage and conduction deficiencies to complete transection requiring surgical intervention (Giuffre et al. 2010; Limthongthang et al. 2013). The location of the injury also affects outcome with

better recovery following damage distal to the DR ganglion (DRG) than following preganglionic injuries located between the DRG and spinal cord (Terzis and Kostopoulos 2007; Giuffre et al. 2010; Limthongthang et al. 2013).

Preganglionic avulsion, where the root is forcibly pulled from the spinal cord, is the most severe type of brachial plexus injury. Surgical intervention is required to reconnect roots to the spinal cord but has limited success in restoring function. As more roots are damaged, surgical intervention becomes more difficult, requiring multiple surgeries over several months (Mannan and Carlstedt 2006; Giuffre et al. 2010; Limthongthang et al. 2013). Although there is no consensus for the treatment of brachial plexus injuries, interventions include neurolysis to free roots from scar tissue, direct root repair, peripheral nerve grafts, and free muscle transplant (Hsu et al. 2004; Shin et al. 2004; Fournier et al. 2005; Mannan and Carlstedt 2006; Chuang 2009; Giuffre et al. 2010; Limthongthang et al. 2013). While motor neurons can partially reinnervate distal muscles leading to partial motor recovery following nerve grafts to the ventral roots (Chuang 2009; Limthongthang et al. 2013), severed sensory axons must regenerate into the spinal cord in order to reconnect with targets. Barriers to regeneration in the CNS largely prevent any restoration of synaptic connectivity.

Barriers to Regeneration in the Central Nervous System

Regeneration in the peripheral nervous system verses the central nervous system. In 1913, Santiago Ramon y Cajal first described the differences in regenerative capacity between neurons in the peripheral nervous system (PNS) and CNS. Using silver staining techniques, Ramon y Cajal observed that transected axons in the CNS and PNS both degenerate in a similar fashion. Although regenerative responses are

initiated in both central and peripheral neurons, regeneration in the PNS continues and severed axons regrow over long distances, whereas neuron sprouts in the CNS become dystrophic and fail to regenerate.

Regeneration in the PNS is dependent on the conditions encountered. When the basil lamina is intact as in crush lesions, conditions are optimal and axons regenerate robustly along their original trajectory at rates of several millimeters a day (Bradbury et al. 2000). Under suboptimal conditions, like following complete nerve transection, many axons encountering the severed end of the nerve form dystrophic end bulbs; some axons, however, exhibit more robust regenerative capacity and are able to navigate across the discontinuous nerve segments to reinnervate peripheral targets, underscoring the tremendous capacity of peripheral axons to regenerate (Bradbury et al. 2000). Ramon y Cajal hypothesized that growing peripheral axons may be attracted to peripheral targets and that myelinating Schwann cells might be supportive of axon growth (1928).

The observed failure of axons to regenerate in the CNS is consistent with the persistent loss of function noted in patients with CNS injuries. Regenerative processes are initiated with short sprouts forming shortly after axons are transection in the CNS but this regeneration is aborted (Ramon y Cajal 1928). Dystrophic end bulbs remain for years following injury. Recent advancements in imaging techniques have allowed researchers to image stalled end bulbs in live mice over weeks to months, observing that they remain completely immobilized and stable for the entire duration studied (Di Maio et al. 2011). Ramon y Cajal hypothesized that physical barriers like scarring and a lack of “catalytic agents” in the adult CNS were the obstacles to axon regeneration, challenging future researchers to overcome these barriers in order to restore CNS function following SCI (1928). To this day, research is still focused on finding therapeutics to overcome these barriers.

Extrinsic barriers to regeneration in the central nervous system. The failure of axons to regenerate in the adult CNS has been attributed to a non-permissive environment and lack of trophic support. For years, central axons were thought to lack regenerative capacity. In paradigm-shifting studies**,** peripheral nerve segments implanted in the CNS demonstrated that some central axons could regenerate given the appropriate environment (Aguayo et al. 1981; David and Aguayo 1981). While CNS axons were able to regenerate in the graft for distances as long as two centimeters, those axons failed to exit the graft, suggesting that the CNS environment was inhospitable for regenerating axons. Studies grafting optic nerve segments to peripheral nerves further suggested that the central environment was inhibitory to growth. Peripheral axons entering the graft grew less than one millimeter and axons reaching the distal nerve stump bypassed the graft (Aguayo et al. 1978). Since these experiments, three major classes of CNS inhibitors have been characterized: myelin-associated inhibitory proteins, members of the canonical axon guidance molecules, and CSPGs.

One major distinction between the environment of the PNS and CNS is the origin and composition of its myelin. Several proteins associated with myelin-debris have been identified that are inhibitory to axonal growth. These most likely serve to promote the stability of synaptic connections in the adult CNS. The prototypical myelin-associated inhibitory proteins are Nogo, myelin-associated glycoprotein (MAG) and oligodendrocyte myelin glycoprotein (OMgp) (Fig. 1-1) (Giger et al. 2010; Lee and Zheng 2011; Geoffroy and Zheng 2014). Each of these proteins signals through the Nogo receptor (NgR) family and paired immunoglobulin-like receptor B (PirB) to effect cytoskeleton rearrangement and neurite inhibition through a signaling pathway involving Rho and

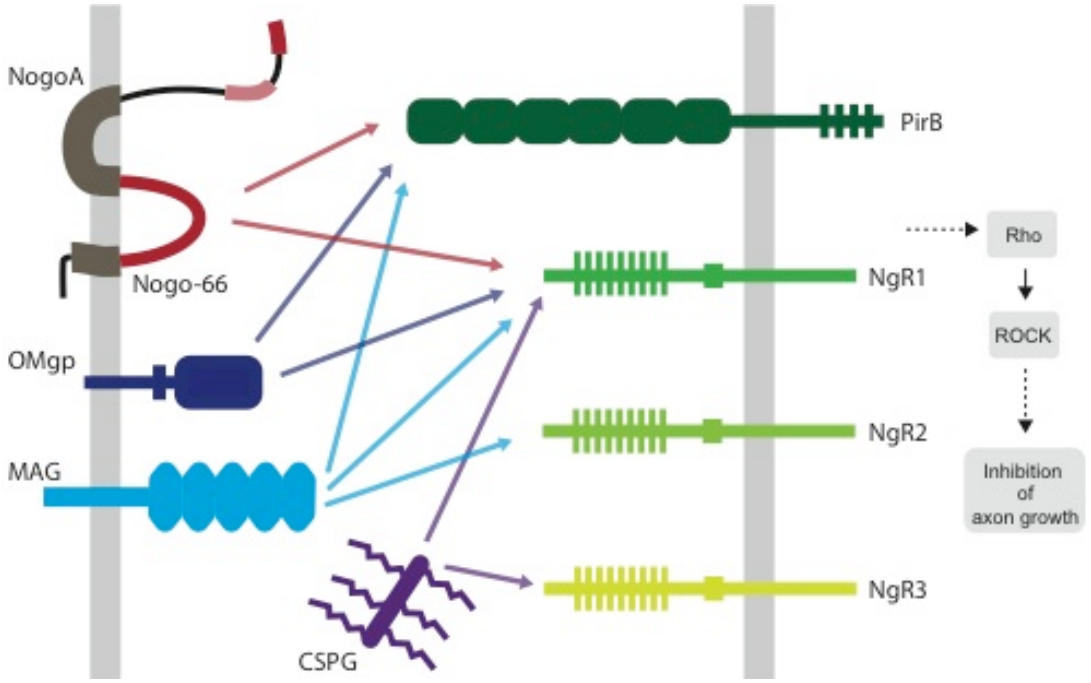

Figure 1-1: Interaction of the myelin inhibitory proteins with their receptors. Nogo, OMgp and MAG all interact with NgR1 and PirB to inhibit axon growth through a signaling pathway involving Rho and ROCK. CSPGs can bind NgR1 and NgR3, thus CSPGs and myelin inhibitory proteins share the same receptors. Figure adapted from Geoffroy and Zheng, 2014.

Rho-associated kinase (ROCK) (Fig. 1-1) (Geoffroy and Zheng 2014; Schwab and Strittmatter 2014). Among these myelin-associated inhibitory proteins, Nogo has been the most widely studied. While varying amounts of corticospinal tract (CST) regeneration have been reported with genetic deletion of Nogo (Kim et al. 2003; Simonen et al. 2003; Zheng et al. 2003), it is now widely accepted that Nogo plays a role in the sprouting of uninjured CST fibers (Simonen et al. 2003; Cafferty et al. 2010; Lee et al. 2010; Schwab and Strittmatter 2014). While blocking Nogo might not promote CST regeneration, our lab has demonstrated that the soluble NgR, which competitively binds Nogo, promotes

regeneration of sensory axons following dorsal root crush (Harvey et al. 2009). Myelin-associated inhibitory proteins and their receptors are incredibly diverse (Fig. 1-1) with many overlapping functions, suggesting that myelin exerts several layers of inhibition.

In addition to the prototypical myelin-associated inhibitory proteins, axon guidance molecules with repulsive effects, such as semaphorins and ephrins, are expressed in the adult CNS after development, are upregulated following injury, and are inhibitory to axon growth (Liebl et al. 2003; Benson et al. 2005; Pasterkamp and Verhaagen 2006; Giger et al. 2010). There is evidence that fibroblasts present in the lesion core upregulate expression of type 3 semaphorins (Sema3s), which may create a repulsive zone at the center of the lesion (Pasterkamp and Verhaagen 2001; Pasterkamp et al. 2001). Blocking SEMA3A promotes regeneration of some neuronal populations, further suggesting a role in inhibition (Kaneko et al. 2006). Adult sensory neurons express receptors for these guidance molecules, suggesting that they are still responsive to the repulsive influence of semaphorins and ephrins. Blockade of neuronally expressed ephrin receptors can induce regeneration and sprouting of CST fibers (Thrasher et al. 2006).

CNS injury leads to recruitment of a heterogeneous population of microglia, oligodendrocyte precursors, meningeal cells and astrocytes. While this cellular infiltration may serve a protective function, isolating the injured portion of the cord from the intact spinal cord, it also provides an additional environmental barrier to axonal regeneration in the form of a glial scar (Silver and Miller 2004; Yiu and He 2006). Many of the infiltrating astrocytes have a reactive phenotype, releasing inhibitory extracellular matrix (ECM) molecules known as chondroitin sulfate proteoglycans (CSPGs). CSPGs are a family of molecules that consist of a protein core with many attached glycosaminoglycan (GAG) side chains (Morgenstern et al. 2002). These are inhibitory to neurite extension *in vitro* and restrict regeneration *in vivo* (Morgenstern et al. 2002; Silver and Miller 2004; Cua et

al. 2013). Digestion of (1) the GAG side chains with chondrotinase ABC, a glycanase enzyme isolated from *Proteus vulgaris*, or (2) the core protein with matrix metalloproteinases promotes axon growth and facilitates recovery (Bradbury et al. 2002; Cua et al. 2013).

Differences in the microglial response to injury and Wallerian degeneration in the PNS and CNS may also contribute to environmental barriers to regeneration. While microglia and macrophages are recruited shortly after injury following both peripheral nerve transection and CNS damage, there is evidence that microglia recruited following CNS damage mount a reduced and delayed response. Despite numerous elongated and multi-vacuolated macrophages observed following CNS injury, toxic myelin debris is not cleared, and trophic factors and cytokines that support regeneration are not released (Avellino et al. 1995; Selzer 2003). This macrophage/microglial layer is inhibitory to axon growth, providing an additional barrier to regeneration beyond that of the astrocyte-derived, CSPG-rich portion of the glial scar (Ramer et al. 2001).

The inhibitory molecules in the adult CNS are diverse in their structure and expression pattern, suggesting an evolutionary role as important mediators preventing inappropriate plasticity. Upregulation of myelin-associated inhibitory proteins and CSPGs coincides with the end of the critical period during development. It appears that the mammalian CNS has eliminated the ability for long-distance regeneration in favor of stability in neurological circuits. Overcoming these extrinsic barriers to regeneration may enhance the regenerative ability of axons.

Neuronal intrinsic barriers to regeneration. In addition to extrinsic barriers to regeneration, neuronal intrinsic barriers also exist, providing additional inhibition to axon regrowth following injury. Recent studies have revealed that simply removing extracellular barriers to regeneration by genetic deletion or pharmacological inhibition

leads to sprouting of uninjured axons but is not sufficient to promote regeneration of many types of CNS neurons (Yiu and He 2006; Cafferty et al. 2010; Lee et al. 2010). Furthermore, implanted fetal or embryonic neurons are able to grow axons in the adult CNS, suggesting that the inhibitory environment is not sufficient to prevent growth of axons in certain developmental stages (Bradbury et al. 2000). There is increasing evidence that mature axons have diminished intrinsic regenerative ability, which contributes significantly to a failure of recovery following SCI.

Peripheral nerve injury leads to reactivation of intrinsic growth capability and allows for robust regeneration not observed with CNS injury. This response requires neurons to sense axonal damage, which is achieved by (1) binding cytokines of the IL-6 family leading to activation of the Janus kinase/signal transducers and activators of transcription (JAK/STAT) pathway; and (2) retrograde transport of injury signals to activate transcriptional pathways (Sun and He 2010; Yang and Yang 2011). Peripheral conditioning lesions increase the rate of axonal growth in the DR injury model, providing evidence that enhancing the intrinsic regenerative response may provide therapeutic benefit following SCI (Bradbury et al. 2000; Di Maio et al. 2011; Yang and Yang 2011).

Several factors may be responsible for the reduced regenerative response that accompanies the transition from immature to mature neurons. cAMP/CREB, PTEN/mTOR and Kruppel-like factors (KLFs) are three such players that are well correlated with axonal regeneration and may be crucial in determining the intrinsic growth properties of CNS neurons (Sun and He 2010; Yang and Yang 2011). Interestingly, targeting several of these pathways simultaneously appears to have a synergistic effect. Recent studies have demonstrated that deletion of SOCS3, leading to upregulation of the JAK/STAT pathway, and deletion of PTEN, leading to increased mTOR levels, results in robust and sustained regeneration of axons in the optic nerve

(Sun et al. 2011). Removing these negative regulators of axon regeneration may allow neurons to regain some intrinsic regenerative ability.

Current research aimed at promoting axon regeneration following SCI is based on overcoming the intrinsic and extrinsic barriers to growth as well as promoting neuroprotective effects after injury. Despite recent advances in understanding the pathways involved in these processes, there has been little advancement in stimulating regeneration of axons. The experiments in this thesis focus on the addition of a growth factor to overcome these barriers in order to promote long-distance regeneration in a model of brachial plexus injury.

Artemin, GFRα3 and RET

The Glial Derived Neurotrophic Factor Family. Neurotrophic factors are a heterogeneous group of proteins responsible for the development and maintenance of the CNS and PNS. The Glial Derived Neurotrophic Factor (GDNF) family of ligands (GFLs), consisting of GDNF, neurturin (NRTN), artemin (ARTN) and persephin (PSPN) (Lin et al. 1993; Kotzbauer et al. 1996; Baloh et al. 1998b; Milbrandt et al. 1998), are members of the transforming growth factor beta (TGF-β) superfamily of ligands. These ligands are involved in the survival, proliferation and differentiation of several neuronal populations in the CNS and PNS, including dopamine, sympathetic, parasympathetic, sensory and enteric neurons (Lin et al. 1993; Baloh et al. 1998b; Airaksinen and Saarma 2002; Paveliev et al. 2004; Paratcha and Ledda 2008).

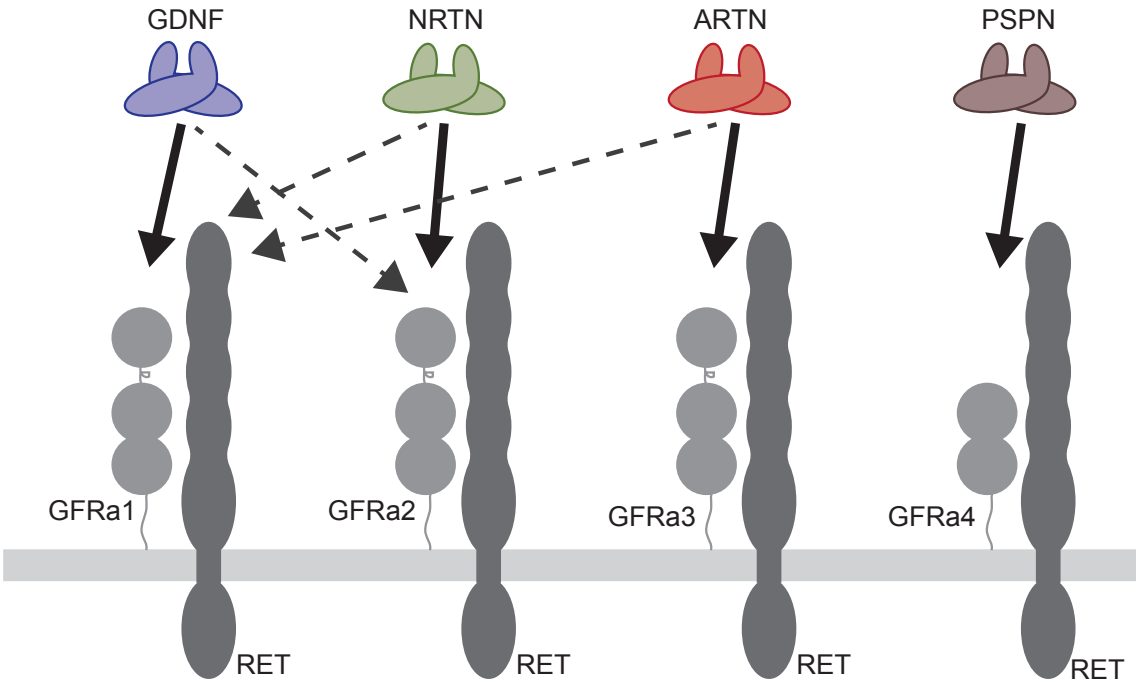

Figure 1-2: Components of the GFL/GFRα/RET complex. GFLs bind RET through an interaction with GFRα family members. GDNF binds GFRα1, NRTN binds GFRα2, ARTN binds GFRα3 and PSPN binds GFRα4. GDNF can also activate RET through low affinity binding of GFRα2, and ARTN and NRTN can act through a low affinity interaction with GFRα1.

The GFLs signal through a multicomponent receptor, consisting of a high-affinity glycosylphosphatidylinositol (GPI)-linked binding component, GDNF receptor family (GFRα1-4), and the RET tyrosine kinase (Baloh et al. 1998b, 2000; Wang et al. 2006; Bespalov and Saarma 2007). GDNF preferentially binds to GFRα1, NRTN to GFRα2, ARTN to GFRα3, and PSPN to GFRα4 (Figure 1-2) (Baloh et al. 1997, 1998b; Jing et al. 1997; Klein et al. 1997). In addition to these preferred reactions, some cross talk is possible, at least *in* vitro, with both ARTN and NRTN showing some affinity to GFRα1 and GDNF showing affinity for GFRα2 (Baloh et al. 1998b).

Although each GFL has specific neurotrophic and regenerative effects, the work presented in this thesis is focused on the regenerative effects of ARTN. We tested the extent to which ARTN promotes long-distance regeneration of sensory afferents to the brainstem in a model of brachial plexus injury. In the following sections, I will describe the structure of ARTN, its preferred binding partner, GFRα3, and the RET tyrosine kinase as well as studies describing the signaling cascades known to be activated downstream of RET. Studies describing the genetic deletion of each of these components will be reviewed for insights into the physiologic role of ARTN during development. Lastly, I will present data from recently published studies demonstrating that ARTN promotes axon regeneration in the CNS and PNS.

Artemin structure and expression. The full-length ARTN protein consists of 139 amino acids, composed of the active ligand, a signal sequence for secretion, and a large pro-region that is cleaved to form the mature 113 amino acid protein (Baloh et al. 1998b). ARTN, like the other GFLs, is a covalently linked homodimer with a conserved cysteine-knot motif (Silvian et al. 2006; Wang et al. 2006). There are three cysteine-rich repeats forming three distinct extracellular domains, two long finger domains formed by beta sheets and a central “wrist” portion composed of a single alpha helix (Baloh et al. 2000; Sah et al. 2005; Wang et al. 2006). The wrist and finger regions are connected by a hinge region which shows the most diversity between GFLs. Fragment swapping experiments have suggested that the second finger and wrist portion form the binding surface for interaction with GFRα, suggesting that the diversity of the hinge region may confer specificity to the different GFL-GFRα interactions (Baloh et al. 2000).

ARTN is expressed predominantly during embryogenesis with expression in the adult limited predominantly to peripheral tissues (Baloh et al. 1998b). In mice at embryonic day 14, ARTN is expressed in the developing nerve roots of the DRG but not

in developing sensory neurons (Baloh et al. 1998b; Honma et al. 2002). Instead, Schwann cells represent the major source of peripheral ARTN expression. Schwann cells from early postnatal rats express ARTN at a much higher level than myelinating Schwann cells of the adult sciatic nerve (Baloh et al. 1998b). Following peripheral nerve transection, ARTN is upregulated in the distal nerve stump. Given that nerve injury causes Schwann cells to transition to a more immature, regeneration-supporting phenotype (Scherer 1997), ARTN expression is regulated appropriately to influence developing and regenerating peripheral nerves. No evidence of ARTN expression has been found in the CNS during development although *in vitro* studies have demonstrated that ARTN can support survival of dopaminergic midbrain neurons (Baloh et al. 1998b).

GFRα3 structure and expression. GFRα3 was simultaneous discovered by three different labs using sequence homology to GFRα1 (Jing et al. 1997; Masure et al. 1998; Worby 1998). The *GFRα3* open reading frame encodes a protein of 397 amino acids, including a C-terminal GPI-linkage sequence and 28 conserved cysteine residues consistent with GFRα1 and GFRα2 (Jing et al. 1997; Masure et al. 1998; Worby 1998). Despite the similarities, GFRα3 shares a lower amino acid identity with GFRα1 (33%) and GFRα2 (36%) than they do with each other (48%) suggesting a more distant relationship (Jing et al. 1997; Worby 1998). GFRα3 is a GPI-linked protein with three globular cysteine-rich domains (Airaksinen and Saarma 2002; Wang et al. 2006). While the first globular domain is not required for ARTN binding and recruitment of RET, the second and third domains are closely packed with highly conserved structure in all members of the GFRα family (Wang et al. 2006).

The expression pattern of GFRα3 is similar to that of ARTN. In contrast to the wide expression of GFRα1 and GFRα2, GFRα3 is expressed at high levels only in developing peripheral nerves and ganglia (Baloh et al. 1998a; Naveilhan et al. 1998;

Worby 1998; Honma et al. 2002). There is no consensus regarding expression in the brainstem or central nervous system: some studies report an absence of GFRα3 expression in the CNS (Baloh et al. 1998b; Orozco et al. 2001), while others report its presence (Masure et al. 1998; Quartu et al. 2007). In addition to expression in nervous tissue, GFRα3 is expressed on cells in several abdominal organs during development and in the adult, with expression reported on several cancer tissues including pancreatic and mammary tumors (Naveilhan et al. 1998; Orozco et al. 2001; Wu et al. 2013).

In the adult nervous system, GFRα3 is expressed predominantly in sensory neurons of the DRG (Bennett et al. 2000; Orozco et al. 2001; Airaksinen and Saarma 2002). In the DRG, several studies have shown that expression of GFRα3 is largely limited to small, nociceptive neurons expressing either calcitonin gene related peptide (CGRP) or isolectin B4 (IB4) (Bennett et al. 2000; Orozco et al. 2001; Keast et al. 2010). Fewer than 1% of GFRα3 expressing sensory neurons are thought to be those with large diameter, myelinated axons expressing the heavy neurofilament chain (NF200) (Keast et al. 2010).

Following peripheral nerve injury, GFRα3 is upregulated, consistent with a role in sensory neuron survival or regeneration (Bennett et al. 2000; Gardell et al. 2003; Keast et al. 2010). One study suggests that this increase in the number of cells expressing GFRα3 results from neurons switching from expressing predominantly GFRα2 to expressing GFRα3 in order to better respond to injury (Wang et al. 2011a). Following DR crush, the total number of DRG neurons expressing GFRα3 increases but there is a concomitant decrease in the number of myelinated neurons expressing GFRα3 from 15% to 5% (Wang et al. 2008). This suggests that there may be a difference in the regulation of GFRα3 expression following central and peripheral nerve injuries.

RET structure and expression. The major mechanism of ARTN signaling is through the RET tyrosine kinase, an interaction that requires binding of the non-signaling coreceptor GFRα3 (Baloh et al. 1998b). RET, a member of the receptor tyrosine kinase superfamily, is the common signaling receptor shared by all the GFLs. It is a single-pass transmembrane protein that contains four cadherin-like repeats followed by a cysteine-rich C-terminal domain in the extracellular portion and a typical intracellular tyrosine kinase domain with multiple tyrosine residues (Airaksinen and Saarma 2002; Kjaer and Ibáñez 2003). Despite its substantial extracellular domain, RET has no inherent affinity for any of the GFLs (Durbec et al. 1996). Ligand binding requires a GFRα member. No difference in tyrosine residue phosphorylation has been observed between the different GFLs, suggesting that activation of RET is similar regardless of whether it is activated by GDNF, NRTN or ARTN (Airaksinen and Saarma 2002).

During development, RET is expressed in the developing kidneys and in neuronal precursors found in the neural crest that become the enteric nervous system (Pachnis et al. 1993; Durbec et al. 1996). In adult peripheral tissues, RET expression—often overlapping with expression of GFRα—is predominantly observed in organs such as liver, intestines, testes and skin. RET is highly expressed in the DRG and in motor neurons in the spinal cord, consistent with expression overlapping that of the GFLs and their coreceptors (Naveilhan et al. 1998; Orozco et al. 2001; Luo et al. 2007). In the brain, RET is expressed in the cerebellum, glomerular layer of the olfactory bulb and is widely expressed in the several regions of the brainstem and midbrain (Trupp et al. 1997).

GFRα3:RET signaling cascades. ARTN signaling requires an active complex composed of two molecules of GFRα3, two of the RET tyrosine kinase, and the ARTN dimer (Schlee et al. 2006). Although GFRα3 has no signaling activity, it is thought to capture ARTN at the cell surface (Ibáñez 2010). GFRα3, like other GPI-linked proteins, is located in lipid rafts, specialized subdomains of the plasma membrane important for the organization of transmembrane signaling events (Airaksinen and Saarma 2002; Paratcha and Ibáñez 2002). The clamped ARTN:GFRα3 compound forms a composite surface that recruits RET, stabilizing it in the lipid raft structure (Paratcha and Ibáñez 2002). The lipid raft inner leaflet is associated with a number of G-proteins and members of the Src-family of kinases, making this an ideal location for neurotrophic signaling. RET activation occurs through the initial binding of ARTN to GFRα3 followed by the sequential recruitment of first one RET and then additional GFRα3 and RET molecules, ultimately leading to RET autophosphorylation and activation (Fig. 1-3) (Schlee et al. 2006; Paratcha and Ledda 2008).

Some cells that are reactive to GFLs do not express RET suggesting a mechanism of signaling that does not require RET and GFRα expression on the same cell. *Trans* activation of RET by neighboring cells with GFL:GFRα complexes has been

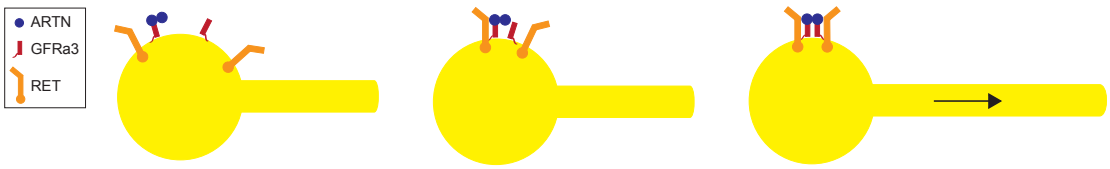

Figure 1-3: The ARTN multicomponent receptor. The ARTN homodimer binds a molecule of GFRα3. This interaction recruits one molecules of RET to the lipid raft, which recruits additional GFRα3 and RET molecules leading to RET auto-phosphorylation and, ultimately regeneration.

described in *in vitro* studies with GDNF (Trupp et al. 1997). Additionally, RET could be activated in *trans* by soluble GFL/GFR a complexes freed from the cell membrane by phospholipase or protease action on the GPI-linkage connecting GFRα molecules to the membrane (Paratcha and Ledda 2008).

RET, once autophosphorylated, has been shown to activate a number of different intracellular cascades, although the precise role of these cascades—in particular growth, survival or proliferative pathways—is unknown. The GDNF/GFRα1/RET complex can initiate the mitogen-activated protein kinase (MAPK), serine/threonine specific protein kinase (Akt), Jun N-terminal kinase (JNK), phospholipase Cγ (PLCγ) and Src-family kinases (SFK) pathways (Takahashi 2001; Airaksinen and Saarma 2002; Paveliev et al. 2004; Jeong et al. 2008; Paratcha and Ledda 2008; Ibáñez 2010). Each of these pathways is important in mediating GDNF-promoted effects on neuron survival, neurite growth, and differentiation. In addition, several studies have found that activation of these intrinsic pathways promote regeneration in other models of SCI, suggesting these are all possible downstream effectors promoting axonal regeneration (Namikawa et al. 2000; Yang and Yang 2011). Although the specific pathways initiated by ARTN/GFRα3/RET activation are less well understood it is likely they are similar to those of other GFL-mediated pathways.

Given that all GFLs signal through the common RET molecule, it is important to understand if they activate different signaling cascades. In culture, all GFLs trigger phosphorylation of the same four tyrosine residues, suggesting there is no difference in downstream signaling. A difference in intracellular signaling between GFLs cannot be entirely ruled out, however, because there are still several intracellular domains that have yet to be investigated and the same tyrosine can bind different adaptors, which could result in biologically different outcomes (Airaksinen and Saarma 2002).

Genetic manipulation of RET, GFRα3 and ARTN. Genetic deletion of RET disrupts signaling from GDNF, NRTN, ARTN and PSPN. These mice die shortly after birth and display dramatic abnormalities in kidney, gastrointestinal tract and lung (Durbec et al. 1996; Taraviras et al. 1999; Airaksinen and Saarma 2002; Viemari et al. 2005). There are also significant defects in the sympathetic and parasympathetic nervous system, enteric nervous system and several sensory neuron populations (Durbec et al. 1996; Enomoto et al. 2001; Golden et al. 2010; Honma et al. 2010). Mutations causing increased activation of RET lead to thyroid cancer and multiple endocrine neoplasia type 2, while germline mutations resulting in a loss of RET lead to aganglionic megacolon (Hirshsprung's disease) (Durbec et al. 1996; Takahashi 2001; Watanabe et al. 2002).

In sharp contrast, mice lacking GFRα3 or ARTN are viable and fertile with ptosis as the only obvious phenotype (Nishino et al. 1999; Honma et al. 2002). In these animals, migration of superior cervical ganglion (SCG) neurons is perturbed and sympathetic innervation of the eyelid elevator muscle is lacking, resulting in ptosis. ARTN expression is temporally regulated, with expression beginning initially near SCG neuron precursors and then shifting to large blood vessels, guiding the SCG axons to their final destination (Nishino et al. 1999; Honma et al. 2002). In the absence of signaling by ARTN, SCG neurons do not connect with their proper targets and thus fail to receive adequate trophic support, resulting in the eventual loss of these neurons. Honma et al. further investigated whether ARTN deletion affected sensory neurons (2002). Surprisingly, the DRGs of $ARTN^{-/-}$ and $GFR\alpha3^{-/-}$ mice were normal in size and morphology. There was no difference observed in the axonal projections of sensory neurons. The lack of observed changes in $ARTN^{-/-}$ and $GFR\alpha3^{-/-}$ DRGs is most likely because these nociceptive neurons express receive overlapping trophic support from NGF (Honma et al. 2002; Elitt et al. 2006).

Although there is no change in DRG neurons in ARTN$^{-/-}$ mice, overexpression of ARTN in the skin leads to an increase in the overall number of neurons in the DRG and an increase in *GFRα3* transcript expression in DRG neurons (Elitt et al. 2006). Interestingly, these increases led to an increase in expression of the transient receptor potential (Trp) channel TRPV1 in DRG neurons and a corresponding increase in thermal sensitivity, consistent with expression of GFRα3 in small nociceptive neurons. This study confirms a functional role of ARTN in the survival and regulation of nociceptive sensory neurons *in vivo*.

These experiments indicate that ARTN is important in the developing sympathetic and sensory systems. Additionally, the similar phenotypes observed in ARTN$^{-/-}$ and GFRα3$^{-/-}$ mice suggest that this ARTN signaling requires GFRα3.

Alternative binding partners. In addition to binding GFRα3, ARTN also binds to heparin sulfate proteoglycans (HSPG) in the extracellular matrix. Analyses of point mutations have shown that the hinge region between finger and wrist sections of ARTN is key to this interaction (Silvian et al. 2006). In addition, regions of the N-terminal domain are important regions for binding HSPG. Removal of the nine N-terminal amino acids by proteolytic cleavage results in a 104 amino acid isoform that has 10-fold lower affinity for HSPG (Silvian et al. 2006). Interestingly, the presence of HSPG enhances the affinity of ARTN to GFRα3:RET. This interaction may serve to restrict diffusion—raising the local ARTN concentration—or may help orient ARTN for proper binding to its receptor complex (Airaksinen and Saarma 2002; Sah et al. 2005; Silvian et al. 2006).

The role of HSPG binding may not be limited to modulating the classical GFRα3:RET pathway. Immobilized ARTN promotes adherence and spreading of a human neuroblastoma cell line lacking RET (Bespalov et al. 2011). This response requires HSPGs and SFK activation, confirming an earlier study showing RET-

independent activation of SFKs (Trupp et al. 1997). SFKs are abundantly located on the inner leaflet of lipid rafts, in close proximity to GPI-linked GFRα3. Additionally, *in vitro* studies indicate that GDNF induces neurite outgrowth in an HSPG and SFK dependent manner (Paveliev et al. 2004; Bespalov et al. 2011). The interaction of ARTN, HSPGs, and GFRα3 on lipid rafts may activate SFKs, promoting axon extension in a RET-independent manner. It is possible that signaling via HSPGs allows for biologically different effects than signaling via RET.

Neural cell adhesion molecule (NCAM) can also bind GFLs in a reaction requiring GFRα members (Paratcha et al. 2003; Ledda et al. 2007). NCAM has three major isoforms, NCAM-180, -140 and -120 with identical ectodomains consisting of five N-terminal immunoglobulin (Ig)-like modules and two fibronectin-like domains (Sjöstrand et al. 2007; Nielsen et al. 2009). NCAM-140 and NCAM-180 are transmembrane proteins with both adhesive properties and signaling properties. They have been implicated in a number of developmental processes including cell migration, neurite outgrowth, and synaptic plasticity (Ibáñez 2010). NCAM can freely associate with GFRα1 through its fourth Ig domain, leading to reduced NCAM-mediated cell adhesion and allowing high-affinity binding of the third Ig domain of NCAM to GDNF, resulting in activation of the SFK Fyn and Schwann cell migration *in vitro* (Paratcha et al. 2003; Sjöstrand et al. 2007; Sjöstrand and Ibáñez 2008). Additionally, GDNF/GFRα1/NCAM interactions promote ligand-induced cell adhesion leading to hippocampal neuritogenesis and synapse formation, suggesting a role in establishing precise synaptic contacts (Ledda et al. 2007; Nielsen et al. 2009). While the majority of the studies involving NCAM have used GDNF as a binding partner, one study demonstrated that ARTN can bind and signal through NCAM in a RET-independent manner to induce release of immunoreactive CGRP in response to capsaicin treatment (Schmutzler et al.

2011). This suggests that NCAM may mediate ARTN-induced effects during development and in the adult.

Artemin treatment *in vivo*. Given that GFRα3 is primarily expressed in nociceptive neurons in the DRG, the potential role of ARTN as a treatment for neuropathic pain was investigated. Repeated systemic injections of ARTN abolished behavioral signs of neuropathic pain in rodents with sciatic nerve ligation and led to significant normalization of the morphological and neurochemical response to the injury state in rodents with sciatic nerve ligation (Gardell et al. 2003). Once ARTN treatment is stopped, neuropathic pain returns and the cellular changes associated with neuropathic pain return. ARTN is currently in Phase 2 trials for the treatment of neuropathic pain.

ARTN treatment causes robust regeneration of axons into the spinal cord following dorsal root crush injury in an adult rat (Wang et al. 2008; Harvey et al. 2010). All classes of sensory fibers, including myelinated, unmyelinated peptidergic, and unmyelinated "peptide-poor" axons, regenerate across the dorsal root entry zone (DREZ) into the spinal cord. By four weeks after injury, labeled axons reinnervate the dorsal horns in ARTN-treated animals, even when treatment is delayed for two days (Wang et al. 2008). Remarkably, regeneration with ARTN is topographically specific. Large, myelinated axons return to deeper laminae while peptidergic fibers remain restricted to the most dorsal aspects of the spinal cord, in laminae I and II (Harvey et al. 2010). Furthermore, axons labeled in the skin are located in more superficial areas in the dorsal horn compared to those receiving information from muscle (Harvey et al. 2010), just as they are on the intact side.

ARTN-promoted regeneration is functional, resulting in restored synaptic connectivity in the spinal cord. Nociceptive responses to noxious thermal, mechanical and chemical stimulation return to normal with ARTN treatment (Wang et al. 2008).

Sensorimotor behaviors are also improved with ARTN. Paw placement on a horizontal ladder, contact-evoked grasping, and skilled walking on a beam are markedly improvement with ARTN treatment (Wang et al. 2008). In addition to improvement on simple behavior tests, synaptic connectivity—assessed electrophysiologically—was restored to approximately 30% of normal (Wang et al. 2008). These data prompted the experiments presented in this thesis, investigating if ARTN similarly promotes regeneration of sensory axons to their targets in the brainstem.

In addition to its effects on centrally projecting axons in the DR, ARTN also promotes regeneration of distal sensory axons traveling to the periphery following spinal root crush, a model of post-ganglionic injury that also induces neuropathic pain (Wang et al. 2013a). Following injury, ARTN induced a time-dependent normalization of tactile sensory thresholds and reduced the hyperalgesia associated with post-ganglionic injury. Similar to findings in the DR crush model, both large, myelinated fibers and small, peptidergic fibers regenerated with ARTN treatment (Wang et al. 2013a). Reinnervation of distal targets persisted after ARTN treatment was stopped but hyperalgesia returned, suggesting that the mechanisms by which ARTN promotes regeneration and reduces neuropathic pain are fundamentally different.

The Dorsal Root Crush Model

In this study, we used the DR crush model of SCI because it is particularly well suited to studying axonal regeneration within the CNS. Sensory neurons reside in the DRG, a structure located in the PNS. These neurons are psuedounipolar with one peripheral axon receiving sensory information from the extremities and a central axon projecting into the spinal cord via the DR. These centrally projecting axons form

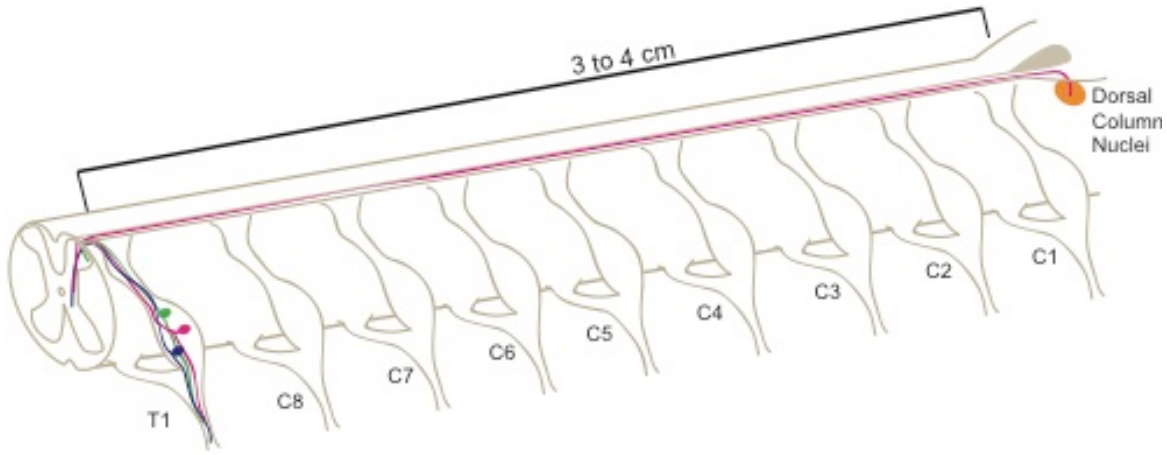

Figure 1-4: Cervical spinal cord and caudal brainstem. Sensory neurons (green, pink, blue) send axons into the spinal cord via the DR to synapse in the dorsal horn. Myelinated neurons (pink) carrying fine touch and proprioceptive information send collaterals directly to the brainstem to connect with the dorsal column nuclei (orange).

synapses with neurons nearby in the dorsal horn of the spinal cord. In addition, sensory neurons receiving fine touch and proprioceptive sense send collaterals long distances in the dorsal columns to connect monosynaptically with targets in the cuneate nucleus of the brainstem, a distance of three to four centimeters in an adult rat (Fig. 1-4).

Damage to the DR interrupts the flow of sensory information from the periphery to the spinal cord. Severed axons degenerate retrogradely toward the cell body while the axon segment separated from the cell body undergoes Wallerian degeneration (Bradbury et al. 2000). DR injury leads to significant proliferation of reactive astrocytes into the DR root and in the white matter of the spinal cord (Fraher 2000; McPhail et al. 2005). These reactive astrocytes deposit CSPGs, producing a glial scar similar to that observed in SCI (Fraher 2000). The glial response and presence of degenerating axons

recruit microglia to the site of injury. In the CNS, removal of myelin debris is limited and this debris may provide an additional barrier to regeneration (Avellino et al. 1995).

After DR injury, axons mount a weak regenerative response, hindered by components of the glial scar and the presence of myelin debris. Regenerating axons halt abruptly at the DREZ, the interface between the PNS, sheathed by Schwann cells, and CNS, myelinated with oligodendrocytes (Bradbury et al. 2000; Fraher 2000; Ramer et al. 2001). In the absence of treatment, growth cones collapse and axons remain permanently arrested at the DREZ, forming stable synapse-like structures on oligodendrocytes expressing NG2 (Ramon y Cajal 1928; Carlstedt et al. 1989; Fraher 2000; Di Maio et al. 2011).

DR crush, a model of pre-ganglionic brachial plexus injury, provides an excellent model for studying long-distance axon regeneration in the spinal cord for several reasons. First, the central projections of sensory afferents are well characterized with axons synapsing directly on local targets in the dorsal horn and distant targets in the brainstem. This allows us to distinguish a failure of axons to regenerate completely from a failure of distant regeneration. Second, DR crush reproducibly damages virtually all sensory afferents, in contrast to contusion or transection models of SCI, which affect variable subtypes of axons. When DRs from C5 to T1 are crushed, all sensory information traveling between the forelimb and spinal cord is interrupted, resulting in complete loss of forelimb sensation (Fig. 1-5). Third, the peripheral location of the DR allows for injury of these axons without affecting the architecture of the spinal cord (McPhail et al. 2005). The cavitation that can occur following direct injury to the spinal cord can provide an insurmountable barrier to regenerating axons.

Regeneration can be assessed anatomically by labeling the peripheral axons of sensory neurons with various neurotracers. These neurotracers are transported transganglionically to label the central projections in the spinal cord, allowing for direct

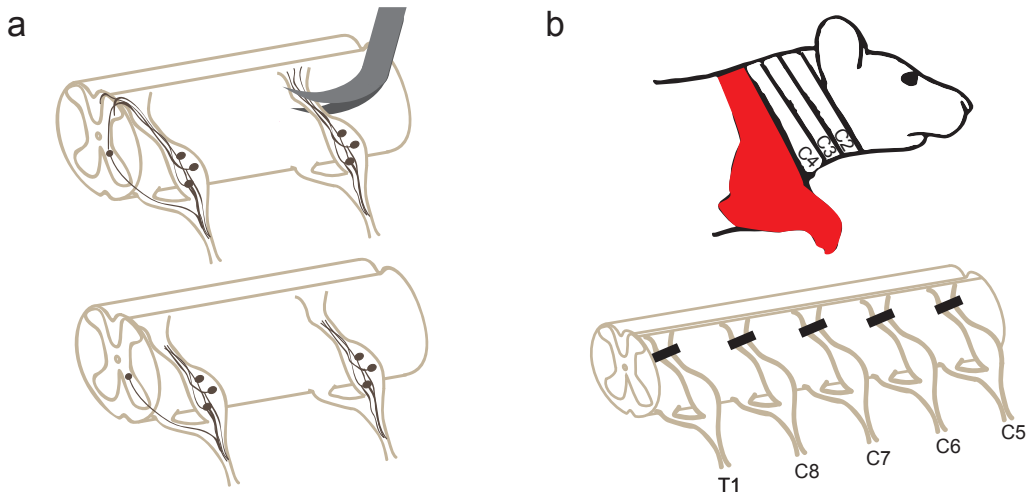

Figure 1-5: The dorsal root crush model of brachial plexus injury. (a) DR are crushed with sharp forceps strongly enough to sever all axons while leaving the epineurium of the root intact. Motor neurons exiting through the DR are not affected. (b) DR crush from cervical level 5 (C5) through thoracic level 1 (T1) results in loss of sensation to the forelimb. The red area in the upper panel depicts the region without sensation. The lower panel depicts the affected roots with black bars marking the location of the DR crush.

visualization of regenerating axons and their synaptic terminals. Restoration of functional connectivity can be evaluated using electrophysiology. Peripheral nerves can be stimulated electrically, permitting precise measurement of functional connectivity with targets in the spinal cord and brainstem. Given its ease of manipulation and the multifaceted approach for assessing the presence of axons and their functional connections, DR crush provides a particularly good model for studying regeneration of sensory axons to the brainstem and reinnervation of targets in the cuneate nucleus.

Regeneration vs. Sprouting

The terms “regeneration” and “sprouting” have been used interchangeably in the literature for decades, resulting in confusing reports of the anatomical events leading to functional recovery following SCI (Steward et al. 2003; Tuszynski and Steward 2012). For the purposes of this thesis, the term “regeneration” will refer to new growth from the cut end of a severed axon extending past the lesion site (Fig. 1-6). In contrast, the term “sprouting” will refer to new growth from uninjured axons.

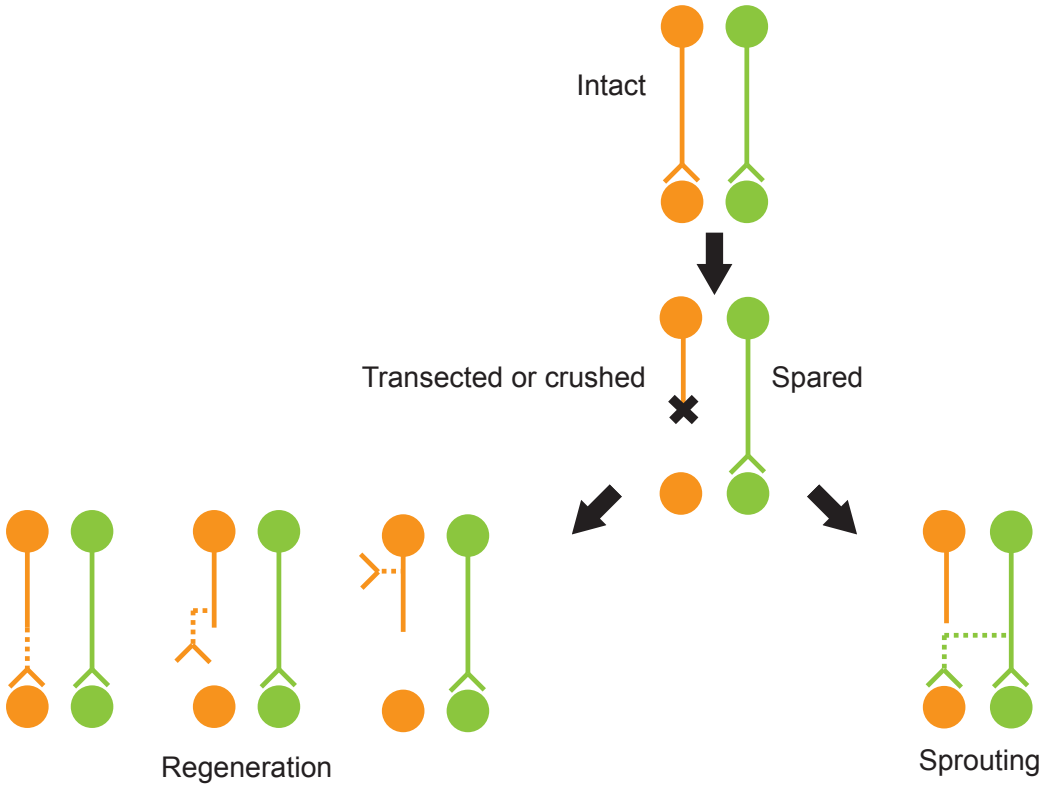

Figure 1-6: Regeneration versus sprouting. The left side of the panel shows different examples of regeneration. Regeneration can occur from the injured tip of the axon, from a region of the axon near to the injured tip, or from a region of the axon remote from the injury. Sprouting, shown on the right, occurs when damage occurs leading to compensatory growth of new connections from nearby undamaged axons.

Sprouting was first described by Liu and Chambers (1958) in experiments using a spared DR preparation where one intact DR was flanked by several cut DRs. They observed an expansion of the normal projections of the undamaged root in the denervated segments of the spinal cord (Liu and Chambers 1958). This was followed by further electrophysiological evidence that demonstrated increased extracellular potentials within the denervated section of the spinal cord 4 weeks following injury (Mendell et al. 1978). Sprouting has been widely demonstrated and further sub-classified depending on its location. Following peripheral injury, reinnervation of muscle arising from very short growth of spared terminals has been termed “terminal sprouting.” Reinnervation arising from a spared axon is termed “collateral sprouting” and has been observed at several different levels in the CNS (Tuszynski and Steward 2012).

A major concern with the DR crush paradigm is that all axons may not be severed in the crush, something we term sparing. Indeed, Di Maio et al. (2011) demonstrated that spared axons were present in many of their DR crush preparations in mice, underscoring the difficulty of transecting all axons. Sensory axons, in particular, are quite capable of undergoing collateral sprouting in the absence of any treatment (Liu and Chambers 1958; Sengelaub et al. 1997). While collateral sprouting may provide for substantial functional improvement following brachial plexus injury or SCI, it is important to be clear about the anatomical events—regeneration versus sprouting—occurring with treatment.

Tuszynski and Steward (2012) recommended guidelines to demonstrate true axonal regeneration including (1) the use of a model where regenerated axons can be definitively differentiated from spared axons, (2) demonstration that regenerating axons exhibit features consistent with new growth, (3) use of a time course demonstrating axons extend actively over time, (4) confirmation of a loss of innervation where possible, and (5) a demonstration of a lack of comparable labeling in a suitable number of controls

(Tuszynski and Steward 2012). Additional support in favor of regeneration over sprouting may come from ectopically located axons. The experiments presented in this thesis, have, to the best of our ability attempted to control for the presence of spared axons by adhering as much as possible to these guidelines.

Significance of this Thesis

In the studies described in this thesis, we assessed the extent to which systemic ARTN treatment might promote regeneration of severed sensory axons to distant targets in the brainstem after DR crush. We aimed to quantify anatomical regeneration to the brainstem using neuroanatomical tracing and the extent of functional reinnervation of the correct nuclei using electrophysiological techniques. Regeneration to the brainstem has been studied in models of SCI lesion in the dorsal columns, a few millimeters from the brainstem. While this resulted in axons reaching the brainstem nuclei, sensory axons did not reestablish functional connections using these methods, underscoring the difficulty of promoting functional regeneration to the brainstem (Alto et al. 2009). In addition, studies of long tract regeneration following dorsal column lesions often demonstrate only modest regeneration despite addition of neurotrophins or conditioning lesions (Neumann and Woolf 1999; Lu et al. 2003; Taylor et al. 2006). Axons can cross the lesion but not reach their targets. In contrast, we used a DR crush model to assess long distance regeneration, allowing us to reproducibly damage all sensory axons receiving input from the forelimb of the rat without affecting the architecture of the spinal cord. This model had a second benefit in that it allowed for easy evaluation of synaptic connections using electrophysiology.

It is critical to understand whether therapeutics promote recovery by inducing regeneration or collateral sprouting. To this end, we developed several experiments to allow us to distinguish between collateral sprouting and regeneration. First, the behavioral changes occurring after DR crush and the timing of regeneration have been well established (Wang et al. 2008; Harvey et al. 2009). We were able to assess the completeness of the crush with simple behavioral tests, allowing us to evaluate animals for the presence of spared axons and eliminate those that recovered use of the forelimb too early to be consistent with regeneration. Second, stimulation of peripheral nerves in the ipsilateral forelimb permitted clear electrophysiological evidence of functional reinnervation. The latency of the synaptic response provided insight into the caliber of regenerating axons. Additionally, cutting the DRs at the termination of the experiment further allowed us to verify that input originated from crushed roots. Lastly, because of the significant distance axons had to travel to reach the brainstem compared to local regeneration to the spinal cord, we could assess the time-dependence of regeneration to the brainstem. This provides a sensitive indication of whether axons were spared following DR crush: spared axons maintain their connections with the brainstem and, thus, recovery rapidly, while transected axons are required to regenerate new connections from the lesion site, a much slower process.

In the experiments comprising the second portion of this thesis, we determined definitively whether the ARTN co-receptor GFRα3 was present on large, myelinated neurons like those that project to the brainstem. Previous studies used immunohistochemistry or *in situ* hybridization to count the number of neurons expressing GFRα3, a technique that is semi-quantitative at best (Bennett et al. 2000; Orozco et al. 2001; Wang et al. 2008; Keast et al. 2010). In studies where more quantitative methods were used to assess expression changes with injury, expression was assessed in

lysates of the whole DRG, which consists of a heterogeneous population of myelinated and unmyelinated sensory neurons (Wang et al. 2011a).

In contrast, we developed a sorting technique where neurotracers conjugated to different fluorescent markers were used to identify myelinated and unmyelinated neurons. These neurons were subsequently separated with fluorescence-activated cell sorting (FACS). This allowed for a more quantitative assessment of GFRα3 expression in each population using the quantitative polymerase chain reaction (QPCR). Not only were we able to assess the presence or absence of the co-receptor, but also the relative expression level of the GFRα3 transcript with and without DR crush. In addition, we optimized and verified the specificity of a GFRα3 antibody in order to ascertain if changes in GFRα3 expression were conserved at the protein level. We quantified immunofluorescence pixel intensity in individual neurons to assess the quantity of protein present rather than simply counting the number of neurons above a threshold level, as was done in earlier studies.

The experiments presented in this thesis identify a new role for ARTN *in vivo*—promoting long-distance axon regeneration of myelinated sensory axons—and suggest that GFRα3 may be expressed on myelinated sensory neurons at levels adequate to promote these effects. These experiments demonstrate that adult neurons can regenerate more than three centimeters to functionally reinnervate appropriate target region in the brainstem. Recovery of function following SCI requires axon regeneration across substantial distances in the adult CNS in order to restore the flow of information from ascending and descending motor and sensory pathways. The data presented here can be applied towards the development and understanding of future therapeutics that can promote recovery following human brachial plexus and spinal cord injuries.

CHAPTER 2

Systemic ARTN Administration Promotes

Regeneration of Sensory Axons

to the Cuneate Nucleus in the Brainstem

Introduction

Spinal cord injury often results in permanent paresis and paralysis, the result, in large part, of a failure of axons to regenerate. Axons fail to regenerate in the adult spinal cord because of myelin- and injury-associated inhibitory barriers and a limited intrinsic regenerative ability (Smith et al. 2012). While there has been some success in removing extrinsic barriers and providing neurotrophic factors to promote functional regeneration over short distances (Ramer et al. 2000; Wang et al. 2008; Harvey et al. 2009), a major limitation is that severed axons need to both regenerate to and reconnect with their original targets, often centimeters away from the lesion. Studies where damaged sensory axons were induced to regenerate to the brainstem failed to show reestablishment of functional synapses (Alto et al. 2009). These findings cast doubt on whether sensory axons at brachial levels can be induced to regenerate functionally to the brainstem.

Dorsal root (DR) crush provides a useful model in which to study long-distance axon regeneration without affecting the architecture of the spinal cord. Fine touch and proprioceptive neurons with cell bodies in the DR ganglion (DRG) connect monosynaptically to neurons in the dorsal column nuclei, a distance of more than three centimeters in the spinal cord of an adult rat. These neurons can be traced using transganglionic labeling methods and are easily studied electrophysiologically, making this an ideal injury model for investigating functional regeneration from the brachial spinal cord to the brainstem.

Previous studies demonstrated that two-week systemic treatment with the neurotrophic factor artemin (ARTN) promotes topographically specific regeneration into the spinal cord one month after DR crush (Wang et al. 2008; Harvey et al. 2010). This

regeneration results in persistent recovery of simple behavioral tasks and recovery of electrophysiological function in the spinal cord. Both myelinated and unmyelinated sensory axons regenerate following ARTN treatment, suggesting that ARTN might also promote functional regeneration of myelinated sensory axons to their distant targets in the brainstem.

In this study, we report that ARTN induces functional regeneration of myelinated sensory axons over several centimeters to the brainstem. Crushed sensory axons regenerate in the dorsal columns to the dorsal column nuclei where they re-establish functional synapses. This regeneration takes several months, consistent with regeneration over the three to four centimeters from the brachial spinal cord to the brainstem.

Materials and Methods

Dorsal Root Crush Surgery. All research procedures were approved by the Institutional Animal Care and Use Committee at Tufts University School of Medicine and conformed to the National Institutes of Health guidelines. Surgery was performed aseptically using 2.5% isoflurane anesthesia. Unilateral DR crush from cervical level 5 (C5) to thoracic level 1 (T1) was performed on male Sprague-Dawley rats (200-250 g; Charles River Labs) as described previously (Wang et al. 2008; Harvey et al. 2009, 2010). Briefly, rats were anesthetized with 2.5% isoflurane and unilateral hemilaminectomy was performed under sterile conditions. A 1-mm width of the spinal cord was exposed from C5 to T2 so the DRs were visible. The dura was cut open over the exposed spinal cord so that the roots were easier to manipulate. Each DR was crushed three times for 10 seconds per

crush, midway between the DRG and the spinal cord, using a sharpened #7 Dumostar forceps; observation of a clearing in the root was required for the crush to be complete. Once surgery was completed, the dura was re-approximated, the muscles were sutured in layers, and the skin was closed using metal clips. Post-operative analgesia (5 mg/kg carprofen or 0.05 mg/kg buprenorphine) was given after surgery and for three days following. Animals were given subcutaneous injections with either 1 mg/kg ARTN104, 3 mg/kg ARTN113, or saline vehicle on a Monday-Wednesday-Friday schedule for two weeks beginning immediately after surgery as previously described (Wang 2008). In addition, the human WT ARTN104 and a variant form were tried in six animals each at concentrations of 6 mg/ml. The human ARTN, both WT and variant, was not effective at promoting regeneration in rats. Following DR crush, animals were closely monitored for persistence of sensory function indicative of spared axons. Correct paw placement and use of the forelimb ipsilateral to the DR crush in the first two weeks suggested that axons were spared in the DR crush and those animals (n=3) were excluded from the study.

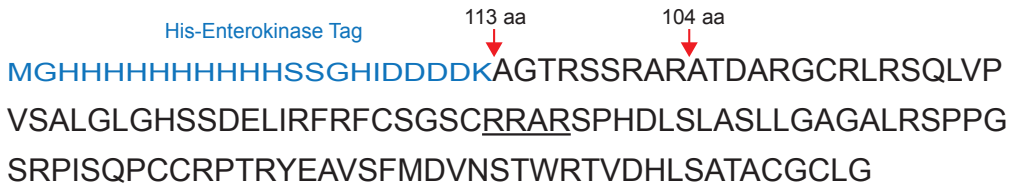

Figure 2-1: The amino acid construct of rat ARTN. The His-Enterokinase tag is shown in blue. Red arrows mark cleavage sites that produce ARTN104 and ARTN113. Underlined amino acids mark the HSPG binding site.

Preparation and purification of ARTN. ARTN samples were generously provided by Biogen Idec. The 104 amino acid and 113 amino acid versions of rat artemin were produced in E.coli from a single construct with an N-terminal his tag as previously described (Figure 2-1) (Silvian et al. 2006). The ARTN was expressed in inclusion bodies, extracted from a washed pellet with guanidine HCl, refolded, and purified prior to removal of the his tag as described. Purified ARTN was treated with endoproteinase Lys-C to generate the 113 amino acid product and with trypsin to generate the 104 amino acid version and then further purified to remove the his tag. Both proteins were purified to >95% and were low in endotoxin suitable for animal studies. By kinase receptor activation (KIRA) enzyme-linked immunosorbent assay (ELISA) the preparations were indistinguishable in their ability to promote RET phosphorylation with EC50 values of 1 nM (Figure 2-2).

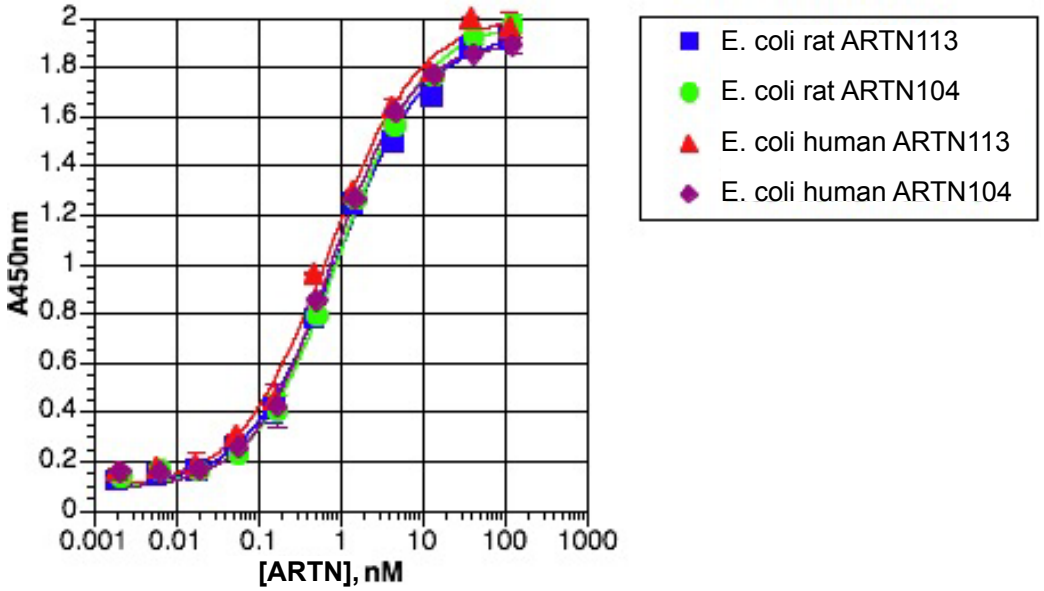

Figure-2-2: ARTN104 and ARTN113 are indistinguishable in their ability to phosphorylate RET *in vitro*. KIRA ELISA showing RET phosphorylation following treatment with human and rat ARTN variants produced in E. coli.

Neuroanatomy. For transganglionic tracing of the central projections of sensory axons, rats were anesthetized with 2.5% isofluorane, the radial nerve was exposed under sterile conditions, and 4 µl of a 1% solution of 10,000 MW mini-Ruby dextran (Life Technologies) in PBS were injected using a 10 µl Hamilton syringe. The triceps muscle was sutured, the skin was closed using metal clips and post-operative care was provided as described above. After allowing 7 to 9 days for the dye to label central projections of sensory axons, rats were perfused intracardially with 4% paraformaldehyde in PBS and the cervical spinal cord and brainstem were removed with DRGs intact. Tissue was cryoprotected in 20% sucrose in PBS and 25 µm frozen sections were cut using a cryostat. Sections were imaged at a resolution of 1024 x 1024 pixels using the 20X objective on a Leica SP2 confocal microscope running the Leica Application Suite software. 10-15 µm Z-stacks were taken using steps of 0.8 µm with 2 line averages and 4 stack averages per focal plane. The 2D average projection was used for quantification. Fixed exposure settings were used and images were adjusted for brightness using the same settings for all photographs. The number of puncta (size limited from 1-50 pixel units to exclude anything larger than an axon) in the dorsal column nuclei was quantified using ImageJ from an equally sized region of interest in all sections. Because the same axons are present in many sections through the brainstem, the number of puncta in three concurrent sections from the caudal cuneate nucleus were averaged per animal. To control for background fluorescence, sections through the brainstem in rats without fluorescent neurotracers were quantified in the same manner and this value was subtracted from the experimental values. All quantification was done by a researcher blinded to the identity and treatment of the animal

Electrophysiology. At least one hour prior to exposure of the brainstem, 1 mg/kg dexamethasone was given to prevent cerebral edema. Animals were anesthetized using 2.5% isofluorane for the duration of all terminal electrophysiology experiments and body temperature was maintained by a 37°C warming pad placed underneath the animal. Under these conditions, animals breathe on their own and evoked field potentials were stable for at least 8 hours. We observed no change in the amplitude, latency or rise time of the synaptic response evoked by stimulation of the peripheral nerves when animals were anesthetized with 2 to 3% isofluorane. The cervical spinal cord was exposed as described above and the brainstem was exposed by careful removal of the occipital bone and retraction of the C2 vertebra with a spinal clamp. The dura was removed just prior to recording. For spinal cord recordings, the spine was stabilized with a spinal clamp on T2. Median and ulnar nerves were dissected and metal hooks were wrapped around the nerves and secured in place using Kwik-Cast Silicon Elastomer (World Precision Instruments), which allowed for stable stimulation for at least 8 hours. Brainstem recordings were made using a 1x16-channel microelectrode with recording spots vertically spaced at 100 μm (NeuroNexus) from three recording sites positioned 0.6 mm caudal to the obex and 1.2 mm, 0.9 mm and 0.6 mm lateral from the midline. The shaft of the electrode was driven 1.5 mm into the brainstem so that the dorsal-most channel was positioned at the dorsal surface. Spinal cord recordings were made using the same microelectrode, positioned 0.8 mm laterally and recordings were taken from the ventral horn (1 mm ventral to the dorsal surface of the cord). The median and ulnar nerves were stimulated with square, 50 μs, 2-V pulses delivered at 5 Hz using an A-M Systems Isolated Pulse Stimulator (Model 2100). Single responses were recorded with a 16 channel amplifier (A-M Systems, Model 3600), filtered (0.3 Hz – 10 kHz) and digitized (16 bits, 20 kHz sampling rate) using a National Instruments system running custom LabVIEW software. At each recording site, 50 individual traces were averaged and

stored for analysis offline. The spinal and brainstem preparations produced stable, replicable neuronal potentials for at least 8 hours. Recordings were made in the cuneate nucleus and each segment of the ventral horn (C5-T1) on both sides in response to ipsilateral stimulation of the brachial nerves. Recordings were made first from the

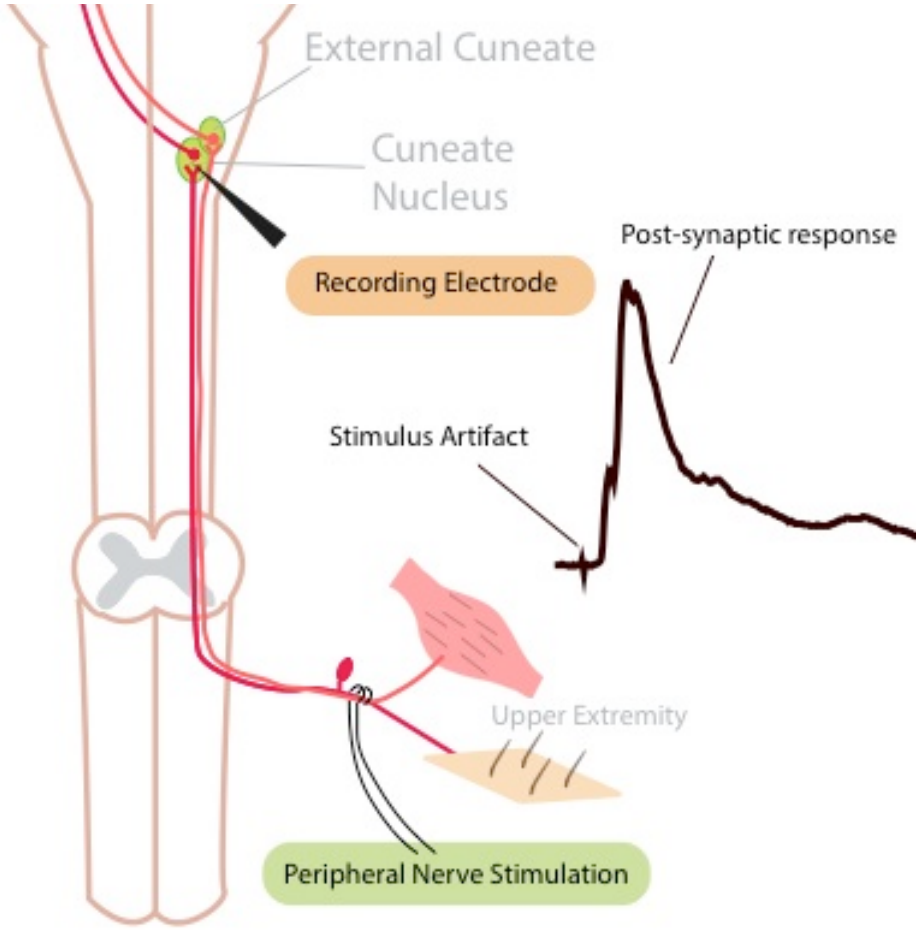

Figure 2-3: Schematic of the electrophysiological method used to record in the brainstem. Peripheral nerves in the forelimb are electrically stimulated using hook electrodes. Extracellular responses are measured in the cuneate nucleus. A representative field potential from an intact animal is shown in black. The stimulus artifact corresponds to electrical stimulation of the peripheral nerves. That is followed by a larger wave corresponding to the post-synaptic response of neurons in the cuneate nucleus.

brainstem and then the spinal cord, always starting with the side ipsilateral to the DR crush and then moving to the intact side to ensure the preparation was in good physiologic condition when regeneration was assessed. The average response from 0.5 to 6.5 ms after the stimulus was used as the physiological measure of the summed short-latency response in the cord and brainstem at each location. Data is expressed as a ratio of the synaptic response on the crushed side over the synaptic response on the intact side to account for any inter-animal variation. Latency was measured from the stimulus artifact to the start of the monosynaptic response. To verify that the observed responses were elicited by regenerated axons, brachial dorsal roots were cut at the end of each experiment. In every case, all of the responses elicited in the brainstem and spinal cord evoked by peripheral nerve stimulation disappeared. We also verified that there was no synaptic input from axons sprouting across the midline from the intact side. Stimulating the contralateral median and ulnar nerves did not evoke a synaptic response in the brainstem.

As an additional control, we performed electrophysiology on animals that were excluded from the study for suspicion of spared axons based on rapid recovery of behavior following DR crush. In the animals excluded for this reason (n=3 of 30), neuronal potentials were observed in the spinal cord and brainstem on the crushed side just 1 month after DR crush with latencies and rise times similar to those on the intact side. Thus, it is reasonable to conclude that a lack of response in the brainstem at early time points is indicative of a complete DR crush.

Statistical analysis. All statistical analyses were done with a Student's t-test or ANOVA, using Bonferroni's post-hoc correction for multiple analyses when appropriate. p-values less than 0.05 were considered significant.

Results

Crushed brachial sensory axons regenerate to the brainstem. To determine if crushed sensory axons regenerate to their distant targets in the brainstem, we performed a unilateral dorsal root (DR) crush from C5 to T1 and treated the rats with either ARTN or vehicle. Six months post-lesion, we examined brainstem sections for the presence of regenerated axons, which were labeled with fluorescent dextran injected into peripheral nerves a week earlier. With intact roots, axon terminals in the cuneate nucleus of the brainstem were robustly labeled and tightly clustered (Fig. 2-4a). On average, there were 437±74 fluorescent puncta quantified on the intact side following injections of the radial nerve. A DR crush bisects all brachial sensory axons traveling to the brainstem, as demonstrated by the large reduction of fluorescent puncta in the cuneate nucleus ipsilateral to the lesion in vehicle-treated animals (Fig. 2-4b). Virtually no labeled axons were present in the spinal cord of vehicle-treated animals at any time point examined (1.5, 3 and 6 months), consistent with the fact that severed sensory axons stop regenerating abruptly at the DR entry zone, the transitional zone between the peripheral nervous system (PNS) and the central nervous system (CNS) (Fraher 2000; Harvey et al. 2010). In animals treated with systemic ARTN104, peripherally labeled axons were present in the cuneate nucleus ipsilateral to the DR crush (Fig. 2-4c), confirming the result from Wang et al. (2008). These regenerating terminals were located in approximately the same relative location in the brainstem as intact axons, suggesting that ARTN can promote directed regeneration even over relatively long distances, although the terminals within the brainstem appear less tightly clustered (Fig. 2-4c). On average, 124±51 fluorescent puncta were quantified in the cuneate nucleus

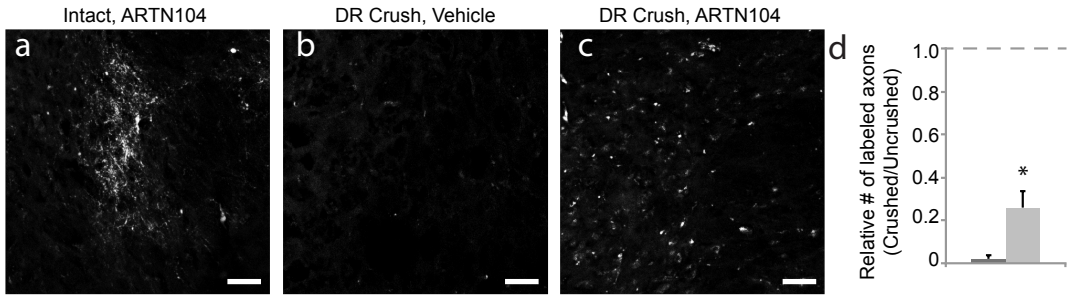

Figure 2-4: Systemic ARTN104 administration promotes axonal regeneration to the dorsal column nuclei in the brainstem within 6 months. (a-c) Representative cross-sections through the cuneate nucleus one week after radial nerve injection with mini-Ruby dextran. On the unlesioned side in an ARTN104-treated animal, axons and terminals are robustly labeled in the cuneate nucleus (a). With vehicle treatment, virtually no axons are present in the cuneate nucleus, indicating that axons were unlikely to be spared in the original crush surgery (b). Labeled axons are present in roughly the correct location in the cuneate nucleus on the crushed side with ARTN104 treatment, although the distribution of axons is more diffuse (c). (d) Quantification of the number of puncta counted in vehicle (n=5) and ARTN104 (n=8) treated animals, expressed as a ratio of the number of fluorescent puncta in the cuneate nucleus ipsilateral to the crush over the number of fluorescent puncta in the cuneate nucleus on the intact side. There are significantly more axons reaching the brainstem with ARTN104-treatment than with vehicle treatment. The dashed line represents complete recovery. Error bars, s.e.m. *$p<0.05$.

ipsilateral to the DR crush following treatment with ARTN104, representing a significant improvement over vehicle-treatment and a return to approximately 25% of the expected number of labeled axons based on the intact side (Fig. 2-4d; $p=0.04$). The small number of fluorescent puncta in vehicle-treated animals ipsilateral to the crush is no greater than

the background fluorescence observed in unlabeled controls. These data suggest that systemic ARTN treatment promotes regeneration of severed brachial sensory axons to the brainstem within six months following DR crush.

Artemin restores synaptic inputs in the brainstem. We assessed recovery of synaptic function in the brainstem by making extracellular recordings from the cuneate nucleus in response to stimulation of the median and ulnar nerves. Most responses mediated by intact sensory axons had latencies of 0.9 to 1.3 ms and synaptic responses, quantified as the average response from 0.5 to 6.5 ms, of 250-400 μV (Fig. 2-5a). These potentials represent excitatory post-synaptic potentials (EPSPs) in brainstem neurons evoked by activity in large-caliber myelinated sensory axons. The synaptic response was similar on the unlesioned side in ARTN104- and vehicle-treated animals. The brainstem EPSPs were abolished by DR crush with vehicle treatment in all animals tested (Fig. 2-5a,c). In contrast, all of the animals treated with systemic ARTN104 showed recovery of synaptic function six months after DR crush (Fig. 2-5a). The ratio of the synaptic responses on the crushed side over the uncrushed side was 0.23 ± 0.02 (n=8), representing significantly more synaptic connectivity than the same ratio in vehicle-treated animals (0.01 ± 0.006, n=5, $p=1.3 \times 10^{-5}$). Similar to previous findings in the spinal cord (Wang et al. 2008; Harvey et al. 2009), EPSP latencies and rise times evoked by regenerating axons were longer than those evoked by unlesioned axons (Fig 2-5a). Latencies to the onset of synaptic activity in ARTN104-treated animals (n=8) were significantly longer on the lesioned side (2.2 ± 0.2 ms) compared to those on the unlesioned side in the same animals (1.1 ± 0.1 ms; n=8; $p=9.4 \times 10^{-7}$), consistent with the smaller diameter of regenerating axons (Di Maio et al. 2011). EPSPs recorded in the spinal cord at six months post-DR crush (Fig. 2-5b,c) were similar to those reported by Wang et al. (2008). To verify that the EPSPs originated from the injured DRs, DRs from

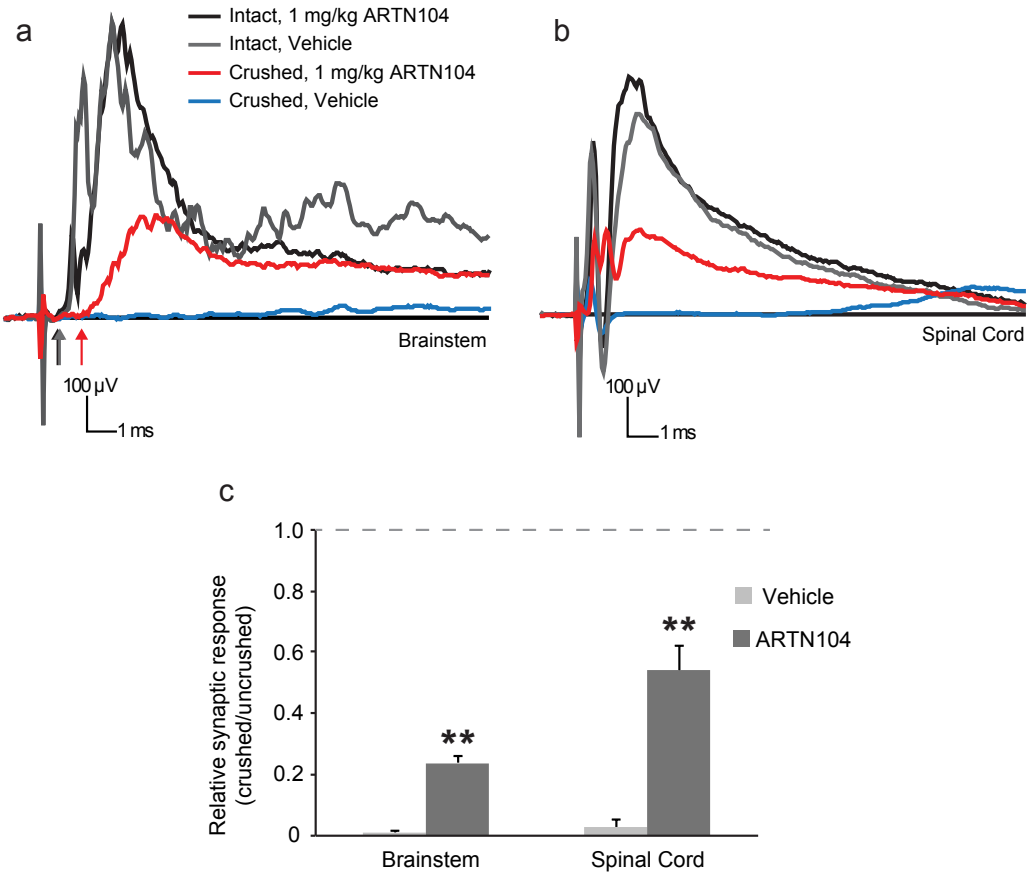

Figure 2-5: ARTN104 treatment restores synaptic responses from regenerated sensory afferent fibers in brainstem neurons. (a,b) Representative traces of field potentials recorded in the brainstem (a) and spinal cord (b) in response to electrical stimulation of median and ulnar nerves in the ipsilateral forelimb 6 months after DR crush. The amplitudes and rise times on the unlesioned side in both vehicle-treated (gray) and ARTN-treated (black) rats were similar. In ARTN-treated rats, there was substantial recovery of synaptic inputs (red) in the brainstem and spinal cord. In contrast, there was no recovery of function after DR crush in vehicle-treated rats (blue), even in the spinal cord. (c) Quantification of the synaptic response evoked by stimulation of median and ulnar nerves in the ipsilateral forelimb recorded in all animals and normalized to the intact side of the same animal (n=8 with ARTN104 treatment; n=5 with vehicle treatment). Dashed line represents complete recovery. Error bars, s.e.m. **p<0.001.

C5-T1 were cut at the end of each electrophysiology session. This completely abolished the EPSPs in the brainstem and spinal cord, indicating that the previously crushed axons mediated the observed synaptic response. These data indicate that, following DR crush and systemic ARTN treatment, regenerating brachial sensory axons reestablish functional synapses with targets in the cuneate nucleus—three to four centimeters from the lesion site—when measured at six months following the crush surgery.

Restoration of synaptic input requires long recovery times. Relatively short recovery times (approximately one month) are required for local regeneration into the spinal cord and restoration of synaptic input in the dorsal horn (Wang et al. 2008; Harvey et al. 2009). In contrast, regeneration to the brainstem should require significantly more time because of the greater distance axons must regenerate from the lesion site. To verify that the synaptic connections we observed in the brainstem following DR crush did not originate from axons spared in the original crush surgery, we assessed the synaptic response in the brainstem and spinal cord in animals that were allowed to recover for 1.5, 3 or 6 months after DR crush. Our initial experiments were carried out in animals treated with ARTN104, a truncated version of ARTN with nine N-terminal amino acids removed to reduce binding to heparin sulfate proteoglycans (Silvian et al. 2006). Because of constraints on our supply of ARTN104, remaining experiments were conducted using a slightly longer form of ARTN containing 113 amino acids, ARTN113. This longer form was previously used in the Wang et al. (2008) studies.

We first assessed if ARTN113, like ARTN104, could restore synaptic input to the brainstem by recording brainstem and spinal cord EPSPs evoked by stimulation of the median and ulnar nerves. With ARTN113 treatment, 50% of animals (3 of 6) had synaptic function restored in the spinal cord and brainstem six months post-lesion, in contrast to all animals treated with ARTN104. In the 3 animals where synaptic input was

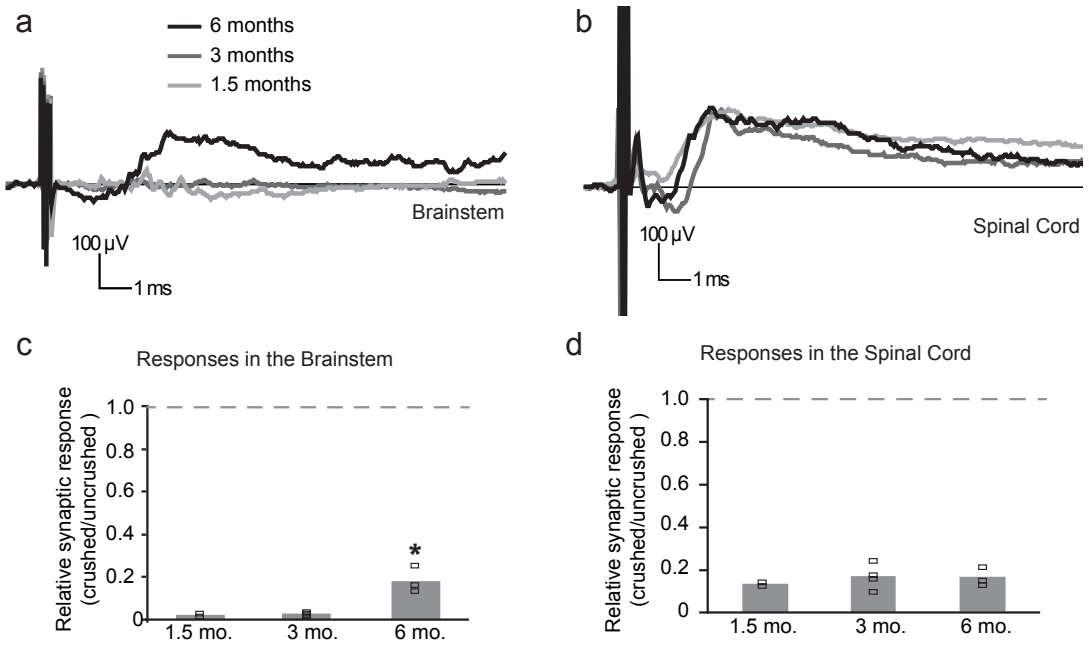

Figure 2-6: Restoration of synaptic function to the brainstem requires long recovery times. (a) Representative field potentials evoked by stimulation of the ipsilateral median and ulnar nerves in the brainstem on the crushed side of ARTN113-treated rats. A synaptic response is present after 6-month recovery (black). There are no synaptic responses after 1.5 or 3 months (light and dark gray, respectively). (b) Representative field potentials in the spinal cord on the crushed side from the same ARTN-treated rats. Similar synaptic responses are present in animals that have recovered for 1.5, 3, or 6 months. The lack of response in the brainstem at 1.5 and 3 months does not indicate failure of ARTN113. (c) Quantification of the synaptic responses in the brainstem normalized to the intact side (1.5 mo., n=2; 3 mo., n=4; 6 mo., n=3), excluding five animals with no regeneration (see Results). By 6-months, ARTN113 promotes significant recovery of synaptic function in the brainstem. No synaptic input is observed in the brainstem at 1.5 or 3 months post-crush. (d) Quantification of the synaptic responses in the spinal cord in the same ARTN-treated animals. Squares show the synaptic response for each animal; bars show average synaptic responses. Dashed line represents complete recovery. *$p<0.05$.

reestablished, EPSP shape, size and latency were similar to the results with ARTN104 (Fig. 2-5 and 2-6). We next verified if restoration of synaptic input to the brainstem did indeed require longer recovery times by examining the recovery of sensory input at 1.5 or 3 months. In animals that had recovered for these shorter time periods, ARTN113 promoted restoration of synaptic connections in the spinal cord in only 6 of 8 animals. In those animals where ARTN113 restored synaptic connectivity in the spinal cord, the synaptic responses recorded in the ventral horn were similar in shape, size and latency for all three recovery times (Fig. 2-6b, d). In contrast, there was no synaptic response in the brainstem on the lesioned side at 1.5 and 3 months post-DR crush in the same animals (Fig. 2-6a). However, by 6 months post-lesion, synaptic function was reestablished in the brainstem of these rats to approximately 18% of normal (Fig.2-6a,c; ANOVA; p=.002). These data indicate that restoration of synaptic function in the brainstem takes significantly longer than restoration of synaptic function in the spinal cord, consistent with the much greater distance axons must regenerate to reach the brainstem. Because spared axons recovery rapidly, the lack of response at 1.5 and 3 mo. suggest that axons are unlikely to be spared following the crush injury. In the few animals excluded from the study because of too rapid behavioral recovery, EPSP latencies and rise times were comparable to those on the uninjured side after just 1.5 months (data not shown).

To further verify that long-distance regeneration is time-dependent, we counted peripherally labeled sensory terminals in the dorsal column nuclei of ARTN113-treated rats that had recovered for 1.5, 3 and 6 months post-crush and had synaptic recovery in the spinal cord. No fluorescent puncta were observed above background in the cuneate nucleus ipsilateral to DR crush at 1.5 (n=2) or 3 months (n=3; Fig. 2-7), despite numerous labeled sensory axons in the dorsal horn of the spinal cord at brachial levels (data not shown). In contrast, numerous fluorescent puncta (188±70) were present in the

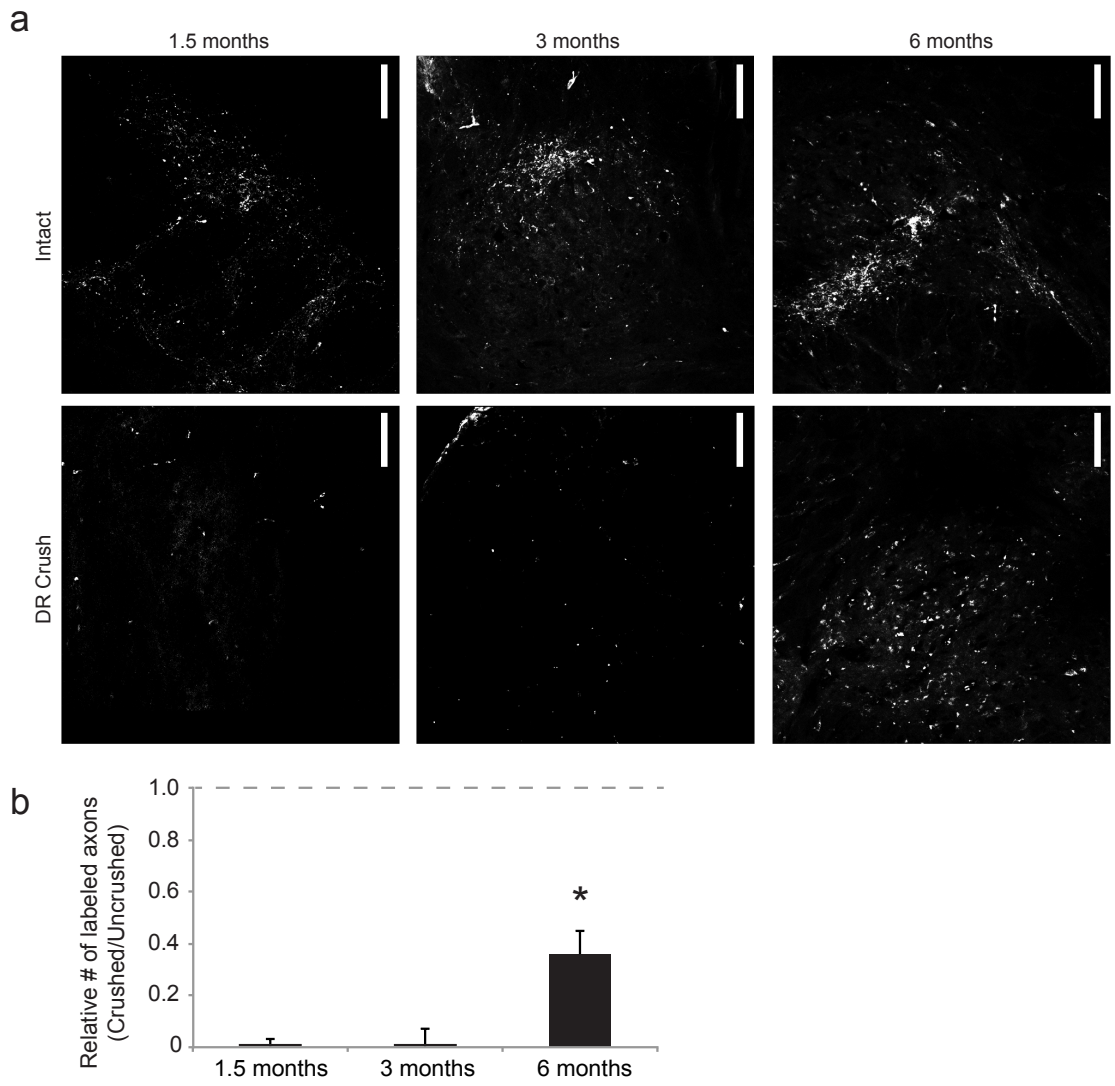

Figure 2-7: Regenerating sensory axons are present in the brainstem of ARTN-treated rats after 6-month recovery. (a) Representative sections through the cuneate nucleus in ARTN113-treated rats 1.5, 3 and 6 months post-crush. On the unlesioned side, axons and terminals are robustly labeled in the cuneate nucleus. At 1.5 and 3 months, no axons are present ipsilateral to the crush, similar to animals with vehicle-treatment (see Fig. 1). By 6 months, numerous puncta are present in the cuneate nucleus ipsilateral to the crush in a diffuse pattern similar to that observed with ARTN104 treatment. (b) Quantification of fluorescent puncta, expressed as the ratio of puncta ipsilateral to the crush over the number on the intact side (1.5 mo., n=2; 3 mo., n=4; 6 mo., n=3). There is significant regeneration to the brainstem by 6 months. Error bars, s.e.m. *p<0.05.

cuneate nucleus of ARTN113-treated animals 6 months post-crush (n=3), a significant improvement when compared to the earlier time-points (Fig. 2-7, ANOVA, p=0.04). In animals with functional regeneration, both ARTN113 and ARTN104 resulted in the recovery of approximately 30% of the normal number of labeled terminals ipsilateral to the crush (Fig. 2-4b; 2-7b). These observations provide strong evidence that virtually no sensory axons are spared following DR crush.

Discussion

Long distance regeneration, often of several centimeters, is required for restoration of function following spinal cord or brachial plexus injury. To date, long distance regeneration in the spinal cord has been limited to several millimeters; in many cases, functional connectivity is not re-established even when axons can regenerate to distant targets. Systemic ARTN treatment promotes the regeneration of crushed sensory axons from the brachial spinal cord to the cuneate nucleus in the brainstem, a distance greater than three centimeters in the adult rat CNS. This regeneration results in the restoration of substantial synaptic connectivity with neurons in the brainstem six months after DR crush (Fig. 2-5). While we could find no behavioral tests to investigate conscious proprioceptive and mechanoreceptive sensation, simple reflexive behaviors are markedly improved with only a 20% restoration of synaptic function in the spinal cord (Wang et al., 2008), suggesting that a 25% restoration of synaptic connectivity in the brainstem might also result in significant behavioral improvement in tasks requiring conscious fine touch and proprioceptive sensation. Return of axons to the brainstem and recovery of synaptic connectivity are time-dependent phenomena. Animals that recover

less than three months do not have any regenerating axons reaching the brainstem (Fig. 2-6, 2-7) despite considerable functional regeneration to the brachial spinal cord at these time points.

One concern about the DR crush model of spinal injury is that axons may be spared in the original crush (Di Maio et al. 2011). Although we never saw axons or EPSPs in the spinal cords of vehicle-treated animals (Fig. 2-4, 2-5), ARTN might promote recovery of damaged sensory axons rather than promoting regeneration of severed axons. Several observations indicate regeneration rather than recovery of spared axons. First, all animals underwent rigorous behavioral testing shortly after crush surgery, and the few animals that recovered the use of their ipsilateral forelimb in the first two weeks after DR crush were excluded from the study. Second, dextran-labeled axons on the injured side were not distributed in the same precise pattern as on the intact side (Fig. 2-4). Third, the latency to the onset of synaptic activity was twice as long in post-synaptic neurons receiving input from crushed axons compared to those receiving input from uninjured axons (Fig. 2-5a), consistent with the smaller caliber of regenerated axons (Wang et al. 2008; Di Maio et al. 2011). Lastly, the fact that axons reappeared and synaptic transmission was restored in the brainstem only over a period of several months (Fig. 2-6, 2-7) provides additional evidence that this recovery was not due to axons that were spared in the original injury. Spared axons recover over the course of days (Di Maio et al. 2011), not months. The most parsimonious explanation for the substantial time requirement before labeled axons appear in the brainstem is that axons regenerated *de novo* to reach these targets more than three centimeters away from the site of injury. These data suggest that ARTN treatment promotes functional regeneration of axons to the brainstem, although we cannot completely rule out a contribution from spared axons.

Remarkably, ARTN promoted functional reinnervation of the correct target areas in the brainstem by severed sensory axons—more than three centimeters away—without additional guidance molecules. Other studies have relied on gradients of neurotrophic factors to guide axons to correct brainstem regions, a technique that, to date, has not resulted in functional connectivity and could just as easily lead axons astray if gradient placement is incorrect (Alto et al. 2009; Bonner et al. 2011). Finding therapeutics that encourage proper guidance and synaptic specificity is paramount to the goal of long-distance regeneration. Many studies attempting to promote long-distance regeneration have cited misguidance as a key limitation (Luo et al. 2013; Pernet et al. 2013). With ARTN treatment, regeneration is topographically specific in the spinal cord, with severed sensory axons reinnervating the correct regions of the dorsal horn (Harvey et al. 2010). Similarly, the results of the present study demonstrate that regenerating axons grow back to the correct general area in the brainstem, suggesting that some guidance cues present during development are likely to persist in the adult CNS. While targeting in this case was not perfect, we hypothesize that ARTN treatment promotes regeneration over long distances, in part, because it stimulates growth in a manner allowing axons to sense these guidance cues. There are two potential reasons that ARTN promotes regeneration in a targeted fashion whereas other therapeutics fail to do so. First, ARTN treatment is administered systemically. Regeneration in the spinal cord is often promoted by administering neurotrophic factors intrathecally or into the spinal cord directly (Zhang et al. 1998a; Ramer et al. 2000; Tang et al. 2007a). Many trophic factors have chemoattractive properties of their own that may overwhelm guidance cues remaining in the adult CNS. Second, ARTN is delivered only for a short time. Six subcutaneous injections over the course of 12 days promoted persistent and continued axon growth. Brief trophic support may activate intrinsic growth pathways, inducing axonal growth until targets are reached. In contrast, viral vectors have been used to

deliver prolonged trophic support, a technique that promotes axon growth but not specificity (Tang et al. 2004, 2007a; Pernet et al. 2013). Perhaps the temporal pattern of trophic support is more important than continuous activation of growth pathways. It is tempting to speculate that two-week ARTN treatment is sufficient to initiate regeneration and activate intrinsic growth pathways. Future experiments are required to ascertain which intrinsic pathways are being activated with ARTN treatment and to understand how ARTN results in a sustained regenerative response.

In summary, systemic ARTN treatment promotes targeted regeneration of adult sensory axons to the brainstem, a distance of more than three centimeters. Regenerating sensory axons reestablish synaptic connectivity with neurons in the cuneate nucleus, suggesting that guidance cues persist in the adult CNS, and adult neurons retain some intrinsic ability to follow these cues to appropriate target areas. To the best of our knowledge, this is the first study to demonstrate centimeters of axon regeneration resulting in functional reinnervation of a correct brainstem target in the absence of external axonal guidance cues. Understanding the intrinsic pathways activated by ARTN can provide insight into new therapeutics to promote targeted axon regeneration in the CNS.

CHAPTER 3

The Artemin Co-Receptor GFRα3

is Expressed on Large, Myelinated Neurons

Introduction

Artemin (ARTN) is a member of the Glial-Derived Neurotrophic Factor (GDNF) family of ligands (GFLs). GFLs have been shown to promote survival, proliferation and differentiation of several different central and peripheral neurons (Baloh et al. 1998b; Airaksinen and Saarma 2002; Paveliev et al. 2004; Paratcha and Ledda 2008). In particular, ARTN has been shown to induce topographically specific regeneration of severed sensory axons *in vivo* (Wang et al. 2008; Harvey et al. 2010). In addition to its regenerative functions, ARTN is in phase 2 trials to treat neuropathic pain. Systemic treatment with ARTN ameliorates thermal and tactile hypersensitivity in animal models of neuropathy (Gardell et al. 2003; Wang et al. 2013b). Given its potential therapeutic value, a precise understanding of the expression pattern of its receptor is essential.

The major mechanism of GFL signaling is through a unique multicomponent receptor composed of a non-signaling GPI-linked co-receptor GFRα and the RET tyrosine kinase (Baloh et al. 1998b, 2000; Airaksinen and Saarma 2002). Each GFL has a preferred GFRα subunit that confers specificity to signaling through RET: GDNF binds to GFRα1, NRTN binds to GFRα2, ARTN binds to GFRα3, and PSPN binds to GFRα4 (Baloh et al. 1997, 1998b; Jing et al. 1997; Klein et al. 1997). Receptor activation requires the initial binding of ARTN to GFRα3 to clamp the ligand at the cell surface, followed by recruitment of two RET molecules and an additional GFRα3 to form the active signaling complex ARTN:$(GFR\alpha3)_2$:$(RET)_2$ (Paratcha and Ibáñez 2002; Schlee et al. 2006). GFRα3 is also required for RET-independent ARTN-mediated signaling through the neural cell adhesion molecule (NCAM) (Paratcha et al. 2003; Nielsen et al. 2009).

Current immunohistochemical evidence suggests that GFRα3 expression in adults is limited primarily to small, nociceptive sensory neurons with very few large, myelinated sensory neurons expressing the protein (Bennett et al. 2000; Orozco et al. 2001; Keast et al. 2010). Despite the apparent limited distribution of the GFRα3 subunit, ARTN treatment promotes axon regeneration in all classes of DRG neurons following DR crush (Wang et al. 2008; Harvey et al. 2010). The mechanism by which ARTN promotes regeneration of large as well as small axons remains unclear.

Given our experiments demonstrating that myelinated sensory axons regenerate to the brainstem in response to ARTN treatment, we required a sensitive method to quantitatively assess whether GFRα3 was expressed on these neurons. We developed a technique to physically separate myelinated and unmyelinated DRG neurons using fluorescence-activated cell sorting (FACS). We then investigated if myelinated neurons expressed *GFRα3* using quantitative PCR (QPCR). In contrast to earlier immunohistochemical studies, these experiments demonstrate that *GFRα3* is expressed in myelinated sensory neurons at levels comparable to expression in unmyelinated sensory neurons, providing a basis for long-distance regeneration discussed in this thesis. We further investigated whether GFRα3 expression changes in response to DR crush injury. While other studies have demonstrated injury-related increases in ARTN expression following peripheral nerve injury (Bennett et al. 2000; Keast et al. 2010), we observed a down-regulation of the receptor at both the transcript and protein level in all DRG neurons, suggesting that GFRα3 expression is regulated similarly in both large and small diameter neurons and that central and peripheral injury affect GFRα3 levels oppositely.

Materials and Methods

Immunohistochemistry. DRGs were fixed in 4% paraformaldehyde and cryoprotected in 20% sucrose solution in PBS. Cryostat sections (25 μm) were mounted on SuperfrostPlus (VWR) glass slides. Slides were washed in PBS and then incubated for one hour in blocking solution (2% normal horse serum, 0.2% Triton X-100 in PBS). Slides were incubated in primary antibodies diluted in blocking solution at 4°C for 18 hours. Goat anti-GFRα3 (1:400, R&D Biosystems), goat anti-GFRα1 (1:400, R&D Biosystems), rabbit anti-NeuN (1:200; Abcam), mouse anti-NF200 (1:1000, Sigma Aldrich), and mouse anti-CGRP (1:1000, Sigma-Aldrich) were used. Binding of primary antibodies was visualized with chicken anti-goat, donkey anti-rabbit, or rabbit anti-mouse secondary antibodies conjugated to AlexaFluor 488 or AlexaFluor 568 (Life Technologies). Slides were coverslipped using Fluoromount and images (1024 x1024 pixels) were captured using the 20X objective of the Leica TCS SP2 confocal microscope running the Leica Application Suite software. Fixed exposure settings were used. 10-15 μm Z-stacks were taken using a step size of 0.5 μm and the 2D projection average was used for quantification as described above. Images were adjusted for brightness, using the same settings for all sections.

We had some concern that the goat anti-GFRα3 antibody might be binding to GFRα1, since it is expressed on large neurons. R&D verified that there was little cross-reactivity using a direct ELISA to measure binding of the GFRα3 antibody to recombinant rat GFRα1 protein and saw that there was less than 2% cross-reactivity in their assay, no more than observed with an unrelated protein. I further verified the specificity by staining consecutive cross-sections through the brainstem with the GFRα1 and GFRα3 antibodies since this is a region where nervous tissue widely expresses

GFRα1 but not GFRα3. For additional verification of the specificity of the GFRα3 antibody, DRG sections from two GFRα3$^{-/-}$ mice and two heterozygous littermate controls (generously provided by the lab of H. Enomoto) were stained with the antibodies to GFRα3 and NeuN using the same protocol described above. Complete genetic deletion was accomplished by inserting the *tau-LacZ* reporter gene into the first coding exon of the *GFRα3* gene by homologous recombination (Honma et al. 2002).

The number of cells positive for a given antibody or neurotracer were quantified by a researcher blinded to the identity of the samples. The threshold feature of ImageJ was used to identify positive cells, using the same settings in all sections quantified. Cells at the periphery of the image were excluded. Numbers are expressed as the proportion of CTB^{+} or WGA^{+} cells expressing CGRP—to identify a subset of unmyelinated neurons—or NF200—to identify myelinated neurons. Cell size was measured using Image J on the same thresholded images, size limiting to 200 pixel units in order to avoid counting labeled axons or partial cells. The automated cell counts were verified by eye for each section.

To quantify the changes in GFRα3 protein expression in DRG neurons two days and twelve days following crush injury, the mean pixel intensity of NeuN positive cells larger from 0-255 was measured using ImageJ. At least 250 cells were counted from brachial DRGs from 3 different animals with unilateral DR crush, excluding cells at the periphery of the image. Quantification was done by a researcher blinded to the identity of the samples. Boxplots with Tukey-style whiskers and widths proportional to the square root of the sample size were used to depict changes is threshold for all cells studied (Krzywinski and Altman 2014). Outliers (more than 1.5 times the interquartile range from the median) were plotted individually.

Fluorescence-Activated Cell Sorting (FACS) and quantification of GFRα3 mRNA levels. To label different populations of DRG neurons, we took advantage of neurotracers with different binding properties. Cholera toxin b (CTB) labels predominantly large, myelinated neurons and wheat germ agglutinin (WGA) labels predominantly small, unmyelinated neurons (ref). A mixture of CTB conjugated to Alexa Fluor 488 (CTB-488; Life Technologies) and WGA conjugated to Alexa Fluor 647 (WGA-647; Life Technologies) was injected into peripheral brachial nerves two days before the DRGs were harvested. Briefly, the median, ulnar and radial nerves were exposed in anesthetized Sprague-Dawley rats (200-250 g; Charles River) under aseptic conditions and 1 µl of 2% CTB-488 and 2.5% WGA-647 in PBS were injected into each nerve using a Hamilton syringe. The muscle and skin were then sutured and post-operative care was provided as described above.

Cultures of dissociated sensory neurons were made using a protocol modified from Malin et al. (2007). In brief, papain and collagenase/dispase enzyme solutions were made as previously described (Malin et al. 2007). For each FACS experiment, brachial DRGs were combined from 12 animals that underwent nerve injection with WGA-647 and CTB-488 and unilateral DR crush two days prior to provide sufficient material for analysis. Animals were perfused with Hank's Balanced Salt Solution without Ca^{2+}/Mg^{2+} (HBSS) and DRGs were removed and placed in HBSS supplemented with 0.01% ascorbic acid on ice, keeping the DRG's from crushed and intact sides separate. DRGs were incubated for 30 minutes, first in papain solution and then in collagenase/dispase. Following enzyme treatment, DRGs were triturated in F-12 media supplemented with 10% fetal bovine serum, 1% penicillin/strepavidin, and 0.01% ascorbic acid. Cells were kept on ice for at least 30 minutes prior to sorting to promote survival. Immediately before sorting, the samples were forced through a 40 µl Flowmi cell strainer (Scienceware) to ensure a suspension of single cells. CTB-488^{+} and WGA-647^{+} cells

were collected in separate tubes containing media supplemented with ascorbic acid using a Beckman Coulter Moflo Legacy Cell sorter. FACs trials were done in triplicate.

cDNA was made from starting material consisting of 5,000 cells suspended in 2 µl using the SuperScript III CellsDirect cDNA synthesis kit (Life Technologies). Cells were lysed and treated with DNase to digest genomic DNA. First strand cDNA synthesis was completed using a mixture of Oligo$(dT)_{20}$ (Life Technologies) and random primers (Life Technologies). Real-Time RT-PCR was performed to determine the extent of expression of *GFRα3* in sensory neurons both with and without prior DR crush. QPCR with equivalent starting material was done using a SYBR green Master Mix (Applied Biosystems) and an MX3000P real-time thermocycler (Agilent) controlled by MXPro QPCR software. Primers were designed using IDT's PrimerQuest software (Table 1). All samples were run in triplicate and every amplification run included reactions run without template as negative controls. Threshold cycle (C_t) values were recorded as a measure of initial template concentration. Relative-fold changes were calculated using the ΔΔCt method with the Pfaffl correction using GAPDH and HPRT as reference genes (Pfaffl 2001). The fold-difference ratios using GAPDH and HPRT were then averaged to get the final value shown in Figure 3-4.

Gene	Forward Primer (5'-3')	Tm (°C)	Reverse Primer (5'-3')	Tm (°C)
GFRα3	CCTTCTGAATGGAAGGTGAAGA	54.4	TGGAGACAGTGCTAGGAGTTA	54.7
GAPDH	CCCTTCATTGACCTCAACTACA	54.4	GATGACCAGCTTCCCATTCT	54.6
HPRT	GACCTCTCGAAGTGTTGGATAC	54.7	TCAAATCCCTGAAGTGCTCAT	54.1

Table 3-1: Primers (sequences and melting temperatures) used for QPCR assays

Statistical analysis. All statistical analyses were done with a Student's t-test or ANOVA, using Bonferroni's post-hoc correction for multiple analyses when appropriate. p-values less than 0.05 were considered significant.

Results

GFRα3 is present in both myelinated and unmyelinated sensory neurons. Earlier immunohistochemical studies suggested that GFRα3 is present predominantly on small, unmyelinated sensory neurons with limited to no expression in large, myelinated neurons (Bennett et al. 2000; Orozco et al. 2001; Keast et al. 2010). Nevertheless, myelinated fibers regenerate well with ARTN treatment, suggesting that GFRα3 may be more widely expressed in large, myelinated sensory neurons than previously reported. To assess GFRα3 expression in large neurons, we stained sections of adult DRGs with antibodies for GFRα3, the neurofilament heavy chain (NF200) to identify large sensory neurons, and calcitonin gene related peptide (CGRP) to identify a subpopulation of small sensory neurons (Fig. 3-1a,b). As expected, numerous CGRP+/GFRα3+ neurons were observed (Fig. 3-1a). Notably, many NF200+/GFRα3+ neurons were observed (Fig. 3-1b), suggesting that the co-receptor is also present in large diameter neurons. Because our results differed from previous reports, we were concerned that the commercially available GFRα3 antibody that we used might bind nonspecifically.

To verify that our GFRα3 antibody distinguished between GFRα1 and GFRα3, we immunolabeled tissue in the brainstem. Although GFRα3 is widely expressed in neurons of the PNS, few areas in the CNS express GFRα3. In particular, neurons in the external cuneate nucleus and fibers in the caudal spinal trigeminal tract (Csp5) are the only cells in the medulla that express GFRα3 whereas many brainstem regions express

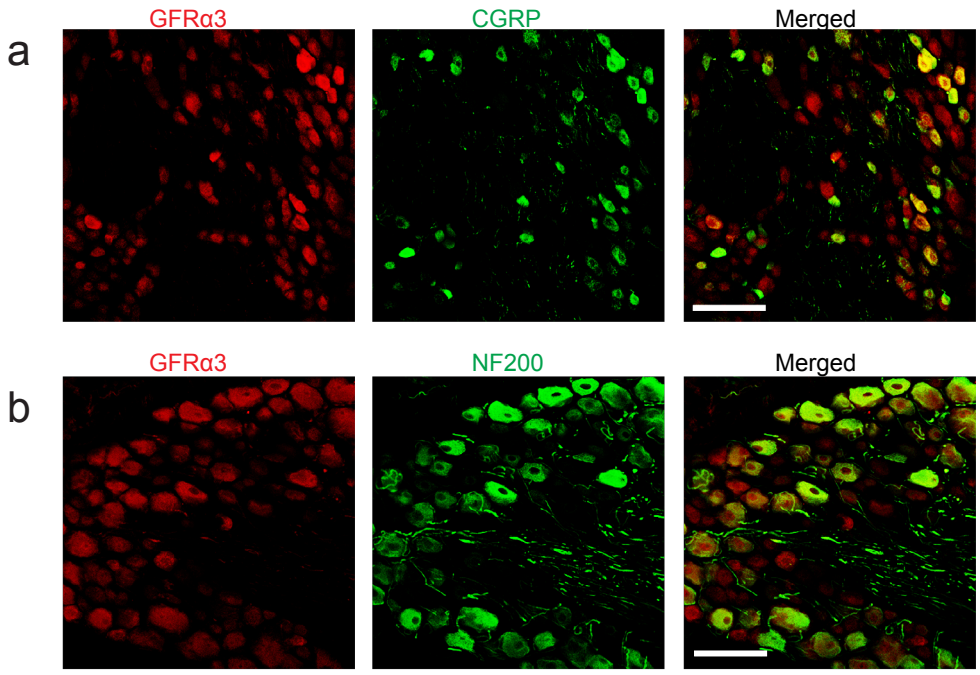

Figure 3-1: GFRα3 is present in both large and small sensory neurons in the DRG. (a) Representative DRG sections stained with antibodies to GFRα3 (red) and CGRP (green). (b) Representative DRG sections stained with antibodies to GFRα3 (red) and NF200 (green). Many GFRα3^{+} cells co-label with both NF200 and CGRP indicating that GFRα3 is likely to be expressed on both small, nociceptive neurons and large, myelinated neurons. Bars, 100 μm.

GFRα1 (Quartu et al. 2007). The antibodies for GFRα1 and GFRα3 labeled distinct areas in the brainstem. The GFRα1 antibody labeled cells in many areas of the medulla (Fig. 3-2a) but the GFRα3 antibody only labeled fibers in Csp5 and a few cells in the external cuneate nucleus (Fig. 3-2b), demonstrating that this GFRα3 antibody does not bind to GFRα1. These results suggest that non-specific binding to GFRα1 is not responsible for the immunolabeling of large sensory neurons. To further verify the specificity of GFRα3 immunolabeling, we immunostained DRG tissue from mice with a genetic deletion of GFRα3 and their heterozygous littermates (Honma et al. 2002).

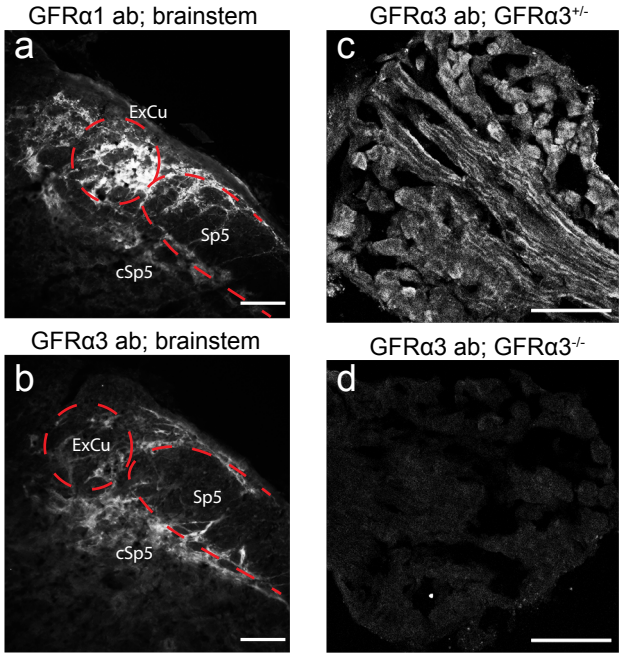

Figure 3-2: The GFRα3 antibody is specific. (a,b) Cross-sections through the brainstem reveal that the GFRα1 and GFRα3 antibodies stain distinct areas of the brainstem. External cuneate nucleus (ExCu), and spinal trigeminal tract (Sp5) are robustly labeled with the GFRα1 antibody (a) while only sparse fibers in the external cuneate and caudal spinal trigeminal tract (cSp5) are labeled with the GFRα3 antibody (b). (c,d) Cross-sections though DRGs of GFRα3$^{-/-}$ mice and GFRα3$^{+/-}$ littermates immunolabeled with the GFRα3 antibody further demonstrate specificity. GFRα3 staining is widespread in the GFRα3$^{+/-}$ DRG (c). In contrast, there is a complete lack of staining in the DRG of the GFRα3$^{-/-}$ mice (d), indicating that the GFRα3 antibody does not bind other proteins. Scale bars, 100 μm.

GFRα3 immunoreactivity in GFRα3+/- murine DRGs was widespread, with nearly all neurons expressing some level of GFRα3 above background (Fig. 3-2c). In contrast, we observed no GFRα3 immunoreactivity in the DRGs of GFRα3-/- mice (Fig. 3-2d), demonstrating that the antibody is specific for GFRα3. Taken together, these results provide strong evidence that GFRα3 is expressed by both large and small sensory neurons in the DRG.

Fluorescence Activated Cell Sorting (FACS) and quantitative PCR confirm that GFRα3 is expressed in both myelinated and unmyelinated neurons. To provide further evidence for GFRα3 expression in large sensory neurons, we developed a method to identify and physically separate large and small neurons so we could assess the expression of GFRα3 mRNA in each type of neuron using QPCR. Populations of small and large neurons were identified by injecting peripheral nerves with WGA-647, which labels a subpopulation of small sensory neurons, and CTB-488, which labels only large, myelinated sensory neurons (LaMotte et al. 1991; Shehab and Hughes 2011). As expected, very few neurons (approximately 4%) were labeled with both WGA and CTB antibodies (Fig. 3-3a,b), verifying that these neurotracers label distinct neuronal populations. The specificity of these labels was confirmed by staining sections of these DRGs with NF200 and CGRP. More than 60% of CTB+ neurons expressed NF200, whereas only 7% express CGRP (Fig. 3-3a-c). When cells labeled with both CTB and WGA are excluded, only 3% of CTB+ neurons express CGRP. In contrast, 48% of WGA+ neurons expressed CGRP and 17% expressed NF200 (Fig. 3-3a-c). The size distribution of the CTB+ and WGA+ neurons was also different. Consistent with previous reports (LaMotte et al. 1991), CTB+ cells are larger than WGA+ cells. More than 20% of CTB+ cells were larger than 1000 μm2 whereas all WGA+ cells were smaller than 1000 μm2 (Fig. 3-3d; CTB+, n=500 cells; WGA+, n=500 cells). The average size of CTB+

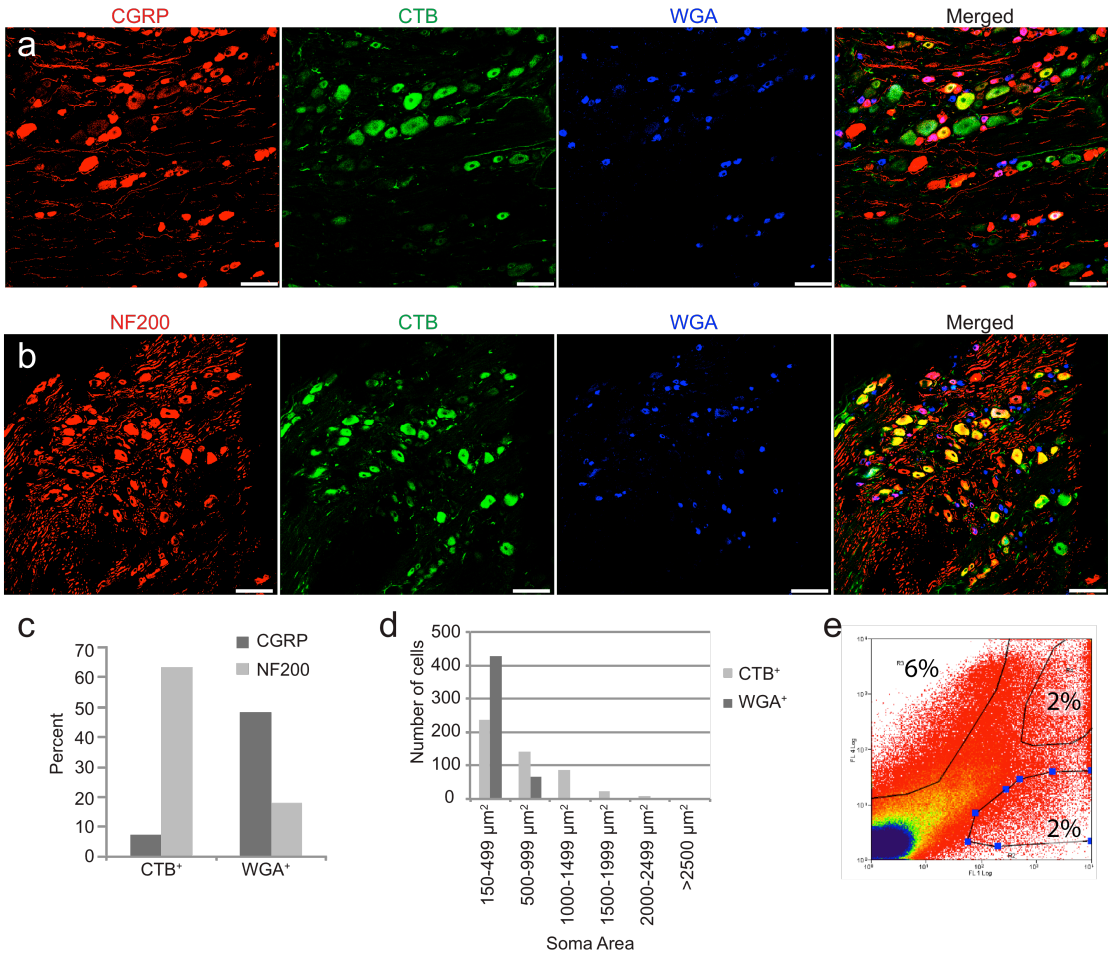

Figure 3-3: WGA and CTB label distinct classes of sensory neurons in the DRG. (a,b) Representative sections through the DRG prelabeled with CTB-488 and WGA-647 and immunolabeled with an antibody to CGRP (a) or NF200 (b). (c) Quantification of the percentage of CTB^+ and WGA^+ cells labeled with NF200 and CGRP antibodies. Most CTB^+ neurons are large, myelinated neurons while many WGA^+ neurons are small, nociceptive neurons. (d) Histogram showing the size distribution of CTB^+ and WGA^+ neurons (n=500). The number of neurons in each 500 μm^2 bin was counted. CTB^+ cells are larger, on average, than WGA^+ cells. (e) FACS profiles of dissociated brachial DRGs prelabeled with CTB and WGA. The percentages of neurons sorted in each condition are labeled in the gated areas. Double-labeled cells, 2% of the total, were not collected. Gates were set to insure

cells (677 ± 20 μm2) is significantly larger than WGA+ cells (approximately 353 ± 7 μm2, p=5x10-44). These data confirm that labeling peripheral nerves with CTB and WGA provides a suitable method for differentiating between large and small sensory neurons in the DRG.

Sensory neurons pre-labeled with WGA and CTB were physically separated using FACS. Two days after labeling, primary neurons were dissociated from brachial DRGs and sorted into separate fractions: small, WGA+-neurons and large, CTB+ neurons. Approximately 6% of dissociated sensory neurons were WGA+ and 2% were CTB+; double-labeled cells were excluded (Fig. 3-3e). QPCR using both GAPDH and HPRT as reference genes showed that the relative levels of GFRα3 message were similar in both CTB+ and WGA+ neurons (Pfaffl ratio for CTB+, 1.03; WGA+, 1.09; p value=0.82). This is consistent with the assertion that both large and small sensory neurons express GFRα3 and their expression levels are similar. The presence of GFRα3 transcript and protein in both neuronal types makes it likely that ARTN promotes the regeneration of both large and small sensory axons via high-affinity binding to GFRα3, which most likely leads to RET activation given that RET is expressed robustly in sensory axons (Luo et al. 2007). We cannot, however, rule out the possibility of other binding partners.

GFRα3 is down-regulated following injury. Using our new method of assessing *GFRα3* levels in different classes of sensory neurons, we assessed the effects of DR crush on *GFRα3* expression. In contrast to the earlier results, we found that *GFRα3* expression was not increased two days after DR crush. Instead, there is a trend towards decreased expression in both large and small neurons, although the reduction did not reach significance (Fig. 3-4a, ANOVA; p=0.10). Combining the results from both large and small neurons, this trend is statistically significant; *GFRα3* message is down-

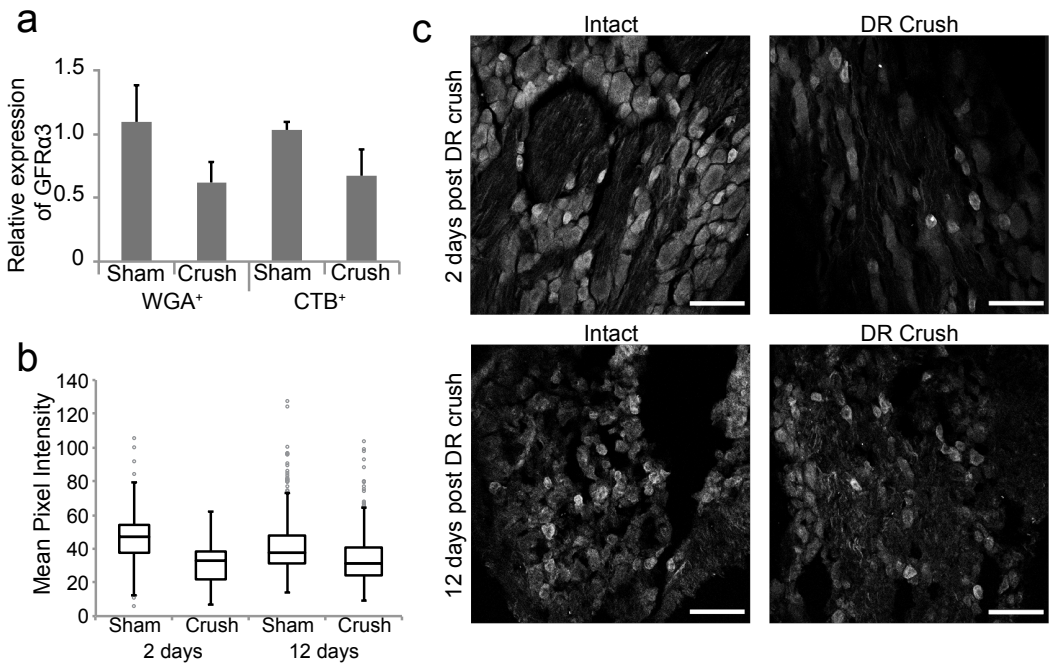

Figure 3-4: GFRα3 expression decreases following DR crush injury. (a) Quantification of the relative ratio of *GFRα3* expression in FACS sorted cells, normalized to both *GAPDH* and *HPRT*. There was no difference in the relative expression of GFRα3 in CTB^+ and WGA^+ sensory neurons. Following DR crush, there was a trend towards reduced GFRα3 expression in both large and small sensory neurons that did not reach statistical significance (ANOVA, p=0.1). (b) Boxplots showing the mean pixel intensity of GFRα3 immunostaining in $NeuN^+$ DRG neurons (2 day intact, n=271; 2 day crush, n=271; 12 day intact, n=400; 12 day crush, n=403). Outliers (>1.5 interquartile range) are depicted with gray circles. (c) Representative cross-sections through DRGs from rats two and twelve days after DR crush stained with the GFRα3 antibody. Scale bars, 100 μm.

regulated with injury (Pffafl ratio for intact neurons, 1.06; DR crush neurons, 0.64; p=0.01) and its expression is likely regulated similarly in both types of sensory neurons. To determine whether this trend also occurs at the protein level, we measured changes in GFRα3 immunoreactivity in DRG neurons from rats with unilateral DR crush two and twelve days prior to DRG collection. There was a significant decrease in mean pixel intensity in $NeuN^+$ DRG cells two days after crush (n=271 cells from 3 animals) when compared to DRG cells from the intact side (n=271 cells from 3 animals) in the same animals (Fig. 3-4b,c). Not only was there a decrease in the average pixel intensity, but also the range of data values was narrower, with no cells expressing high levels of GFRα3. This decrease in average immunoreactivity for GFRα3 protein was still observed 12 days after crush (intact, 41.3; crush, 34.3; $p=4x10^{-10}$; Fig. 3-4b,c). While the majority of cells have decreased GFRα3 expression, there are some cells expressing high levels of the protein, indicating that some neurons up-regulate protein expression by 12 days post-injury (Fig. 3-4b). These data suggest that there is a slight decrease in GFRα3 expression levels following DR crush injury that is maintained for at least several days.

Discussion

ARTN signals predominantly through the RET tyrosine kinase, an interaction that requires the binding of a non-signaling co-receptor GFRα3 (Baloh et al. 1998b; Wang et al. 2006). Previous studies suggested that GFRα3 is expressed on only a few myelinated sensory neurons (Bennett et al. 2000; Orozco et al. 2001; Keast et al. 2010), yet ARTN promotes robust regeneration of large sensory axons in several different injury

models (Wang et al. 2008, 2013b; Harvey et al. 2010). Given our experiments demonstrating that myelinated sensory axons regenerate long distances to the brainstem with ARTN treatment, we devised a technique using FACS and QPCR to assess quantitatively if GFRα3 mRNA is expressed in these neurons. Using this method, we found that expression of GFRα3 is similar in large and small neurons (Fig. 3-4a). These data confirm our immunohistochemistry findings indicating that GFRα3 colocalizes with NF200 and CGRP in adult rat DRGs (Fig. 3-1). Given that RET is expressed on all classes of sensory neurons (Luo et al. 2007), ARTN likely acts through the binding of GFRα3 and the RET tyrosine kinase to promote regeneration in both myelinated and unmyelinated neurons, although signaling through the non-canonical NCAM-mediated pathway cannot be ruled out.

Several earlier studies reported an increase in the number of cells expressing GFRα3 following injury, leading us to ask if GFRα3 expression changed in response to DR crush. Interestingly, we observed a trend toward down-regulation of *GFRα3* in response to DR crush injury in myelinated and unmyelinated neurons (Fig. 3-4a), suggesting that expression of the receptor is similarly regulated in both types of sensory neuron. We further found that GFRα3 protein levels are reduced in DRG neurons beginning shortly after DR crush and persisting for at least 12 days (Fig. 3-4b,c). Our results most likely differ from the previous studies due to methodological differences. Most of the earlier studies examined changes in expression in response to peripheral nerve injury rather than DR injury (Bennett et al. 2000; Keast et al. 2010; Wang et al. 2011a). Peripheral nerve injury leads to up-regulation of growth promoting pathways while DR injury generally does not. It is, therefore, not surprising that we would observe a similar phenomenon in GFRα3 expression. In one study using the DR crush model of injury, Wang et al. (2008) used immunohistochemistry to quantify changes in the number of GFRα3$^+$ cells, finding an increase overall but a concomitant decrease in the number of

myelinated GFRα3^{+} neurons. In contrast, we used QPCR to determine if there were changes in the relative amount of *GFRα3* expressed in DRG cells and verified that protein levels were also decreased by measuring the mean pixel intensity of fluorescent GFRα3 immunoreactivity in DRG neurons. Differences in the sensitivity and resolution of these testing methods may account for the discrepancy between these results.

These results advance our understanding of the mechanism by which ARTN promotes distant regeneration. Given that GFRα3 is expressed at equivalent levels on large and small diameter neurons, ARTN most likely promotes regeneration of both types of sensory neurons through high-affinity binding to GFRα3. ARTN:GFRα3 interactions are required for RET and NCAM signaling, both of which are expressed in the DRG and contribute to ARTN mediated affects *in vitro* (Baloh et al. 1998b; Ledda et al. 2007; Paratcha and Ledda 2008). Understanding the intrinsic pathways activated by ARTN can provide insight into new therapeutics to promote targeted axon regeneration in the CNS.

CHAPTER 4

Discussion

Summary of this thesis

Artemin promotes functional regeneration of severed sensory axons to the brainstem. We have demonstrated that two-week systemic artemin (ARTN) treatment promotes targeted long-distance regeneration of brachial sensory afferents to the brainstem following dorsal root (DR) crush. Sensory axons regenerated appropriately in the dorsal columns and synapsed with targets in the cuneate nucleus in the absence of externally applied guidance cues. We observed that synaptic potentials in the cuneate nucleus ipsilateral to the crush were approximately 25% of those on the intact side. Although we have found no rodent behavioral tests that depend upon synaptic activity in the cuneate nucleus, a restoration of synaptic connectivity in the dorsal horn of the spinal cord to 20% of normal resulted in robust improvement in several simple behaviors, including paw placement, contact-evoked grasping, and sensation of thermal and tactile pain (Wang et al. 2008). We expect that 25% restoration of brainstem connectivity would similarly result in behaviorally relevant functional improvements.

This is the first study demonstrating functional regeneration of sensory axons to targets in the brainstem. The observed regeneration was time-dependent; more than three months of recovery were required for sensory axons to extend from brachial levels of the spinal cord to the brainstem and restore synaptic connectivity.

Several lines of evidence suggest that ARTN induces true regeneration from injured axons. First, our anatomical tracing and electrophysiological techniques ensured that synaptic responses originated from injured brachial DRs. Manipulation of peripheral brachial nerves only affects axons entering through cervical level 5 (C5) through thoracic level 1 (T1). Axons sprouting from neighboring spinal levels are, therefore, not responsible for the observed synaptic responses and do not contribute to the presence

of fluorescently labeled axons in the brainstem or spinal cord. Second, we saw no electrophysiological evidence of axons crossing the midline when nerves on the intact side were stimulated, suggesting that axons from the uninjured side do not contribute to the presence of fluorescently labeled axons on the crushed side. This is consistent with the result from Sengelaub et al. (1997) that sprouting across the midline does not occur. Lastly, the substantial time requirement for axons to reach the cuneate nucleus is consistent with true regeneration rather than sprouting of spared fibers. Spared fibers recover quickly (Di Maio et al. 2011). If they were responsible for the observed effects, we would see anatomical and electrophysiological improvements at the earliest time point. Instead, connectivity was reestablished in a time frame consistent with regeneration. Given that a span of three to four centimeters separates the lesion site and the cuneate nucleus in the brainstem, the average rate of regeneration was approximately 0.2 to 0.4 millimeters per day.

These experiments emphasize the substantial therapeutic benefit of ARTN for the treatment of DR injuries, not only because ARTN promotes functional regeneration in the CNS across unprecedented distances, but also because of the ease with which ARTN is administered. ARTN promotes regeneration when delivered subcutaneously. Subcutaneous injections are associated with significantly fewer risks than neurosurgical therapeutic techniques such as administration in the CSF or injection of viral vectors, both of which have been used to deliver other experimental therapeutic agents for SCI (Zhang et al. 1998b; Ramer et al. 2000; Alto et al. 2009; Harvey et al. 2009; Parikh et al. 2011; Lu et al. 2012). In addition, these experiments demonstrate that regeneration continues for several months, even though ARTN is delivered for only two weeks. Shorter durations of treatment will potentially be less expensive and will likely increase patient compliance, resulting in more successful therapy. Moreover, the limited expression of ARTN's high-affinity binding partner GFRα3—restricted in adults primarily

to cells in the DRG—and the short treatment window required for robust regeneration will reduce, and may even prevent, some of the harmful side effects observed with systemic administration of other neurotrophic factors in clinical trials.

GFRα3 is expressed on large, myelinated neurons in the dorsal root ganglion. Previous immunohistochemical studies suggested that expression of GFRα3, the high-affinity binding partner for ARTN, was limited to small, nociceptive neurons in the DRG (Baloh et al. 1998b; Orozco et al. 2001; Keast et al. 2010). Given our evidence that large neurons regenerate long distances in the spinal cord, we investigated if GFRα3 was expressed on these cells. Both large neurons that express NF200 and small, peptidergic neurons that express CGRP were immunoreactive for GFRα3. Using a sorting method to separate small and large DRG neurons, we demonstrated quantitatively that expression of GFRα3 transcript is similar in both classes of neurons, confirming our immunohistochemical results. GFRα3 transcript and protein are indeed expressed in both small and large sensory neurons. Given that RET is expressed in all classes of adult sensory neurons in the DRG (Luo et al. 2007), ARTN most likely promotes regeneration by signaling through GFRα3:RET.

Using the same sorting technique, we determined that *GFRα3* transcript is moderately down-regulated in both large and small neurons two days after DR crush. We observed a similar reduction in GFRα3 protein two and twelve days after crush. These results suggest that expression is regulated similarly in large and small neurons. Previous studies have shown that GFRα3 is up-regulated following peripheral nerve injury, suggesting a role of ARTN in promoting peripheral axonal regeneration. Given the differences in the propensity for peripheral and central axons to regenerate, it is not surprising that DR crush and peripheral nerve injury result in opposite regulation of GFRα3 expression. This is also observed in several other neurotrophic factor systems

(Bradbury et al. 2000). Unfortunately, we were unable to determine whether treatment with ARTN leads to a normalization of these injury-induced expression changes because we no longer have adequate supplies of bioactive ARTN. Treatment with ARTN has been shown to increase the number of $NF200^{+}$ DRG neurons that are immunoreactive for GFRα3 following DR crush (Wang et al. 2008). This evidence suggests that we might observe a similar stabilization of transcript and protein expression using our more quantitative methods. Future experiments are needed to determine whether expression of GFRα3 is altered with ARTN treatment.

These results contribute to the current understanding of the mechanism by which ARTN promotes regeneration of large, myelinated fibers. It is likely that high-affinity binding through GFRα3 expressed on the surface of sensory neurons contributes to ARTN-induced regeneration of both myelinated and unmyelinated axons. ARTN:GFRα3 binding is required for signaling through RET and NCAM, both of which are expressed in the DRG and contribute to GFL effects *in vitro* (Baloh et al. 1998b; Schmutzler et al. 2011). Given the myriad potential therapeutic benefits of ARTN *in vivo*, a complete understanding of the mechanism by which ARTN acts is essential.

Proposed Mechanism by which Artemin Promotes Distant Regeneration

Our results demonstrate that ARTN promotes long-distance regeneration of myelinated sensory axons to their targets in the brainstem. Remarkably, just two weeks of systemic ARTN treatment is sufficient to promote sustained axon regeneration for more than three months, suggesting that brief trophic support may initiate intrinsic growth programs that remain active until axons reach their targets. As a result, several

different experimental questions arise regarding the mechanism of ARTN-promoted long distance regeneration. In the following sections, I will address how ARTN might reach the DRG, the role of heparin binding in ARTN-mediated signaling, potential binding partners for ARTN:GFRα3, and potential down-stream effector molecules. Lastly, I will discuss how the two main therapeutic functions of ARTN—axon regeneration and treatment of neuropathic pain—may result from different ARTN signaling mechanisms.

Artemin might reach the dorsal root ganglion through the circulatory system. There are several lines of evidence that suggest that ARTN might reach the DRG through the circulatory system. First, ARTN protein is detected in the DRG after a 12-day treatment course with subcutaneous ARTN (Harvey 2009). This same subcutaneous administration of ARTN results in serum plasma concentration of ARTN in the 1 to 5 ng/ml range, suggesting a likely avenue by which ARTN might reach neurons in the DRG. Second, ARTN immunoreactivity is observed in the extracellular matrix (ECM) of the DRG, not in neuron cell bodies, suggesting that axonal transport is an unlikely mechanism by which ARTN reaches the DRG (Harvey 2009).

Further evidence that ARTN reaches sensory neurons via the circulatory system comes from studies investigating neuropathic pain. One study in particular demonstrated that ARTN reduces hyperalgesia when spinal nerves were cut, crushed or ligated very near the DRG (Wang et al. 2013b). In these experiments, the only manner by which ARTN could reach the sensory neurons is through the circulation. Axonal transport was completely disrupted as demonstrated by a failure of dextran and CTB to be transported to the DRG following peripheral nerve injection in the models where spinal nerves were cut or ligated (Wang et al. 2013b). Although ARTN-promoted regeneration appears to be mechanistically different from ARTN-induced treatment of neuropathic pain, it is likely that ARTN reaches the cell body by traveling in the circulation in both cases.

The Role of Heparin Binding. We observed functional long-distance regeneration with both forms of ARTN, the version with 104 amino acids and the longer form with 113 amino acids. While both forms of ARTN show similar activation of RET using KIRA ELISA, ARTN104 has a 10-fold lower affinity for heparin sulfate proteoglycans (HSPGs), leading to an increase in the level of ARTN in plasma (Silvian et al. 2006). Consistent with higher plasma levels, 1 mg/kg of ARTN104 promoted better regeneration than 3 mg/kg of ARTN113. This suggests that high-affinity HSPG binding is not required for regeneration.

HSPGs are important binding partners for GFLs (Airaksinen and Saarma 2002; Sah et al. 2005; Silvian et al. 2006; Bespalov et al. 2011). The presence of HSPGs increases the affinity of ARTN for GFRα3 *in vitro* (Silvian et al. 2006). It has been hypothesized that HSPGs restrict diffusion of GFLs, which may serve to raise the concentration of GFLs near the cell membrane. Binding of HSPGs may also orient GFLs for proper binding to the receptor complex. While HSPG-restricted diffusion might be a useful component of ARTN signaling during development when ARTN is secreted by nearby cells, HSPG binding may sequester exogenously administered ARTN from the bloodstream, preventing it from reaching the DRG. Additionally, HSPGs may have a role in GFL-mediated signaling; HSPG binding is required for activation of the Src family of kinases (SFK) in a RET- and GFRα-independent manner *in vitro* (Bespalov et al. 2011).

Given our finding that both ARTN104 and ARTN113 promote functional regeneration of large diameter axons, high-affinity heparin binding must not be required for axon regeneration. In fact, ART104 promoted more robust axon regeneration than ARTN113, suggesting that reduced HSPG binding might be beneficial. This is most likely because ARTN104 is more bioavailable than ARTN113 and circulates at higher plasma concentrations. This provides some additional evidence that ARTN reaches the DRG by

traveling in the bloodstream. While ARTN104 has reduced HSPG binding, cleavage of the nine N-terminal amino acids does not completely block interactions with HSPGs in the extracellular matrix (ECM) because the putative HSPG binding motif is still intact. Interactions with HSPGs could still be important for neurite extension or immobilization of ARTN near DRG cells. The role of HSPG binding could be addressed definitively by assessing local and distant regeneration following treatment with a version of ARTN in which targeted mutations completely abolish the HSPG binding site (Silvian et al. 2006).

Potential ARTN:GFRα3 binding partners. Our data indicate that myelinated axons regenerate with ARTN treatment and that these neurons express GFRα3 at levels similar to unmyelinated neurons. Thus, it is likely that ARTN promotes regeneration in a GFRα3-dependent manner, although GFRα3-independent effects cannot be excluded because *in vivo* regeneration experiments have never been done in GFRα3$^{-/-}$ animals. GFRα3 is thought to capture and stabilize ARTN on lipid rafts in the cell membrane for binding to RET and NCAM (Paratcha and Ibáñez 2002). Aside from positioning ARTN ideally to promote signal transduction, it is unknown whether GFRα3 is required for downstream signaling. Future experiments will be done in collaboration with Dr. Alan Kopin's laboratory in the Molecular Pharmacology Research Center at Tufts Medical Center to determine if tethering ARTN to lipid rafts in the cell membrane is sufficient for activation of RET or to promote neurite outgrowth in cells that do not express GFRα3.

High-affinity interactions between ARTN and GFRα3 are required for activation of both RET and NCAM (Baloh et al. 1998b; Paratcha and Ibáñez 2002; Paratcha et al. 2003; Ledda et al. 2007). RET is considered the classical signaling partner for each GFL including ARTN and is expressed in most tissues that express GFRα3. Activation of RET has been implicated in GFL-mediated cell survival, neurite outgrowth and differentiation making this tyrosine kinase a good candidate signal-transduction molecule mediating

ARTN-promoted long-distance regeneration. Likewise, NCAM has been implicated as an ARTN:GFRα3 binding partner (Schmutzler et al. 2011). NCAM is important both for its adhesive properties and its ability to signal through the SFK Fyn (Beggs et al. 1994; Paratcha et al. 2003).

Given that both RET and NCAM seem equally likely to bind to ARTN:GFRα3 and promote regeneration, *in vivo* assays are required to assess which partner is required for regeneration. For example, an ARTN variant could be engineered with alterations in the second finger and hinge motifs, abolishing its ability to activate RET without affecting NCAM binding (Wang et al. 2006). Likewise, an ARTN variant that cannot bind NCAM could also be engineered (Sjöstrand et al. 2007; Sjöstrand and Ibáñez 2008). By assessing regeneration following DR crush and subcutaneous treatment with these ARTN variants, it may be possible to unravel which signaling component—RET or NCAM—is required for regeneration.

Intrinsic downstream growth pathways activated by artemin treatment. Few studies have investigated which downstream effector molecules are activated with ARTN treatment, and none of these studies have addressed this issue *in vivo*, making it difficult to determine which mechanism of ARTN action is important for promoting distant regeneration. Several pathways have been implicated as mediators of ARTN function *in vitro* including cAMP/CREB, SFK, Erk1/2, MAPK and Akt (Park and Hong 2006; Jeong et al. 2008; Zhou et al. 2009; Schmutzler et al. 2011).

Zhou et al. (2009) demonstrated that a protein kinase A (PKA) inhibitor blocked ARTN-promoted neurite extension in a dose-dependent manner. In this study, ARTN treatment increased phosphorylation of CREB, which was attenuated by treatment with the PKA inhibitor, and arginase I levels increased following ARTN treatment. The authors therefore proposed a mechanism by which ARTN promotes regeneration via a

cascade involving cAMP, PKA, CREB and arginase I to inhibit Rho/ROCK mediated myelin inhibition (Zhou et al. 2009). In a similar study, Jeong et al. (2008) demonstrated that an SFK inhibitor and extracellular signal-related kinase 1/2 (ERK1/2) inhibitor prevented ARTN-induced neurite outgrowth. In contrast, a phospho-inositide 3 kinase (PI3K) inhibitor had no effect on neurite extension (Jeong et al. 2008). Taken together, these results suggest that signaling through ARTN may activate several different downstream kinases, the interaction of which could affect neurite outgrowth, cell survival, actin dynamics and regeneration. To sort out these possibilities, new tools must be developed to elucidate the down-stream effector molecules resulting in ARTN-promoted regeneration.

The use of microarray technology would allow the determination of how various genes are regulated in response to ARTN treatment *in vivo*. In one study, microarray analysis performed on an *ex vivo* whole DRG preparation revealed widespread changes in expression of transcripts related to actin polymerization twelve hours after ARTN treatment (Park and Hong 2006). In addition to changes in genes related to actin dynamics, the most dramatic difference noted was the up-regulation of Akt (S. Park, personal communication). These results provide some evidence that the Akt pathway may be important for downstream ARTN signaling. Because DRGs were stripped of both the central and peripheral axons for the *ex vivo* preparation, and ARTN was delivered at a much higher dose than would be expected with *in vivo* systemic treatment, it is difficult to draw conclusions about the molecular changes that might accompany ARTN administration in more physiologically relevant situations. It would be interesting to perform these types of gene expression analyses with DRGs taken from animals treated with subcutaneous ARTN following unilateral crush. Investigation of transcript expression changes at several time points, both during and in the months following

ARTN treatment, might provide some insight into the signaling pathways through which ARTN promotes sustained regeneration.

The sorting method we developed to study GFRα3 expression in large and small cells may also be a useful tool for gaining additional insight into the molecular changes that occur in response to ARTN treatment. It is possible that large and small diameter cells respond differently to crush and ARTN treatment. The use of microarray technology on sorted cells would begin to address if different pathways are activated with ARTN treatment in different classes of neurons. In developing a way to physically separate classes of neurons, we have created a flexible tool that is capable of sorting more than just large and small diameter neurons. Because this sorting method relies on fluorescent neurotracers, it can be used for labeling neurons that have responded to treatment. Retrograde labeling of axons by injecting a neurotracer in the spinal cord one week post-DR crush would allow the collection of DRG neurons that have regenerated across the DREZ without diluting the sample with cells that did not regenerate. Techniques to assess gene expression or protein phosphorylation could then be used to elucidate which growth-promoting pathways are involved in this regenerative response. Understanding the molecular mechanism by which ARTN promotes substantial axon regeneration will be instrumental in developing new therapeutics for treating SCI.

The mechanism by which artemin promotes regeneration is different from the manner by which artemin ameliorates neuropathic pain. ARTN has two main therapeutic functions, the treatment of neuropathic pain and the promotion of sensory axon regeneration. Interestingly, a recent study suggests that these two functions may have fundamentally different mechanisms. As previously noted, two-week systemic ARTN promotes sustained regeneration after treatment is terminated, leading to recovery of synaptic function in the spinal cord within four weeks (Wang et al. 2008) and

continued regeneration to the brainstem over several months. In contrast, neuropathic pain requires continuous treatment with ARTN (Gardell et al. 2003; Wang et al. 2013a). Once treatment is terminated, hyperalgesia returns. In a recent study, Wang et al. (2013) demonstrated that sensory axon regeneration did not relieve neuropathic pain using a post-ganglionic spinal nerve crush that severed peripheral axons and led to hyperalgesia. Brief systemic ARTN treatment led to functional regeneration and briefly alleviated hyperalgesia symptoms. Once ARTN treatment was terminated, neuropathic pain returned within 5 days despite the fact that many sensory fibers reinnervated their peripheral targets. ARTN also relieved hyperalgesia without regeneration when physical continuity of the nerve was disrupted (Wang et al. 2013a). These results suggest that neuropathic pain is caused not by denervation, specifically, but by some other injury-induced mechanism, likely inflammatory in nature. It further suggests that downstream molecules promoting regeneration might differ from those that alleviate neuropathic pain.

NCAM and RET are both important for enhanced capsaicin-induced immunoreactive CGRP release with ARTN treatment *in vitro*, suggesting that signaling through both molecules may modulate the pain response (Schmutzler et al. 2011). This depends on the SFKs c-Src and Fyn. Although the MAPK and Erk1/2 pathways are activated with ARTN treatment, inhibitors of these particular pathways had no effect on the enhanced release of immunoreactive CGRP (Schmutzler et al. 2011). ARTN may modulate the pain response through SFKs but activation of MAPK and Erk1/2 following ARTN treatment must result in some other functional outcome. It seems likely that the MAPK and Erk1/2 pathways are important for the ARTN-promoted regenerative response. In addition to the microarray experiments described above, this could be tested definitively by evaluating ARTN-promoted regeneration following DR crush in animals with siRNA knockdown of MAPK and Erk1/2 in the DRG.

Schmutzler et al. (2011) also demonstrated that GDNF, NRTN and ARTN mediate the pain response through different downstream pathways. Erk1/2 is important in mediating immunoreactive CGRP release with GDNF treatment while PI3K was important for mediating its release with NRTN treatment (Schmutzler et al. 2011). This suggests that GFLs activate distinct downstream signaling cascades despite the fact that each initiates signaling in the same manner, by binding to the transmembrane molecules RET and NCAM. It is possible that different intracellular RET adaptor proteins account for the diversity of GFL-mediated signaling. This study further suggests that it may not be appropriate to make generalizations about ARTN's mechanism of action based on results from the many studies using GDNF.

Rate of Axon Growth

In the present experiments, it took between 3 and 6 months for axons to reconnect with their targets in the brainstem. Thus, regeneration to the brainstem occurred at an average rate between 0.2 and 0.4 millimeters per day, much slower than rates of axon growth reported in other studies. Several studies have reported that sensory axons reach the DREZ within one week after DR crush, indicating that sensory axons grow in the DR at a rate of 1.0 to 1.5 millimeters per day (Ramer et al. 2001; Di Maio et al. 2011). Functional regeneration of axons into the dorsal horn occurs one month after DR crush, suggesting that crossing the barrier into the spinal cord and reconnecting to synaptic targets requires substantially more time than regeneration in the peripheral environment of the DR (Ramer et al. 2000; Wang et al. 2008; Harvey et al. 2010).

In a study investigating regeneration in degenerating white matter tracts, Davies et al. (1999) discovered that adult sensory neurons transplanted in the dorsal columns rostral to a dorsal column lesion grew axons that were several millimeters in length by ten days post-transplant. These studies indicated that axons are capable of growing as much as 1.0 millimeter per day in white matter tracts undergoing Wallerian degeneration, demonstrating that molecules such as NOGO, MAG and OMgp—all abundant in this degenerating tract—must not provide an insurmountable barrier to regeneration (Davies et al. 1999). While we also saw substantial sensory axon regeneration, our results show a much slower rate of growth. There may be several reasons for this finding. First, the neurons transplanted into lesioned dorsal columns were completely denervated in order to dissociate them for transplantation. Stripping a neuron of both its central and peripheral axons can result in transcriptional changes leading to a robust regenerative response. In contrast, our preparation only injured the central axon, which does not produce a strong regenerative response. Second, because Davies and co-workers transplanted neurons rostral to the lesion, growing axons did not encounter the CSPG-rich glial scar until several millimeters of axon growth had occurred. In a DR crush model, axon regeneration slows upon reaching the DREZ, and CSPGs produce a substantial barrier at the DREZ, dorsal horns and dorsal columns near the site of injury (Ramer et al. 2001). In our preparation, this CSPG-rich area would extend from C5 to T1, a distance of at least 1.5 centimeters through which regenerating axons might grow at a slower rate. Lastly, Davies et al. (1999) described a slowing of axon elongation at the border between the dorsal columns and the dorsal column nuclei. Crossing this border may take substantial time, slowing the overall rate of axon growth.

We observed robust regeneration at average rates of 0.2 to 0.4 millimeters per day. Although growth was slower than other studies have reported, the fact that invasive conditioning lesions were not required provides a significant clinical advantage.

Furthermore, axons may extend at rates equal to those observed in other studies under ideal conditions. Studies will need to be done at more frequent time points over the six-month recovery time to assess the rate of axon regeneration more completely.

Implications for Targeted Regeneration

An unfulfilled goal of spinal cord regeneration remains the reinnervation of appropriate neuronal targets. As therapeutic strategies are developed that promote longer distance regeneration, the challenge will become one of reestablishing correct synaptic input. Several studies have attempted to use molecules with tropic or repulsive effects as exogenously applied guidance cues to promote targeted reinnervation (Tang et al. 2007a; Alto et al. 2009; Bonner et al. 2011). These studies have had limited success. In the spinal cord, injecting semaphorin in the ventral cord stopped nociceptive neurons from regenerating to aberrant locations deep in the cord, limiting axons to more superficial laminae and restoring some function (Tang et al. 2007a). In contrast, studies promoting regeneration to sites in the brainstem using an attractive trophic factor gradient have been less successful; synaptic connectivity was not reestablished with neurons in the cuneate nucleus and, in some cases, misplacement of the trophic gradient resulted in misguidance (Alto et al. 2009; Bonner et al. 2011).

Remarkably, we observed that sensory neurons regenerated in the dorsal columns to the appropriate brainstem areas and formed synapses with targets in the cuneate nucleus without the application of exogenous guidance cues. In addition, ARTN treatment promotes topographically specific regeneration of neurons in the dorsal horn of the spinal cord (Harvey et al. 2010). These data suggest that (1) axon guidance cues must persist in the adult CNS; (2) adult axons are capable of sensing those cues; and

(3) ARTN treatment permits adult axons to follow those cues. To the best of our knowledge, ARTN is the first therapeutic agent that promotes targeted regeneration in this fashion. While other therapeutic agents can produce robust regeneration, axons often project aberrantly (Zhang et al. 1998b; Ramer et al. 2000; Tang et al. 2004, 2007a; Harvey et al. 2010). In fact, ectopically located axons have become a useful feature for distinguishing regeneration from sprouting of spared fibers (Tuszynski and Steward 2012). While misguidance makes it easier to distinguish between sprouting and regeneration, it may be detrimental to the goal of long-distance regeneration. Two recent studies have cited misguidance as a key limitation preventing long-distance regeneration (Luo et al. 2013; Pernet et al. 2013).

There are several key reasons why ARTN may promote targeted regeneration. First, ARTN is delivered systemically. Several studies promote regeneration by administering trophic factors into the cerebrospinal fluid (CSF) (Zhang et al. 1998b; Ramer et al. 2000). Many neurotrophic factors, including ARTN, have chemoattractive properties, and application of these agents directly into the CSF may overwhelm minor guidance cues present in the adult CNS. In contrast, systemic ARTN may stimulate regeneration by binding to the cell body, promoting axon growth in a manner allowing local guidance cues to be followed. Second, ARTN is delivered briefly; two-week ARTN treatment promotes sustained and targeted regeneration for several months. In contrast, several studies provide prolonged trophic support using viral vectors (Tang et al. 2004, 2007a; Pernet et al. 2013). Our experiments suggest that brief trophic support may be important for initiating axon regeneration that is sustained by naturally occurring cues. This may better recapitulate events during development, allowing axons to follow guidance cues to the appropriate location. Lastly, ARTN treatment does not effect the molecular environment of the spinal cord. Studies blocking environmental inhibitors of axon growth can result in robust sensory axon regeneration but do not result in

topographically specific reinnervation (Harvey et al. 2009, 2010). It is possible that blocking inhibitory molecules in the CNS also has profound affects on guidance, particularly since several repulsive guidance cues during development become barriers to regeneration in adulthood. Alteration of how ARTN is delivered—sustained systemic administration, viral delivery, or intrathecal administration—could easily be used to test these hypotheses.

It is possible that there is some alternative and unique aspect of ARTN treatment that results in targeted regeneration. During development, axon guidance and topographical specificity is achieved through the complex interactions resulting from attractive and repulsive guidance cues interacting with their transmembrane receptors and cell-cell interactions mediated by adhesion molecules. Synaptic pruning maintains and strengthens appropriate connections and removes inappropriate ones. An understanding of the molecular components that contribute to ARTN-promoted regeneration would be instrumental for understanding the molecular events leading to specific regeneration and the development of novel therapeutic strategies that induce axons to reinnervate correct target areas.

Development of Therapeutic Strategies for Spinal Cord Injury

Despite remarkable advances in our understanding of the molecular events that follow SCI and the factors that prevent axonal regeneration, no effective therapeutic agent has been developed to promote axon regeneration and restore synaptic connectivity to areas that have been denervated following neuronal injury. Currently available treatments are designed to limit damage following injury, relying primarily on

surgical techniques. Methylprednisone, the only FDA-approved therapeutic agent for SCI, is falling out of favor because its undesirable side effects outweigh its limited clinical benefit (Kwon et al. 2010). The therapeutic agents that have advanced to clinical trials have focused on neuroprotection, but treatment with these therapies has failed to produce much functional improvement because there is little axonal regeneration. Although several therapeutic agents have advanced to clinical trials, off-target interactions leading to severe, unexpected side effects have prevented these potential therapies from passing initial safety trials in humans.

Understanding how a molecule will affect different classes of cells, both in the nervous system and in other organ systems, is critical for the development of therapeutic agents for spinal cord injury. Therapeutic agents must be easily delivered and should produce functional improvements that persist once treatment is terminated. In addition, agents that are useful for treating in the chronic phase of injury would have tremendous utility given that 250,000 Americans are currently living with SCI. It seems likely that combinatorial therapies must be developed to address the different injury modalities and neuronal types affected in order to promote complete recovery following SCI.

Thorough characterization of which neurons respond to treatment and the extent to which they respond is required. SCI is extremely variable, often affecting several different ascending and descending tracts depending on the location of the injury. Rarely are all neuronal classes disrupted. Drug therapies for SCI must be optimized to (1) promote regeneration of damaged pathways to appropriate local and distant targets, (2) leave undamaged pathways intact, and (3) promote sprouting of appropriate collateral pathways.

In this thesis, we have further characterized the effects of ARTN on large sensory neurons. Notably, ARTN promotes regeneration of large sensory axons across several

centimeters in the spinal cord to reestablish functional synapses with appropriate targets in the brainstem. We observe no inappropriate sprouting of intact neurons from nearby spinal segments or from the uncrushed side, suggesting that ARTN-promoted regeneration requires an injury response. This could be an important feature for preventing intact axons from connecting inappropriately with other neurons but it may also preclude potentially useful collateral sprouting.

In addition, we have sought to understand the mechanism by which ARTN initiates signaling in DRG neurons to help understand what types of cells might respond to treatment. We have established that expression of GFRα3, ARTN's high-affinity binding partner, is equivalent on large and small DRG neurons, suggesting that binding to GFRα3 is the initial step in ARTN-promoted regeneration in both types of neurons. An alternative, undiscovered receptor is probably not responsible for axon regeneration. High-affinity HSPG binding is also not required for ARTN to elicit a regenerative response. It will be important to determine whether ARTN treatment causes alteration in non-neuronal cell types, especially because there are several organ systems in the abdomen that express low levels of GFRα3.

Location and timing of drug delivery. The mechanism and timing of administration of a therapeutic agent will need to be optimized to produce the most successful treatment. An effective therapy for SCI requires that the therapeutic agent be easily administered with a broad treatment window to allow for administration at times compatible with the surgical and medical needs of the patient.

Often patients presenting with SCI are unstable, requiring several different clinical specialists to manage the complex medical and surgical needs arising from severe trauma. Therapies to promote axon regeneration may not be addressed until the patient is hemodynamically stable. Systemic treatment is highly advantageous over

more invasive treatment methods that require neurosurgical intervention for delivery because it can be administered quickly, safely, and easily by many different clinical providers.

Subcutaneous treatment of ARTN is effective at promoting axonal regeneration. High levels of GFRα3 are restricted primarily to neurons in the DRG, a benefit because off-target side effects will be limited. While peripheral effects were not evaluated here, we observed no side effects suggesting involvement of other organ systems. Unpublished data from Biogen idec indicate that there are no harmful peripheral effects (M. Arnold, personal communication). In addition, ARTN is in Phase 2 trials for the treatment of neuropathic pain, so intravenous (IV) delivery of ARTN has passed initial safety trials in humans. More work must be done to optimize IV administration of ARTN to promote the maximum amount of regeneration.

Another advantage of ARTN treatment is that only brief treatment is required to promote regeneration. Two-week treatment promotes functional regeneration that persists for at least six months after treatment has been terminated (Wang et al. 2008). In this study, we further demonstrated that regeneration continues for several months, leading to recovery of synaptic connectivity with distant targets several months later. This is beneficial because it increases the likelihood that patients will adhere to the treatment regimen, and because patients can be exposed to lower amounts of the drug, potentially reducing harmful side effects. This could be a major advantage because prolonged treatments for SCI, including ARTN, may have oncogenic effects (Wu et al. 2013). Optimization of treatments will require balancing maximal regeneration with more harmful side effects.

Therapeutic agents should be able to treat pre-existing conditions. More than 250,000 Americans are currently living with some form of SCI (Silva et al. 2013) and

treatments that are able to promote regeneration and functional recovery in this population are desperately needed. To date, no studies have demonstrated a positive result with chronic injury underscoring the difficulty of finding therapeutic agents that will work for these patients.

It is unknown whether chronically injured axons will be able to respond to delayed treatment or whether the original targets will persist for synaptic connectivity to be reestablished. Evidence suggests that injured neurons might survive and retain some regenerative capability long after SCI. First, axons from severed DRG neurons remain stable at the DREZ for months to years and only 2% of DRG neurons die in the absence of treatment (Ramon y Cajal 1928; Hu and McLachlan 2003; Chew et al. 2008; Di Maio et al. 2011). Second, rubrospinal neurons can be induced to regenerate into peripheral nerve grafts one year after injury with BDNF treatment (Kwon et al. 2002). Thus, it may be possible to find effective therapies to promote regeneration after injury has become chronic. Evidence suggesting that target neurons will persist is mixed. Some neurons, including motor neurons, lose trophic support once peripheral connections are lost, leading to cell death (Kawamura and Dyck 1981; Yan et al. 1992; Chen et al. 2002). In contrast, studies have shown that neurons in the dorsal column nuclei persist for at least several months after sensory connections are lost (Sengelaub et al. 1997). They suggest that collateral sprouting may be important for preventing cell death caused by deafferentation (Sengelaub et al. 1997).

Although we did not delay ARTN treatment in this study, previous studies demonstrated that ARTN treatment promotes some regeneration after a three-day delay post-injury (Wang et al. 2008). With more prolonged delays in treatment, ARTN is no longer effective. Given that intact neurons do not respond to ARTN treatment by sprouting, some acute injury-related signal might be required for ARTN to promote

regeneration. Inducing this response, either using a conditioning lesion or some molecular means, might promote regeneration in more chronically injured patients.

In this study, we observed that regenerating sensory axons were able to reconnect with targets in the cuneate nucleus several months after DR crush removed sensory input to these neurons. This suggests that targets in the brainstem can persist for more than three months after injury and are available to make functional connections with fibers reaching these targets even once an injury has become chronic. Further experiments are needed to understand how long synaptic connections can be lost before treatment no longer results in functional reconnection.

Combinatorial treatment modalities will be required to treat all aspects of spinal cord injury. SCI often injures several different ascending and descending axon tracts and neuronal populations, induces inflammation in the spinal cord, leads to autonomic dysfunction, and causes systemic immunodeficiency, which increases the risk for infections (Dobkin and Havton 2004; Kwon et al. 2010; Silva et al. 2013). Treatment of this multifactorial injury state will require several different treatment modalities to target all aspects causing dysfunction.

ARTN treatment is thought to promote regeneration only of sensory axons with cell bodies in the DRG. In order to promote complete recovery following SCI, regeneration-promoting therapies will need to be combined to promote functional regeneration of all classes of injured neurons. In addition, SCI leads to cell death of neurons and glial cells in the spinal cord. Therapies leading to sprouting of collateral fibers may need to be used in concert with regeneration-promoting therapies to induce recovery when neurons are too damaged. Treatments capable of bridging the cavity and extensive glial scar present at the lesion site must be engineered. It will be necessary to develop targeted anti-inflammatory agents that are specific to the events occurring in the

spinal cord to prevent cell death caused by inflammation without also increasing infection risk. Lastly, patients will require extensive rehabilitation and supportive care. Each patient will pose a slightly different set of problems, as no two injuries are exactly the same, presenting a challenge to clinicians and researchers alike.

Concluding Comments

Spinal cord injury has catastrophic implications, both personally for the affected individual, and for society in terms of the enormity of healthcare and living expenses. In the past several decades, there have been drastic improvements in the understanding of SCI. Research has focused on understanding the molecular, cellular and systemic events following SCI, leading to a much clearer understanding of events contributing to widespread dysfunction. Yet, despite gains in knowledge and understanding and significant improvements in our ability to treat SCI experimentally, there are still no effective clinical treatments for SCI.

The discovery of a treatment that achieves axonal regeneration with functional improvement would be an extraordinary step in developing clinical therapies that lead to recovery following SCI. The unprecedented level of functional regeneration we observed with systemic ARTN treatment makes it an attractive candidate for future clinical trials. If human studies continue to show no deleterious side effects and if efficacy can be demonstrated in human subjects following injuries where sensory axons are damaged, ARTN would be a novel therapy to restore sensory input to the spinal cord and brainstem following brachial plexus injury and SCI.

Appendix A

A Method for Assessing

Topographical Specificity in the Brainstem

Introduction

As more effective regeneration-promoting therapeutics are developed, it will be important to understand the extent to which regeneration is topographically specific. Incorrect connectivity could result in greater dysfunction than no connectivity at all, as aberrant circuitry could lead to seizure activity, debilitating neuropathic pain, or other behavioral dysfunction.

To date, treatment with ARTN is the only therapeutic agent in which the specificity of regenerating connections has been confirmed. With systemic ARTN treatment following DR crush, different classes of sensory neuron regenerate to the appropriate laminae in the spinal cord; pain fibers terminate in superficial laminae, fibers receiving cutaneous sensory information terminate deeper and those receiving information from muscles terminate nearest to motor neurons in the deepest laminae (Harvey et al. 2010). The extent to which ARTN-promoted long-distance regeneration is topographically specific in the cuneate nucleus is unknown.

The cuneate nucleus is a major relay site for ascending brachial somatosensory information. Sensory neurons receiving fine touch and vibratory sensation from spinal segments C2 through T6 synapse in the cuneate nucleus in a stereotyped somatotopic pattern that has been well characterized using transganglionic labeling techniques (Maslany et al. 1991, 1992). To date, there is no simple method to characterize the somatotopic distribution of these sensory fibers electrophysiologically.

We have developed a novel electrophysiological technique that allows us to easily assess the topographical specificity of synaptic connections in the cuneate nucleus. Here, we report that current passed through cuff electrodes placed over forepaw digits exclusively activates cutaneous sensory neurons. Stimulation of

cutaneous fibers innervating a particular digit evokes synaptic responses in discrete locations in the cuneate nucleus. Our results suggest that this technique is sensitive enough to determine the precise somatotopic distribution of cutaneous sensory axons in the cuneate nucleus and spinal cord. Because of limitations on our supply of bioactive ARTN, the topographical specificity of long-distance regeneration has only been assessed in one animal. Although there is no consensus regarding the specificity of regeneration, synaptic responses evoked by cutaneous axons were present in the cuneate nucleus, suggesting that this method is sensitive enough to assess specificity following regeneration.

Materials and Methods

At least one hour prior to exposure of the brainstem, 1 mg/kg dexamethasone was given to prevent cerebral edema. Animals were anesthetized using 2.5% isofluorane for the duration of all terminal electrophysiology experiments and body temperature was maintained by a 37°C warming pad placed underneath the animal. Under these conditions, animals breathe on their own and evoked field potentials were stable for at least 8 hours. The cervical spinal cord was exposed as described above and the brainstem was exposed by careful removal of the occipital bone and retraction of the C2 vertebra with a spinal clamp. Gentle suction was used to remove the entire cerebellum in order to have better access to the cuneate nucleus. The dura was removed just prior to recording. The median and ulnar nerves were dissected and metal hooks were wrapped around the nerves and secured in place using Kwik-Cast Silicon Elastomer (World Precision Instruments) and stimulated as described in Chapter 2.

Skin over the digits was stimulated using novel cuff electrodes. Cuff electrodes were made by filling small polyethylene tubing with electrode conductive gel (Signagel) and fitting the distal end with a wire. These were placed on the first and fourth digit of the forelimb. The return electrode wires were inserted just under the skin at the base of the digit (Fig. A-1). The digits were stimulated with square, 50 μs, 10-V pulses delivered at 5 Hz using an A-M Systems Isolated Pulse Stimulator (Model 2100).

Brainstem recordings were obtained using a 1x16-channel microelectrode with recording spots vertically spaced at 100 μm (NeuroNexus). Using a stereotactic micromanipulator, we were able to record field potentials from a two-dimensional grid covering a 0.9 mm^2 area. Extracellular recordings were measured from 7 mediolateral recording sites positioned 100 μm apart from 1.2 mm through 0.6 mm lateral to the midline and 0.6 mm caudal to the obex. The shaft of the electrode was driven 1.5 mm into the brainstem so that the dorsal-most channel was positioned at the surface. Single responses were recorded with a 16 channel amplifier (A-M Systems, Model 3600), filtered (0.3 Hz – 10 kHz) and digitized (16 bits, 20 kHz sampling rate) using a National Instruments system running custom LabVIEW software. At each recording site, 50 individual traces were averaged and stored for analysis offline. Recordings were made in the spinal cord using the same recording locations described in Chapter 2 to verify that only cutaneous fibers were being stimulated with this technique.

The amplitude of the synaptic response was used as a measure of the summed, short latency (monosynaptic) response in the brainstem at each location. Three-dimensional maps were used to visualize the amplitude of the synaptic responses at each location in the two-dimensional grid.

Results

Finger cuff electrodes stimulate cutaneous sensory afferents. To assess if the cuff electrodes specifically stimulated cutaneous fibers, we first recorded extracellular potentials in the spinal cord of intact animals. Synaptic potentials evoked by stimulation of the digits are more dorsally located than those evoked by stimulation of mixed nerves, which contain input from muscle afferents as well as cutaneous. The location where the synaptic response was largest was located approximately 0.3 mm from the dorsal surface of the spinal cord whereas stimulation of mixed nerves resulted in maximal

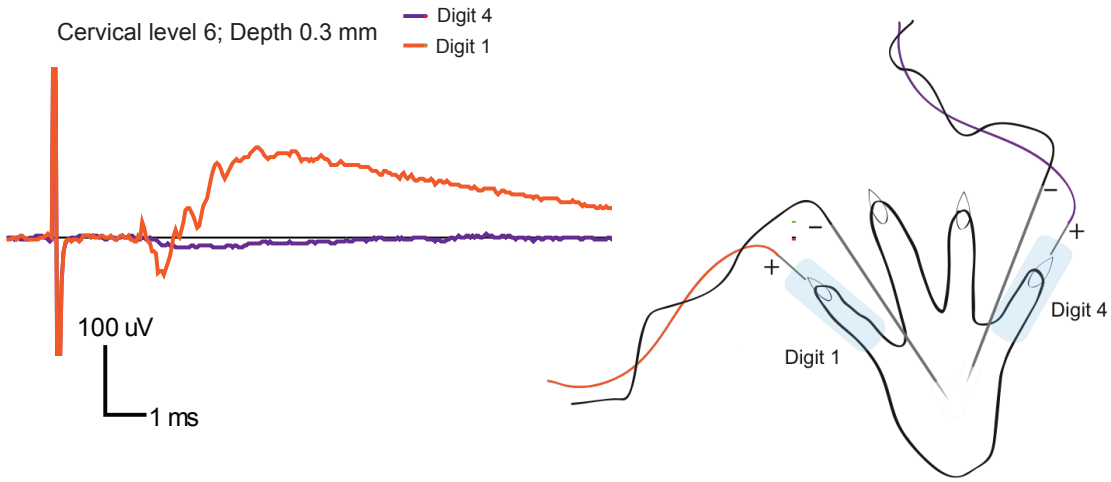

A-1: Cuff electrodes stimulate cutaneous sensory fibers. The panel on the left shows spinal cord field potentials recorded from the C6 spinal level with stimulation of digit 1 (orange) or digit 4 (purple). At C6, a synaptic response is present for digit 1 at a depth of 0.3 mm into the spinal cord. There is no response for digit 4 at this spinal level. The panel on the right depicts the placement of the cuff electrodes and return electrodes on the rat forepaw.

responses located approximately 1.0 mm from the dorsal surface of the spinal cord (Fig. A-1). In addition, stimulation of the digits did not produce a visible muscle response with any stimulus tested from 2 V to 12 V. These data demonstrate that our technique stimulates cutaneous sensory afferents.

Individual stimulation of the skin over the first and fourth digits evoked synaptic responses in different spinal segments. Axons receiving cutaneous information from the first digit synapsed primarily in the C6 spinal segment (Fig. A-1) while those from the fourth digit synapsed primarily in the C8 segment, as would be predicted by dermatome maps. These data indicate that this cuff-electrodes placed over the digits allow for the sensitively determination of the topographical distribution of cutaneous afferents in the spinal cord.

The first and fourth digits are represented in discrete locations in the brainstem. We next recorded synaptic potentials in the brainstem of intact animals using the same digit stimulation technique. Stimulation of cutaneous fibers with cuff-electrodes evoked EPSPs in the brainstem similar in latency to those observed with mixed nerve stimulation. Amplitudes were approximately 150 μV at the location of greatest synaptic input, 10-fold smaller than what was observed with direct stimulation of the median nerve. To determine whether this technique could assess the precise pattern of synaptic input from the first and fourth digits, we created a three-dimensional contour map showing the amplitudes of the synaptic responses in the cuneate nucleus at all 112 locations from which we recorded. For each digit, a clear peak was observed (Fig. A-2). We consistently observed that the first digit synapsed in a dorsomedial location in the cuneate nucleus while the fourth digit synapsed deeper and more laterally in the cuneate nucleus (Fig. A-2). In the four animals tested, we observed similar innervation patterns in all but one animal. Patterns were very similar on the left and right side in all animals.

These data indicate that electrophysiological mapping of the projection pattern of cutaneous sensory afferents is a sensitive method for assessing the somatotopic map in the cuneate nucleus in uninjured animals.

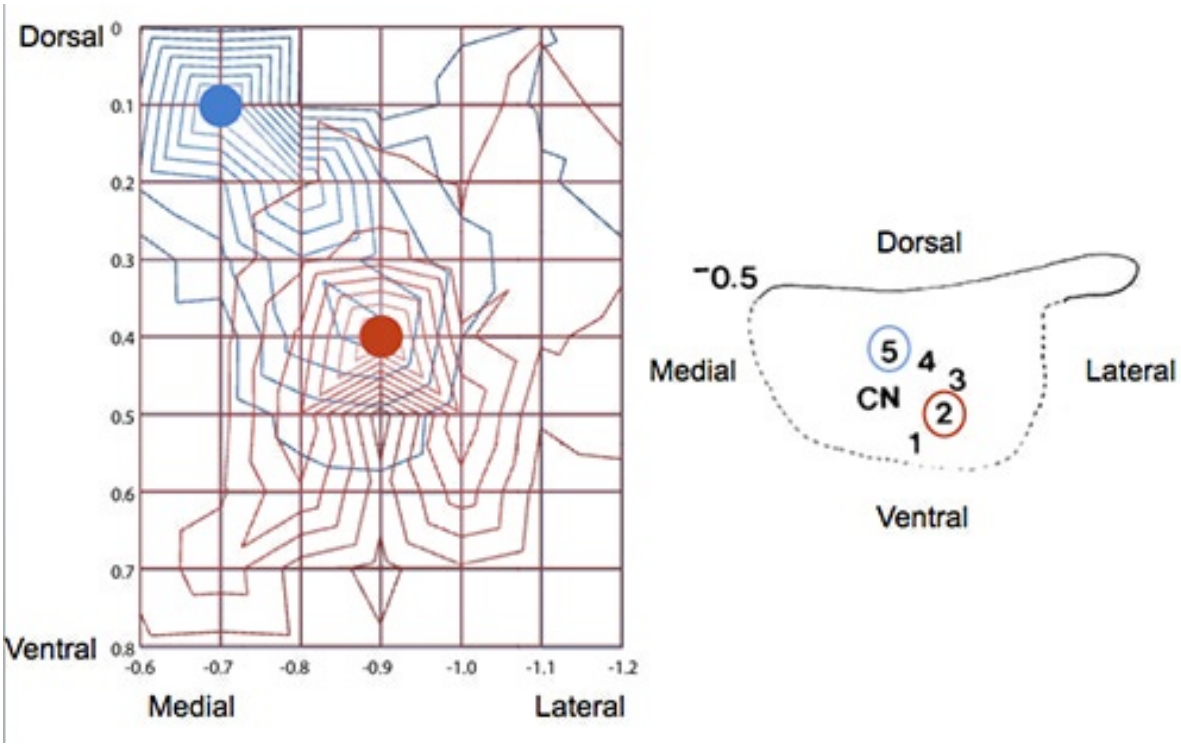

A-2: Digits 1 and 4 project to distinct regions in the cuneate nucleus. The panel on the left shows a contour map displaying the amplitudes at each location map. Each line represents 20 μV. Digit 4 connects with neurons in a discrete area centralized at 0.1 mm from the surface and 0.7 mm from the midline while Digit 1 connects with neurons centralized at 0.4 mm from the surface and 0.9 mm from the midline. This corresponds well with maps of axonal projections developed from transganglionic labeling studies (left panel). Maslany et al. (1991) included the pollux nub as digit 1, which accounts for the discrepancy in numbering.

Cutaneous fibers regenerate to the cuneate nucleus with ARTN treatment. Although we were not able to assess the extent to which axon regeneration is topographically specific because of limitations on the supply of bioactive ARTN, we were able to map the synaptic input from the digits in one animal following DR crush, ARTN treatment and 6 months for recovery. We observed small but appreciable synaptic responses in the cuneate nucleus evoked by digit stimulation on the crushed side in an ARTN-treated animal 6 months after DR crush. The amplitude of the maximal response

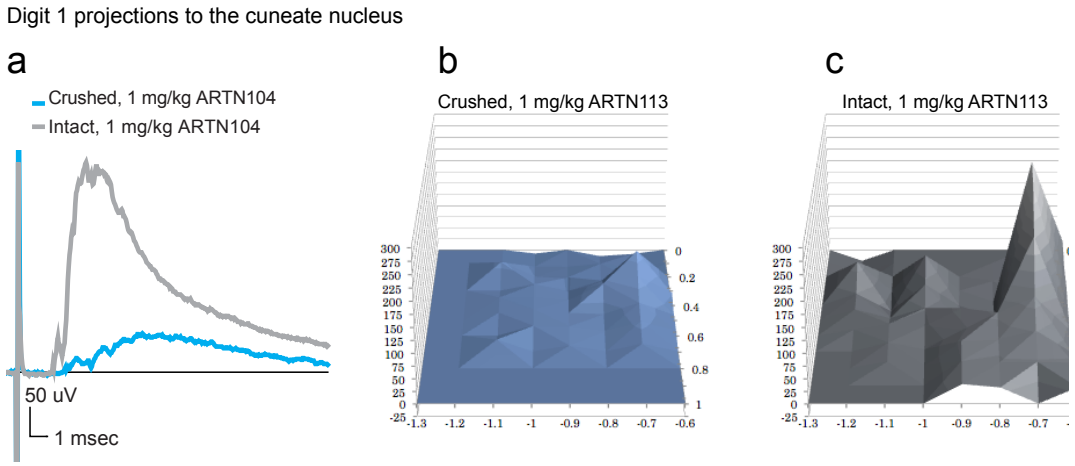

A-3: ARTN113 promotes functional regeneration of cutaneous sensory fibers to the cuneate nucleus following DR crush. (a) Synaptic responses recorded on the crushed and intact side evoked by stimulation of the first digit. There are clearly cutaneous fibers regenerating to the cuneate nucleus following DR crush and ARTN treatment. (b,c) Three-dimensional maps with the mediolateral position on the x-axis, the dorsoventral position on the y-axis and the amplitude of the response on the z-axis for the crushed (b) and intact (c) sides. Given the size of the potentials, on the crushed side, it is difficult to determine whether there is a peak in this one animal.

was approximately 25 μV. This suggests that cutaneous fibers regenerate back to the cuneate nucleus. When we mapped the location of all the responses, we did not observe the same precise pattern. The peak synaptic response appeared more spread out than the distribution on the intact side, consistent with the less organized pattern of axon terminals noted in the anatomical tracing experiments (Figs. 2-3, 2-5). These data suggest that this technique is sensitive enough to determine the extent to which regenerating axons project back to the correct locations in the brainstem.

Discussion

Only recently have investigators begun to study whether regeneration might result in topographically specific or targeted regeneration (Tang et al. 2007b; Harvey et al. 2010; Smith et al. 2012). As such, new, more sensitive methods for assessing the somatotopic map are required. In this study, we have demonstrated that use of a novel cuff-electrode placed over the digit stimulates cutaneous fibers. We have further demonstrated that this technique is sensitive enough to allow mapping of distinct somatotopic distributions in the intact spinal cord and brainstem. Lastly, our results suggest that this method is sensitive enough to assess the topographic distribution of sensory axons following regeneration in an animal after DR crush and ARTN treatment.

Although we only assessed specificity in one animal after regeneration, these data provide additional evidence that regeneration to the brainstem is targeted. Cutaneous fibers reach the cuneate nucleus and synapse with neurons there. While we currently have no method to determine if incorrect sensory modalities project to the cuneate nucleus, this provides some evidence that cutaneous fibers—at least in one

animal—are reaching their appropriate target region. We did, however, observe limitations in ARTN's ability to promote topographically specific regeneration. In this animal, we did not observe discrete projection areas of cutaneous sensory afferents from the different digits in the cuneate nucleus on the injured side. This preliminary experiment will need to be repeated in order to determine the extent to which ARTN promotes specific regeneration.

Electrophysiology is a powerful tool for assessing functional connections. Unlike previous methods using transganglionic tracing with CTB or WGA that only allow determination of the anatomical distribution of axons (Maslany et al. 1991, 1992), electrophysiology has the benefit of assessing whether synaptic connections are topographically correct. Additionally, this electrophysiological method has the advantage of using cuff-electrodes that reproducibly stimulate cutaneous fibers. Older studies used manual manipulation of skin and muscle to map areas in the brainstem, which is both time consuming and sensitive to human error (Campbell et al. 1974). A functional and reproducible measure of specificity will provide valuable insight into the degree of recovery in animal models of SCI. Potential therapeutics might promote regeneration that is anatomically non-specific—with widespread axonal growth—but that synaptic connections might be topographically specific due to synaptic pruning, interactions with cell adhesion molecules or other properties affecting synaptogenesis. This tool combined with neurotracing techniques would allow us to answer these questions and evaluate future therapeutic agents in their ability to promote specific regeneration.

Appendix B

HAM Sandwich:

A Surgical Method for Repairing Avulsed Roots

Introduction

Traction injury caused by high-speed motor vehicle accidents (MVA) and severe falls frequently result in avulsion of brachial plexus roots, completely separating roots from the spinal cord (Midha 1997; Moran et al. 2005; Giuffre et al. 2010; Limthongthang et al. 2013). Brachial plexus injuries disrupt the flow of information between the spinal cord and brain, resulting in paralysis and paresis of the arm. Avulsions carry the worse prognosis of all brachial plexus injuries.

Reconnecting avulsed brachial plexus roots to the spinal cord pose a major surgical challenge. While nerves can be surgically reconnected in some cases, these surgeries are complicated, often involving harvesting extraplexus nerves (i.e. intercostal nerves) (Shin et al. 2004; Chuang 2009; Giuffre et al. 2010; Limthongthang et al. 2013). Since 70% of brachial plexus injuries affect all of the roots from cervical level 5 (C5) through thoracic level 1 (T1), finding enough nervous tissue to repair all roots is difficult (Hsu et al. 2004). The prognosis worsens as more roots are damaged. Even when surgical means can be used to reattach the severed roots, axons fail to regrow into the spinal cord, resulting in permanent loss of sensory function. Thus, there is a need for a new surgical technique that allows avulsed roots to be reattached to the spinal cord so axons, given appropriate therapeutic agents, can regenerate through the lesion, and into the spinal cord.

A suture-less light-activated technique has been developed to repair delicate tissue, including injuries to the eyelid skin, corneal surface, and vocal folds, by reconnecting extracellular matrix (ECM) proteins with a photochemical bond to close the wound with a continuous seal (Franco et al. 2011; Wang et al. 2011b; Ni et al. 2012; Yang et al. 2012; Fairbairn et al. 2014). Recently, this technique has been modified to

repair transected peripheral nerves by cross-linking devitalized human amniotic membrane (HAM) to the nerve sheath (O'Neill et al. 2009). HAM that has been soaked in Rose Bengal (RB), a photochemically activated dye, is wrapped around the peripheral nerve stumps, sutured in place and then bonded to the collagen in the epineurium using a laser. The illumination of RB with laser light induces collagen fiber cross-linking between the HAM and the nerve sheath. This creates an isolated endoneurial environment, which promotes significant regeneration of peripheral sensory axons (O'Neill et al. 2009).

Here, we report that HAM can be used to cross-link cut dorsal roots (DRs) to the spinal cord, inducing regeneration across the lesion. This requires no sutures and can easily repair multiple roots by sandwiching them between pieces of HAM. We have named this surgical method the "HAM sandwich" technique. Axons terminate at the DR entry zone (DREZ) similar to axons following DR crush. In a few animals treated with low-dose ARTN113, we observed $CGRP^+$ axons crossing into the dorsal horn and several $CGRP^+$ axons in laminae 1 and 2 suggesting that this method repairs roots well enough to allow regeneration into the spinal cord.

Materials and Methods

These experiments were done using 9 Sprague-Dawley rats (Charles River Laboratory). All animal experiments are done using 2.5% isofluorane anesthesia. Body temperature is maintained using a 37°C warming pad placed under the rat. Unilateral hemilaminectomy was performed from C5 to T1 on the left side so the DRs are visible. The dura was opened over the dorsal roots and each DR is gently isolated using forceps and glass hooks.

Isolated HAM (provided by the laboratory of Dr. Robert Redmond) stored on parafilm is cut into a strip approximately 1 mm wide and at least twice as long as the root area (about 30 mm long). This is soaked in RB for 10 minutes and transferred to waxed paper backing. #7 Dumostar forceps are used to gently pull HAM and backing underneath each root from C5 through T1. Once HAM is in place, waxed paper backing is removed. The brachial roots are cut midway between the DRG and spinal cord using Vannas spring scissors with a 2.5 mm cutting edge angled to the side (Fine Science Tools). The extra length of HAM is folded over creating a sandwich and gently pressed to create a seal. The area is thoroughly dried and the exposed roots are illuminated with a 532 nm laser beam for 3 minutes (Fig. B-1).

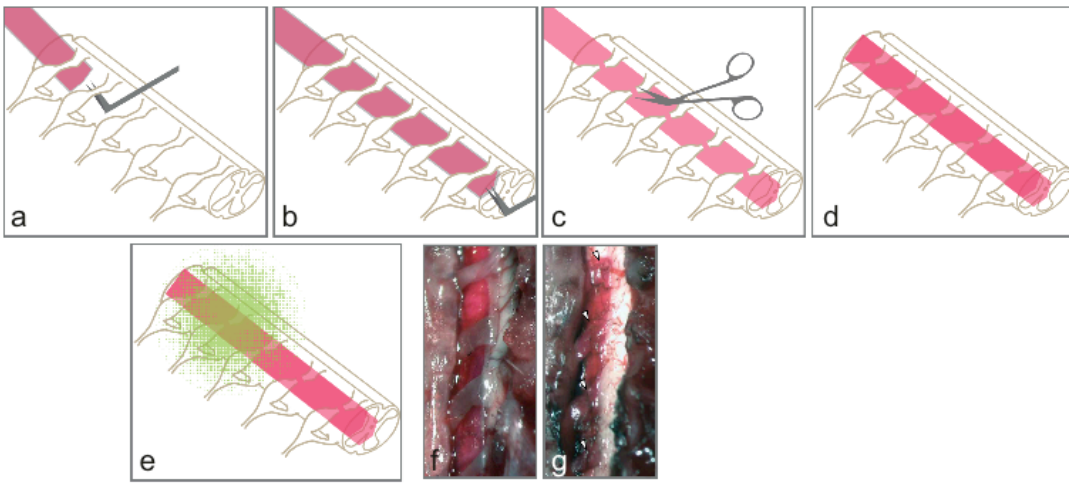

Figure B-1: Scheme showing the HAM sandwich technique for repair of cut dorsal roots. RB soaked HAM is pulled underneath DRs with fine forceps (a,b). DRs are cut and then the remaining HAM is folded over to make a sandwich around the cut DRs (c,d). The area is illuminated with 532 nm laser for 5 minutes (e). (f) HAM and backing pulled underneath the roots before they are cut. (g) After irradiation, HAM is bonded to the roots. Arrowheads mark the cuts and distal stumps are touching proximal stumps.

The muscle is closed over the spinal cord in layers and the skin is closed. Post-operative care is provided as described earlier (Chapter 2). Animals recover for 6 weeks to allow for regeneration. 1 week before the tissue is harvested, 4 µl of a 1% solution 10,000 MW dextran conjugated to Alexa Fluor 488 (Life Sciences) in PBS is injected into the radial, median and ulnar nerve using a 10 µl Hamilton syringe. In a cohort of 3 animals, we administered 1 mg/kg ARTN113 via subcutaneous injection on a 2 week, Monday-Wednesday-Friday schedule and did not inject the nerves before harvesting tissue. Animals were perfused with 4% paraformaldehyde and the spinal cords with DRGs attached were removed. Tissue was cryoprotected in 20% sucrose in PBS.

To assess regeneration in the DR, whole-mounts of the root were imaged at a resolution of 1024 x 1024 pixels using the 10X objective on a Leica SP2 confocal microscope running the Leica Application Suite software. 30 µm Z-stacks were made using 1.5 µm steps with 2 line averages and 4 stack averages per focal plane. Fixed exposure settings were used and the images were adjusted for brightness. To assess regeneration into the spinal cord, 25 µm cryostat sections were visualized either directly for the presence of dextran labeled axons. These were imaged using the same settings described previously (Chapter 2). Cryostat sections from the 3 ARTN113-treated animals were immunostained for the presence $CGRP^{+}$ axons as described earlier (Chapter 3).

Results

The "HAM Sandwich" technique repairs roots so that axons can regenerate across the lesion. To assess the ability to repair cut DRs using HAM, we imaged DR whole mounts for the presence of dextran-labeled axons 6 weeks after DR cut and repair. HAM could still be observed holding the roots together after 6 weeks and had to

be removed carefully for imaging. Once HAM had been removed, roots were delicate but held together suggesting that HAM promoted tissue repair. Dextran labeled axons were abundant distal to the root. The lesion was clearly visible and axons were observed crossing through the lesion into the proximal root (Fig. B-2). These data indicate that roots were adequately repaired with HAM so that axons could regenerate across the lesion. In the absence of pharmacological treatment, no axons were observed crossing the DREZ and entering the dorsal horn, similar to what is observed following DR crush in the absence of treatment.

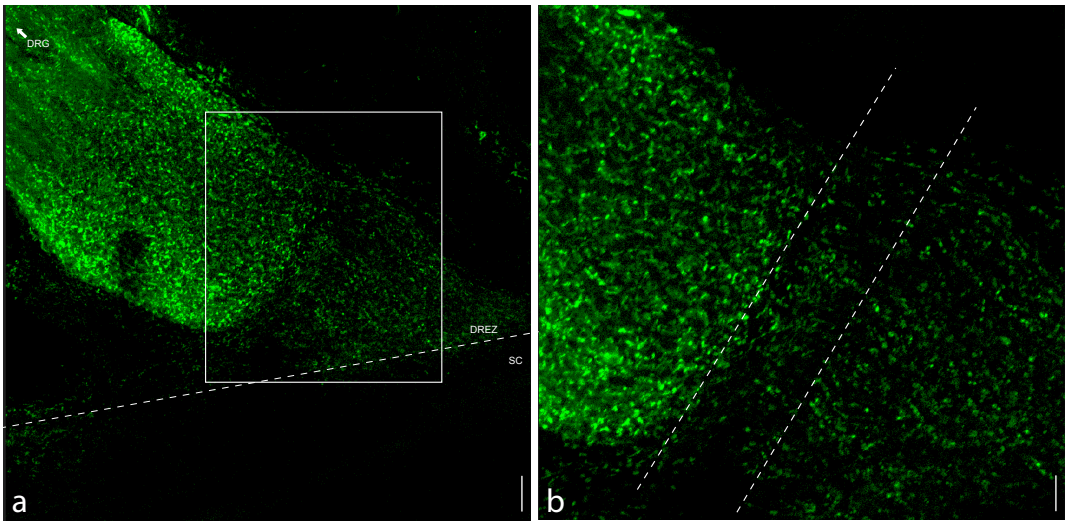

Figure B-2: Axons regenerate past the lesion. (a). Representative image of a DR whole mount showing abundant dextran-labeled axons distal to the lesion and several dextran-labeled axons regenerating through the lesion. (b) Close up of the area in the box. Dotted lines mark the lesion. Scale bars are 50 μm in (a) and 100 μm (b).

Low-dose artemin-treatment combined with HAM repair promotes regeneration of cut axons across the DREZ. To test the regenerative capacity of sensory axons after DR HAM-repair, 3 animals were treated with 1 mg/kg ARTN113. At this dose, this batch

of ARTN113 did not result in regeneration of large diameter axons into the spinal cord following DR crush but small diameter nociceptive fibers were able to regenerate (data not shown). Cross-sections through the spinal cord and DR from animals with "HAM sandwich" repair and low-dose ARTN treatment were immunostained for CGRP, a marker for small, nociceptive fibers. We observed many $CGRP^+$ axons crossing the lesion in the DR. Remarkably, we also observed a few $CGRP^+$ axons in the most superficial laminae in the dorsal horn, suggesting that axons can regenerate into the spinal cord after DR cut (Fig. B-3). We assessed CGRP staining in the C7 segment, which is flanked by cut DRs two segments rostral and caudal to it. Therefore, it is unlikely that the observed immunoreactive axons are sprouting from neighboring uninjured roots. Furthermore, we observed no CGRP immunoreactivity in the spinal cord

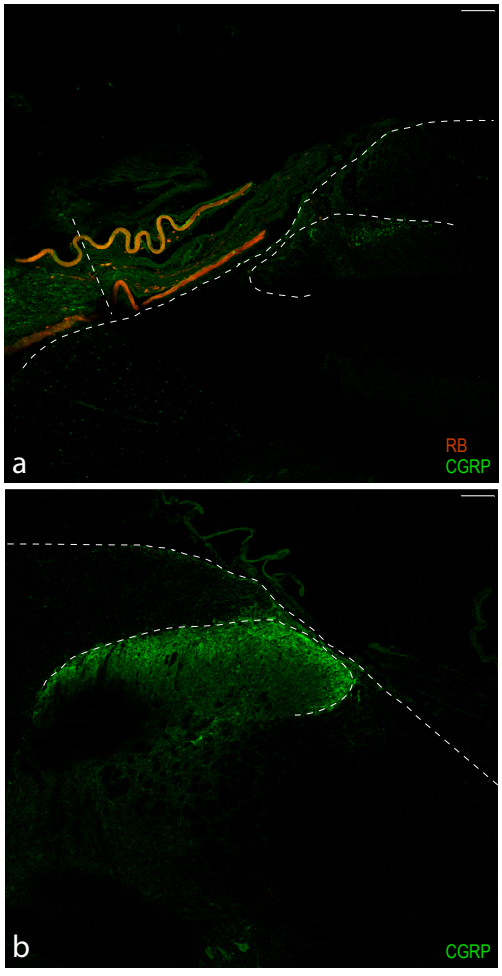

Figure B-3: Axons regenerate into the dorsal horn with ARTN113 and HAM sandwich repair. (a) Cross-section through the DR and spinal cord on the crushed side shows $CGRP^+$ axons regenerating through the lesion. $CGRP^+$ axons are present in the spinal cord indicating some regenerated across the DREZ. RB soaked HAM is still bound to the DR after 6 weeks recovery. (b) A cross-section through the spinal cord on the intact side in the same animal showing abundant CGRP label in the superficial laminae of the dorsal horn.

in HAM repaired, untreated rats suggesting that these axons indeed represent regeneration.

Discussion

Reconnecting avulsed roots to the spinal cord poses a major surgical challenge. Here, we have developed a novel surgical technique, called “HAM sandwich,” for reconnecting cut roots to the proximal nerve stump in a rat model of dorsal root avulsion. The discontinuity is repaired by ensheathing the root in HAM, which is then bonded to the epineurium using RB and laser light. In the absence of pharmacological treatment, axons regenerate across the lesion, indicating that the HAM acts as a conduit. As expected, these axons stop regenerating when they reach the inhibitory barrier of the DREZ, similar to axons in a DR crush model of injury. When animals were treated with low-dose ARTN and the HAM sandwich surgical technique, peptidergic axons were readily able to cross the DREZ and enter the spinal cord where they terminated in laminae 1 and 2 in the dorsal horn. Because of limits on our supply of ARTN113, we were not able to treat animals with an appropriately higher dose to promote regeneration of large diameter fibers. It would be interesting to determine if large diameter neurons are equally able to regenerate following DR cut.

An advantage to DR cut model of brachial plexus injury is that it virtually eliminates all concern regarding spared axons because the roots are physically disconnected from the spinal cord. Until now, surgical repair in a rodent model was impossible. Roots could not be reconnected with sutures because they are too friable and other methods using fibrin glue or extra-plexus nerve donors to reconnect roots were met with limited success (Huang et al. 2009; Li et al. 2004; Wu et al. 2009). Using

this model, one can study sensory axon regeneration in rodent models without conflating sprouting and true regeneration.

In human avulsion injuries, traction forcibly pulls the DR from the spinal cord leaving no proximal stump with which to connect the distal end. In a more clinically relevant injury model, an alternative HAM repair technique will be necessary. HAM binds to the collagen of the DR and spinal cord as well as it does to itself. Preliminary experiments suggest that HAM may be able to bind the root to the spinal cord without sandwiching the tissue between two layers. Future work will be needed to determine if HAM could hold avulsed DRs against the cord, allowing axons to regenerate into the cord with appropriate neurotrophic support.

These data indicate that HAM sandwich is a viable method for repairing avulsed dorsal roots. Given the ease with which these materials could be adapted and approved for use in human brachial plexus injuries, this technique provides an exciting prospect for the repair of avulsed brachial roots.

References

Aguayo AJ, David S, Bray GM. Influences of the glial environment on the elongation of axons after injury: transplantation studies in adult rodents. J Exp Biol. 1981 Dec;95(1981):231–40.

Aguayo AJ, Dickson R, Trecarten J, Attiwell M, Bray GM, Richardson P. Ensheathment and myelination of regenerating PNS fibres by transplanted optic nerve glia. Neurosci Lett. 1978 Oct;9(2-3):97–104.

Airaksinen MS, Saarma M. The GDNF family: signalling, biological functions and therapeutic value. Nat Rev Neurosci. 2002 May;3(5):383–94.

Alto LT, Havton L a, Conner JM, Hollis Ii ER, Blesch A, Tuszynski MH. Chemotropic guidance facilitates axonal regeneration and synapse formation after spinal cord injury. Nat Neurosci. Nature Publishing Group; 2009 Sep;12(9):1106–13.

Avellino AM, Hart D, Dailey AT, MacKinnon M, Ellegala D, Kliot M. Differential macrophage responses in the peripheral and central nervous system during wallerian degeneration of axons. Exp Neurol. 1995 Dec;136(2):183–98.

Baloh RH, Gorodinsky a, Golden JP, Tansey MG, Keck CL, Popescu NC, et al. GFRalpha3 is an orphan member of the GDNF/neurturin/persephin receptor family. Proc Natl Acad Sci U S A. 1998 a May 12;95(10):5801–6.

Baloh RH, Tansey MG, Golden JP, Creedon DJ, Heuckeroth RO, Keck CL, et al. TrnR2, a novel receptor that mediates neurturin and GDNF signaling through Ret. Neuron. 1997 May;18(5):793–802.

Baloh RH, Tansey MG, Johnson EM, Milbrandt J. Functional mapping of receptor specificity domains of glial cell line-derived neurotrophic factor (GDNF) family ligands and production of GFRalpha1 RET-specific agonists. J Biol Chem. 2000 Feb 4;275(5):3412–20.

Baloh RH, Tansey MG, Lampe P a, Fahrner TJ, Enomoto H, Simburger KS, et al. Artemin, a novel member of the GDNF ligand family, supports peripheral and central neurons and signals through the GFRalpha3-RET receptor complex. Neuron. 1998 b Dec;21(6):1291–302.

Beggs HE, Soriano P, Maness PF. NCAM-dependent neurite outgrowth is inhibited in neurons from Fyn-minus mice. J Cell Biol. 1994 Nov 1;127(3):825–33.

Bennett DLH, Boucher TJ, Armanini MP, Poulsen KT, Michael GJ, Priestley J V, et al. The Glial Cell Line-Derived Neurotrophic Factor Family Receptor Components Are Differentially Regulated within Sensory Neurons after Nerve Injury. Neurosci Res. 2000;20(1):427–37.

Benson MD, Romero MI, Lush ME, Lu QR, Henkemeyer M, Parada LF. Ephrin-B3 is a myelin-based inhibitor of neurite outgrowth. Proc Natl Acad Sci U S A. 2005 Jul 26;102(30):10694–9.

Bespalov MM, Saarma M. GDNF family receptor complexes are emerging drug targets. Trends Pharmacol Sci. 2007 Feb;28(2):68–74.

Bespalov MM, Sidorova Y a, Tumova S, Ahonen-Bishopp A, Magalhães AC, Kulesskiy E, et al. Heparan sulfate proteoglycan syndecan-3 is a novel receptor for GDNF, neurturin, and artemin. J Cell Biol. 2011 Jan 10;192(1):153–69.

Bonner JF, Connors TM, Silverman WF, Kowalski DP, Lemay M a, Fischer I. Grafted neural progenitors integrate and restore synaptic connectivity across the injured spinal cord. J Neurosci. 2011 Mar 23;31(12):4675–86.

Bradbury EJ, McMahon SB, Ramer MS. Keeping in touch: sensory neurone regeneration in the CNS. Trends Pharmacol Sci. 2000 Oct;21(10):389–94.

Bradbury EJ, Moon LDF, Popat RJ, King VR, Bennett GS, Patel PN, et al. Chondroitinase ABC promotes functional recovery after spinal cord injury. Nature. 2002 May;416(6881):636–40.

Cafferty WBJ, Duffy P, Huebner E, Strittmatter SM. MAG and OMgp synergize with Nogo-A to restrict axonal growth and neurological recovery after spinal cord trauma. J Neurosci. 2010;30:6825–37.

Campbell SK, Parker TD, Welker W. Somatotopic Organization of the External Cuneate Nucleus in Albino Rats. Brain Res. 1974;77:1–23.

Carlstedt T, Cullheim S, Risling M, Ulfhake B. Nerve fibre regeneration across the PNS-CNS interface at the root-spinal cord junction. Brain Res Bull. 1989 Jan;22(1):93–102.

Chen H-H, Tourtellotte WG, Frank E. Muscle spindle-derived neurotrophin 3 regulates synaptic connectivity between muscle sensory and motor neurons. J Neurosci. 2002 May;22(9):3512–9.

Chew DJ, Leinster VHL, Sakthithasan M, Robson LG, Carlstedt T, Shortland PJ. Cell death after dorsal root injury. Neurosci Lett. 2008 Mar;433(3):231–4.

Chuang DC-C. Adult brachial plexus reconstruction with the level of injury: review and personal experience. Plast Reconstr Surg. 2009;124:e359–e369.

Cua RC, Lau LW, Keough MB, Midha R, Apte SS, Yong VW. Overcoming neurite-inhibitory chondroitin sulfate proteoglycans in the astrocyte matrix. Glia. 2013 Jun;61(6):972–84.

David S, Aguayo AJ. Axonal elongation into peripheral nervous system “bridges” after central nervous system injury in adult rats. Science. 1981;214:931–3.

Davies SJ, Goucher DR, Doller C, Silver J. Robust regeneration of adult sensory axons in degenerating white matter of the adult rat spinal cord. J Neurosci. 1999 Jul 15;19(14):5810–22.

Dobkin BH, Havton L a. Basic advances and new avenues in therapy of spinal cord injury. Annu Rev Med. 2004 Jan;55(1):255–82.

Durbec PL, Larsson-Blomberg LB, Schuchardt a, Costantini F, Pachnis V. Common origin and developmental dependence on c-ret of subsets of enteric and sympathetic neuroblasts. Development. 1996 Jan;122(1):349–58.

Elitt CM, McIlwrath SL, Lawson JJ, Malin S a, Molliver DC, Cornuet PK, et al. Artemin overexpression in skin enhances expression of TRPV1 and TRPA1 in cutaneous sensory neurons and leads to behavioral sensitivity to heat and cold. J Neurosci. 2006 Aug 16;26(33):8578–87.

Enomoto H, Crawford P a, Gorodinsky a, Heuckeroth RO, Johnson EM, Milbrandt J. RET signaling is essential for migration, axonal growth and axon guidance of developing sympathetic neurons. Development. 2001 Oct;128(20):3963–74.

Fairbairn NG, Randolph M a, Redmond RW. The clinical applications of human amnion in plastic surgery. J Plast Reconstr Aesthet Surg. Elsevier Ltd; 2014 Jan 31;

Fournier HD, Mercier P, Menei P. Repair of avulsed ventral nerve roots by direct ventral intraspinal implantation after brachial plexus injury. Hand Clin. 2005. p. 109–18.

Fraher JP. The transitional zone and CNS regeneration. J Anat. 2000 Jan;196 (Pt 1:137–58.

Franco R a, Dowdall JR, Bujold K, Amann C, Faquin W, Redmond RW, et al. Photochemical repair of vocal fold microflap defects. Laryngoscope. 2011 Jul;121(6):1244–51.

Gardell LR, Wang R, Ehrenfels C, Ossipov MH, Rossomando AJ, Miller S, et al. Multiple actions of systemic artemin in experimental neuropathy. Nat Med. 2003 Nov;9(11):1383–9.

Geoffroy CG, Zheng B. Myelin-associated inhibitors in axonal growth after CNS injury. Curr Opin Neurobiol. 2014 Mar 6;27C:31–8.

Giger RJ, Hollis ER, Tuszynski MH. Guidance molecules in axon regeneration. Cold Spring Harb Perspect Biol. 2010 Jul 1;2(7):a001867.

Giuffre JL, Kakar S, Bishop AT, Spinner RJ, Shin AY. Current Concepts of the Treatment of Adult Brachial Plexus Injuries. J Hand Surg Am. 2010;35:678–88.

Golden JP, Hoshi M, Nassar M a, Enomoto H, Wood JN, Milbrandt J, et al. RET signaling is required for survival and normal function of nonpeptidergic nociceptors. J Neurosci. 2010 Mar 17;30(11):3983–94.

Harvey P. Functional Regeneration of Sensory Afferents in a Model of Brachial Plexus Injury. Tufts University; 2009.

Harvey P a, Lee DHS, Qian F, Weinreb PH, Frank E. Blockade of Nogo receptor ligands promotes functional regeneration of sensory axons after dorsal root crush. J Neurosci. 2009 May 13;29(19):6285–95.

Harvey P, Gong B, Rossomando AJ, Frank E. Topographically specific regeneration of sensory axons in the spinal cord. Proc Natl Acad Sci U S A. 2010 Jun 22;107(25):11585–90.

Honma Y, Araki T, Gianino S, Bruce A, Heuckeroth R, Johnson E, et al. Artemin is a vascular-derived neurotropic factor for developing sympathetic neurons. Neuron. 2002 Jul 18;35(2):267–82.

Honma Y, Kawano M, Kohsaka S, Ogawa M. Axonal projections of mechanoreceptive dorsal root ganglion neurons depend on Ret. Development. 2010 Jul;137(14):2319–28.

Hsu SPC, Shih Y-H, Huang M-C, Chuang T-Y, Huang W-C, Wu H-M, et al. Repair of multiple cervical root avulsion with sural nerve graft. Injury. 2004 Oct;35(9):896–907.

Hu P, McLachlan EM. Distinct functional types of macrophage in dorsal root ganglia and spinal nerves proximal to sciatic and spinal nerve transections in the rat. Exp Neurol. 2003 Dec;184(2):590–605.

Ibáñez CF. Beyond the cell surface: new mechanisms of receptor function. Biochem Biophys Res Commun. Elsevier Inc.; 2010 May 21;396(1):24–7.

Jeong DG, Park WK, Park S. Artemin activates axonal growth via SFK and ERK-dependent signalling pathways in mature dorsal root ganglia neurons. Cell Biochem Funct. 2008;(September 2007):210–20.

Jing S, Yu Y, Fang M, Hu Z, Holst PL, Boone T, et al. GFRalpha-2 and GFRalpha-3 are two new receptors for ligands of the GDNF family. J Biol Chem. 1997 Dec;272(52):33111–7.

Kaneko S, Iwanami A, Nakamura M, Kishino A, Kikuchi K, Shibata S, et al. A selective Sema3A inhibitor enhances regenerative responses and functional recovery of the injured spinal cord. Nat Med. 2006 Dec;12(12):1380–9.

Kawamura Y, Dyck PJ. Permanent axotomy by amputation results in loss of motor neurons in man. J. Neuropathol. Exp. Neurol. 1981. p. 658–66.

Keast JR, Forrest SL, Osborne PB. Sciatic nerve injury in adult rats causes distinct changes in the central projections of sensory neurons expressing different glial cell line-derived neurotrophic factor family receptors. J Comp Neurol. 2010 Aug 1;518(15):3024–45.

Kim JE, Li S, GrandPré T, Qiu D, Strittmatter SM. Axon regeneration in young adult mice lacking Nogo-A/B. Neuron. 2003 May 24;38(2):187–99.

Kjaer S, Ibáñez CF. Identification of a surface for binding to the GDNF-GFR alpha 1 complex in the first cadherin-like domain of RET. J Biol Chem. 2003 Nov 28;278(48):47898–904.

Klein RD, Sherman D, Ho WH, Stone D, Bennett GL, Moffat B, et al. A GPI-linked protein that interacts with Ret to form a candidate neurturin receptor. Nature. 1997 Jul;387(6634):717–21.

Kotzbauer PT, Lampe PA, Heuckeroth RO, Golden JP, Creedon DJ, Johnson EM, et al. Neurturin, a relative of glial-cell-line-derived neurotrophic factor. Nature. 1996 Dec;384(6608):467–70.

Krzywinski M, Altman N. Points of Significance: Visualizing samples with box plots. Nat Methods. Nature Publishing Group; 2014 Jan 30;11(2):119–20.

Kwon BK, Liu J, Messerer C, Kobayashi NR, McGraw J, Oschipok L, et al. Survival and regeneration of rubrospinal neurons 1 year after spinal cord injury. Proc Natl Acad Sci U S A. 2002 Mar;99(5):3246–51.

Kwon BK, Sekhon LH, Fehlings MG. Emerging repair, regeneration, and translational research advances for spinal cord injury. Spine (Phila Pa 1976). 2010 Oct 1;35(21 Suppl):S263–70.

LaMotte CC, Kapadia SE, Shapiro CM. Central projections of the sciatic, saphenous, median, and ulnar nerves of the rat demonstrated by transganglionic transport of choleragenoid-HRP (B-HRP) and wheat germ agglutinin-HRP (WGA-HRP). J Comp Neurol. 1991 Sep 22;311(4):546–62.

Ledda F, Paratcha G, Sandoval-Guzmán T, Ibáñez CF. GDNF and GFRalpha1 promote formation of neuronal synapses by ligand-induced cell adhesion. Nat Neurosci. 2007 Mar;10(3):293–300.

Lee JK, Geoffroy CG, Chan AF, Tolentino KE, Crawford MJ, Leal MA, et al. Assessing Spinal Axon Regeneration and Sprouting in Nogo-, MAG-, and OMgp-Deficient Mice. Neuron. 2010;66:663–70.

Lee JK, Zheng B. Role of myelin-associated inhibitors in axonal repair after spinal cord injury. Exp Neurol. Elsevier Inc.; 2011 May 7;1–10.

Liebl DJ, Morris CJ, Henkemeyer M, Parada LF. mRNA expression of ephrins and Eph receptor tyrosine kinases in the neonatal and adult mouse central nervous system. J Neurosci Res. 2003 Jan 1;71(1):7–22.

Limthongthang R, Bachoura A, Songcharoen P, Osterman a L. Adult brachial plexus injury: evaluation and management. Orthop Clin North Am. Elsevier Inc; 2013 Oct;44(4):591–603.

Lin LF, Doherty DH, Lile JD, Bektesh S, Collins F. GDNF: a glial cell line-derived neurotrophic factor for midbrain dopaminergic neurons. Science. 1993 May;260(5111):1130–2.

Liu CN, Chambers WW. Intraspinal sprouting of dorsal root axons; development of new collaterals and preterminals following partial denervation of the spinal cord in the cat. AMA Arch Neurol Psychiatry. 1958 Jan 1;79(1):46–61.

Lu P, Blesch a., Graham L, Wang Y, Samara R, Banos K, et al. Motor Axonal Regeneration after Partial and Complete Spinal Cord Transection. J Neurosci. 2012 Jun 13;32(24):8208–18.

Lu P, Jones L., Snyder E., Tuszynski M. Neural stem cells constitutively secrete neurotrophic factors and promote extensive host axonal growth after spinal cord injury. Exp Neurol. 2003 Jun;181(2):115–29.

Luo W, Wickramasinghe SR, Savitt JM, Griffin JW, Dawson TM, Ginty DD. A hierarchical NGF signaling cascade controls Ret-dependent and Ret-independent events during development of nonpeptidergic DRG neurons. Neuron. 2007 Jun 7;54(5):739–54.

Luo X, Salgueiro Y, Beckerman SR, Lemmon VP, Tsoulfas P, Park KK. Three-dimensional evaluation of retinal ganglion cell axon regeneration and pathfinding in whole mouse tissue after injury. Exp Neurol. Elsevier Inc.; 2013 Sep;247(2013):653–62.

Di Maio A, Skuba A, Himes BT, Bhagat SL, Hyun JK, Tessler A, et al. In vivo imaging of dorsal root regeneration: rapid immobilization and presynaptic differentiation at the CNS/PNS border. J Neurosci. 2011 Mar 23;31(12):4569–82.

Malin S a, Davis BM, Molliver DC. Production of dissociated sensory neuron cultures and considerations for their use in studying neuronal function and plasticity. Nat Protoc. 2007 Jan;2(1):152–60.

Mannan K, Carlstedt T. Injuries to the brachial plexus. Surgery. 2006. p. 409–14.

Maslany S, Crockett DP, Egger MD. Somatotopic organization of the dorsal column nuclei in the rat: transganglionic labelling with B-HRP and WGA-HRP. Brain Res. 1991 Nov 8;564(1):56–65.

Maslany S, Crockett DP, Egger MD. Organization of cutaneous primary afferent fibers projecting to the dorsal horn in the rat: WGA-HRP versus B-HRP. Brain Res. 1992 Jan 8;569(1):123–35.

Masure S, Cik M, Pangalos MN, Bonaventure P, Verhasselt P, Lesage a S, et al. Molecular cloning, expression and tissue distribution of glial-cell-line-derived neurotrophic factor family receptor alpha-3 (GFRalpha-3). Eur J Biochem. 1998 Feb 1;251(3):622–30.

McPhail LT, Plunet WT, Das P, Ramer MS. The astrocytic barrier to axonal regeneration at the dorsal root entry zone is induced by rhizotomy. Eur J Neurosci. 2005 Jan;21(1):267–70.

Mendell LM, Sassoon EM, Wall PD. Properties of synaptic linkage from long ranging afferents onto dorsal horn neurones in normal and deafferented cats. J Physiol. 1978 Dec;285(1978):299–310.

Midha R. Epidemiology of brachial plexus injuries in a multitrauma population. Neurosurgery. 1997;40:1182–1188; discussion 1188–1189.

Milbrandt J, de Sauvage FJ, Fahrner TJ, Baloh RH, Leitner ML, Tansey MG, et al. Persephin, a novel neurotrophic factor related to GDNF and neurturin. Neuron. 1998 Mar;20(2):245–53.

Moran SL, Steinmann SP, Shin AY. Adult brachial plexus injuries: mechanism, patterns of injury, and physical diagnosis. Hand Clin. 2005 Feb;21(1):13–24.

Morgenstern DA, Asher RA, Fawcett JW. Chondroitin sulphate proteoglycans in the CNS injury response. Prog Brain Res. 2002. p. 313–32.

Namikawa K, Honma M, Abe K, Takeda M, Mansur K, Obata T, et al. Akt/protein kinase B prevents injury-induced motoneuron death and accelerates axonal regeneration. J Neurosci. 2000 Apr 15;20(8):2875–86.

Naveilhan P, Baudet C, Mikaels a, Shen L, Westphal H, Ernfors P. Expression and regulation of GFRalpha3, a glial cell line-derived neurotrophic factor family receptor. Proc Natl Acad Sci U S A. 1998 Feb 3;95(3):1295–300.

Neumann S, Woolf CJ. Regeneration of dorsal column fibers into and beyond the lesion site following adult spinal cord injury. Neuron. 1999 May;23(1):83–91.

Ni T, Senthil-Kumar P, Dubbin K, Aznar-Cervantes SD, Datta N, Randolph M a, et al. A photoactivated nanofiber graft material for augmented Achilles tendon repair. Lasers Surg Med. 2012 Oct;44(8):645–52.

Nielsen J, Gotfryd K, Li S, Kulahin N, Soroka V, Rasmussen KK, et al. Role of glial cell line-derived neurotrophic factor (GDNF)-neural cell adhesion molecule (NCAM) interactions in induction of neurite outgrowth and identification of a binding site for NCAM in the heel region of GDNF. J Neurosci. 2009 Sep 9;29(36):11360–76.

Nishino J, Mochida K, Ohfuji Y, Shimazaki T, Meno C, Ohishi S, et al. GFR alpha3, a component of the artemin receptor, is required for migration and survival of the superior cervical ganglion. Neuron. 1999 Aug;23(4):725–36.

O'Neill AC, Randolph MA, Bujold KE, Kochevar IE, Redmond RW, Winograd JM. Preparation and integration of human amnion nerve conduits using a light-activated technique. Plast Reconstr Surg. 2009 Aug;124(2):428–37.

Orozco OE, Walus L, Sah DWY, Pepinsky RB, Sanicola M. SHORT COMMUNICATION GFRalpha3 is expressed predominantly in nociceptive sensory neurons. 2001;13.

Pachnis V, Mankoo B, Costantini F. Expression of the c-ret proto-oncogene during mouse embryogenesis. Development. 1993 Dec;119(4):1005–17.

Paratcha G, Ibáñez CF. Lipid rafts and the control of neurotrophic factor signaling in the nervous system: variations on a theme. Curr Opin Neurobiol. 2002 Oct;12(5):542–9.

Paratcha G, Ledda F. GDNF and GFRalpha: a versatile molecular complex for developing neurons. Trends Neurosci. 2008 Aug;31(8):384–91.

Paratcha G, Ledda F, Ibáñez CF. The neural cell adhesion molecule NCAM is an alternative signaling receptor for GDNF family ligands. Cell. 2003 Jun 27;113(7):867–79.

Parikh P, Hao Y, Hosseinkhani M, Patil SB, Huntley GW, Tessier-Lavigne M, et al. Regeneration of axons in injured spinal cord by activation of bone morphogenetic protein/Smad1 signaling pathway in adult neurons. Proc Natl Acad Sci U S A. 2011 May 10;108(19):E99–107.

Park S, Hong Y-W. Transcriptional regulation of artemin is related to neurite outgrowth and actin polymerization in mature DRG neurons. Neurosci Lett. 2006 Aug 14;404(1-2):61–6.

Pasterkamp RJ, Anderson PN, Verhaagen J. Peripheral nerve injury fails to induce growth of lesioned ascending dorsal column axons into spinal cord scar tissue

expressing the axon repellent Semaphorin3A. Eur J Neurosci. 2001 Mar;13(3):457–71.

Pasterkamp RJ, Verhaagen J. Emerging roles for semaphorins in neural regeneration. Brain Res Brain Res Rev. 2001 Mar;35(1):36–54.

Pasterkamp RJ, Verhaagen J. Semaphorins in axon regeneration: developmental guidance molecules gone wrong? Philos Trans R Soc Lond B Biol Sci. 2006 Oct 29;361(1473):1499–511.

Paveliev M, Airaksinen MS, Saarma M. GDNF family ligands activate multiple events during axonal growth in mature sensory neurons. Mol Cell Neurosci. 2004 Mar;25(3):453–9.

Pernet V, Joly S, Dalkara D, Jordi N, Schwarz O, Christ F, et al. Long-distance axonal regeneration induced by CNTF gene transfer is impaired by axonal misguidance in the injured adult optic nerve. Neurobiol Dis. Elsevier Inc.; 2013 Mar;51:202–13.

Pfaffl MW. A new mathematical model for relative quantification in real-time RT-PCR. Nucleic Acids Res. 2001 May 1;29(9):e45.

Quartu M, Serra MP, Boi M, Ferretti MT, Lai ML, Del Fiacco M. Tissue distribution of Ret, GFRalpha-1, GFRalpha-2 and GFRalpha-3 receptors in the human brainstem at fetal, neonatal and adult age. Brain Res. 2007 Oct 10;1173:36–52.

Ramer MS, Duraisingam I, Priestley J V, McMahon SB. Two-tiered inhibition of axon regeneration at the dorsal root entry zone. J Neurosci. 2001 Apr 15;21(8):2651–60.

Ramer MS, Priestley J V, McMahon SB. Functional regeneration of sensory axons into the adult spinal cord. Nature. 2000 Jan 20;403(6767):312–6.

Ramon y Cajal S. Degeneration & regeneration of the nervous system. London: Oxford University Press; 1928.

Sah DWY, Ossipov MH, Rossomando A, Silvian L, Porreca F. New approaches for the treatment of pain: the GDNF family of neurotrophic growth factors. Curr Top Med Chem. 2005 Jan;5(6):577–83.

Scherer SS. The biology and pathobiology of Schwann cells. Curr Opin Neurol. 1997;10:386–97.

Schlee S, Carmillo P, Whitty A. Quantitative analysis of the activation mechanism of the multicomponent growth-factor receptor Ret. Nat Chem Biol. 2006 Nov;2(11):636–44.

Schmutzler BS, Roy S, Pittman SK, Meadows RM, Hingtgen CM. Ret-dependent and Ret-independent mechanisms of Gfl-induced sensitization. Mol Pain. BioMed Central Ltd; 2011 Jan;7(1):22.

Schwab ME, Strittmatter SM. Nogo limits neural plasticity and recovery from injury. Curr Opin Neurobiol. Elsevier Ltd; 2014 Mar 11;27C:53–60.

Selzer ME. Promotion of axonal regeneration in the injured CNS. Lancet Neurol. 2003 Mar;2(3):157–66.

Sengelaub DR, Muja N, Mills a C, Myers W a, Churchill JD, Garraghty PE. Denervation-induced sprouting of intact peripheral afferents into the cuneate nucleus of adult rats. Brain Res. 1997 Sep 26;769(2):256–62.

Shehab S a S, Hughes DI. Simultaneous identification of unmyelinated and myelinated primary somatic afferents by co-injection of isolectin B4 and Cholera toxin subunit B

into the sciatic nerve of the rat. J Neurosci Methods. Elsevier B.V.; 2011 Jun 15;198(2):213–21.

Shin AY, Spinner RJ, Bishop AT. Nerve transfers for brachial plexus injuries. Oper. Tech. Orthop. 2004. p. 199–212.

Silva N a, Sousa N, Reis RL, Salgado AJ. From basics to clinical: A comprehensive review on spinal cord injury. Prog Neurobiol. 2013 Nov 20;114(2014):25–57.

Silver J, Miller JH. Regeneration beyond the glial scar. Nat Rev Neurosci. 2004 Feb;5(2):146–56.

Silvian L, Jin P, Carmillo P, Boriack-Sjodin PA, Pelletier C, Rushe M, et al. Artemin crystal structure reveals insights into heparan sulfate binding. Biochemistry. 2006 Jun 6;45(22):6801–12.

Simonen M, Pedersen V, Weinmann O, Schnell L, Buss A, Ledermann B, et al. Systemic deletion of the myelin-associated outgrowth inhibitor Nogo-A improves regenerative and plastic responses after spinal cord injury. Neuron. 2003 May 24;38(2):201–11.

Sjöstrand D, Carlsson J, Paratcha G, Persson B, Ibáñez CF. Disruption of the GDNF binding site in NCAM dissociates ligand binding and homophilic cell adhesion. J Biol Chem. 2007 Apr 27;282(17):12734–40.

Sjöstrand D, Ibáñez CF. Insights into GFRalpha1 regulation of neural cell adhesion molecule (NCAM) function from structure-function analysis of the NCAM/GFRalpha1 receptor complex. J Biol Chem. 2008 May 16;283(20):13792–8.

Smith GM, Falone AE, Frank E. Sensory axon regeneration: rebuilding functional connections in the spinal cord. Trends Neurosci. 2012 Mar;35(3):156–63.

Steward O, Zheng B, Tessier-Lavigne M. False resurrections: distinguishing regenerated from spared axons in the injured central nervous system. J Comp Neurol. 2003 Apr 21;459(1):1–8.

Sun F, He Z. Neuronal intrinsic barriers for axon regeneration in the adult CNS. Curr Opin Neurobiol. 2010 Aug;20(4):510–8.

Sun F, Park KK, Belin S, Wang D, Lu T, Chen G, et al. Sustained axon regeneration induced by co-deletion of PTEN and SOCS3. Nature. Nature Publishing Group; 2011 Nov 6;480(7377):372–5.

Takahashi M. The GDNF/RET signaling pathway and human diseases. Cytokine Growth Factor Rev. 2001 Dec;12(4):361–73.

Tang X-Q, Cai J, Nelson KD, Peng X-J, Smith GM. Functional repair after dorsal root rhizotomy using nerve conduits and neurotrophic molecules. Eur J Neurosci. 2004 Sep;20(5):1211–8.

Tang X-Q, Heron P, Mashburn C, Smith GM. Targeting sensory axon regeneration in adult spinal cord. J Neurosci. 2007 a May 30;27(22):6068–78.

Tang X-Q, Heron P, Mashburn C, Smith GM. Targeting sensory axon regeneration in adult spinal cord. J Neurosci. 2007 b May 30;27(22):6068–78.

Taraviras S, Marcos-Gutierrez C V, Durbec P, Jani H, Grigoriou M, Sukumaran M, et al. Signalling by the RET receptor tyrosine kinase and its role in the development of the mammalian enteric nervous system. Development. 1999 Jul;126(12):2785–97.

Taylor L, Jones L, Tuszynski MH, Blesch A. Neurotrophin-3 gradients established by lentiviral gene delivery promote short-distance axonal bridging beyond cellular grafts in the injured spinal cord. J Neurosci. 2006 Sep 20;26(38):9713–21.

Terzis JK, Kostopoulos VK. The surgical treatment of brachial plexus injuries in adults. Plast Reconstr Surg. 2007 Apr 1;119(4):73e–92e.

Thrasher A, Brennan C, Bolsover S, Fabes J, Anderson P, Ya RJ. Accumulation of the inhibitory receptor EphA4 may prevent regeneration of corticospinal tract axons following lesion. 2006;(September 2005):1721–30.

Trupp M, Belluardo N, Funakoshi H, Ibáñez CF. Complementary and overlapping expression of glial cell line-derived neurotrophic factor (GDNF), c-ret proto-oncogene, and GDNF receptor-alpha indicates multiple mechanisms of trophic actions in the adult rat CNS. J Neurosci. 1997 May 15;17(10):3554–67.

Tuszynski MH, Steward O. Concepts and methods for the study of axonal regeneration in the CNS. Neuron. Elsevier Inc.; 2012 Jun 7;74(5):777–91.

Viemari JC, Maussion G, Bévengut M, Burnet H, Pequignot JM, Népote V, et al. Ret deficiency in mice impairs the development of A5 and A6 neurons and the functional maturation of the respiratory rhythm. Eur J Neurosci. 2005 Nov;22(10):2403–12.

Wang R, King T, Ossipov MH, Rossomando AJ, Vanderah TW, Harvey P, et al. Persistent restoration of sensory function by immediate or delayed systemic artemin after dorsal root injury. Nat Neurosci. 2008 Apr;11(4):488–96.

Wang R, Rossomando A, Sah DWY, Ossipov MH, King T, Porreca F. Artemin induced functional recovery and reinnervation after partial nerve injury. Pain. International Association for the Study of Pain; 2013 a Nov 21;

Wang R, Rossomando A, Sah DWY, Ossipov MH, King T, Porreca F. Artemin induced functional recovery and reinnervation after partial nerve injury. Pain. International Association for the Study of Pain; 2013 b Nov 21;

Wang T, Molliver DC, Jing X, Schwartz ES, Yang F-C, Samad OA, et al. Phenotypic switching of nonpeptidergic cutaneous sensory neurons following peripheral nerve injury. PLoS One. 2011 a Jan;6(12):e28908.

Wang X, Baloh RH, Milbrandt J, Garcia KC. Structure of artemin complexed with its receptor GFRalpha3: convergent recognition of glial cell line-derived neurotrophic factors. Structure. 2006 Jun;14(6):1083–92.

Wang Y, Kochevar IE, Redmond RW, Yao M. A light-activated method for repair of corneal surface defects. Lasers Surg Med. 2011 b Aug;43(6):481–9.

Watanabe T, Ichihara M, Hashimoto M, Shimono K, Shimoyama Y, Nagasaka T, et al. Characterization of gene expression induced by RET with MEN2A or MEN2B mutation. Am J Pathol. American Society for Investigative Pathology; 2002 Jul;161(1):249–56.

Worby C a. Identification and Characterization of GFRalpha -3, a Novel Co-receptor Belonging to the Glial Cell Line-derived Neurotrophic Receptor Family. J Biol Chem. 1998 Feb 6;273(6):3502–8.

Wu Z-S, Pandey V, Wu W-Y, Ye S, Zhu T, Lobie PE. Prognostic significance of the expression of GFRα1, GFRα3 and syndecan-3, proteins binding ARTEMIN, in mammary carcinoma. BMC Cancer. BMC Cancer; 2013 Jan;13(1):34.

Yan Q, Elliott J, Snider WD. Brain-derived neurotrophic factor rescues spinal motor neurons from axotomy-induced cell death. Nature. 1992;360:753–5.

Yang P, Yang Z. Enhancing intrinsic growth capacity promotes adult CNS regeneration. J Neurol Sci. Elsevier B.V.; 2011 Sep 15;312(1-2):1–6.

Yang P, Yao M, DeMartelaere SL, Redmond RW, Kochevar IE. Light-activated sutureless closure of wounds in thin skin. Lasers Surg Med. 2012 Mar;44(2):163–7.

Yiu G, He Z. Glial inhibition of CNS axon regeneration. Nat Rev Neurosci. 2006 Aug;7(8):617–27.

Zhang Y, Dijkhuizen PA, Anderson PN, Lieberman AR. Rapid Communication NT-3 Delivered by an Adenoviral Vector Induces Injured Dorsal Root Axons to Regenerate Into the Spinal Cord of Adult Rats. 1998 a;562(June):554–62.

Zhang Y, Dijkhuizen PA, Anderson PN, Lieberman AR. Rapid Communication NT-3 Delivered by an Adenoviral Vector Induces Injured Dorsal Root Axons to Regenerate Into the Spinal Cord of Adult Rats. 1998 b;562(June):554–62.

Zheng B, Ho C, Li S, Keirstead H, Steward O, Tessier-Lavigne M. Lack of enhanced spinal regeneration in Nogo-deficient mice. Neuron. 2003 Apr 24;38(2):213–24.

Zhou Z, Peng X, Fink DJ, Mata M. HSV-mediated transfer of artemin overcomes myelin inhibition to improve outcome after spinal cord injury. Mol Ther. Nature Publishing Group; 2009 Jul;17(7):1173–9.